Positive Grassmannian, lectures by A. Postnikov

October 2, 2013

Contents

1 Lecture 1, 2/8/2012

1.1 Introduction

Fix $0 \leq k \leq n$ and a field $\mathbf{F}$ (e.g., $\mathbb{C}, \mathbb{R}, \mathbf{F}_q$). The **Grassmannian** $\mathbf{Gr}(k,n,\mathbf{F})$ be the manifold of k-dimensional linear subspaces in $\mathbf{F}^n$. (It has nice geometry it is projective algebraic variety/smooth,...)

Example 1.1. $k = 1$, $\mathbf{Gr}(1,n) = \mathbb{P}^{n-1}$ the projective space:

$$\begin{aligned}\mathbb{P}^{n-1} &= \{(x_1,\ldots,x_n) \neq (0,\ldots,0)\}\backslash(x_1,\ldots,x_n) \sim (\lambda x_1,\ldots,\lambda x_n)\\ &= \{(x_1 : x_2 : \cdots : x_n)\}.\end{aligned}$$

□

Take a $k \times n$ matrix A with rank k then

$$\mathbf{Gr}(k,n) = \{k \times n \text{ matrices of rank } k\}\backslash \text{ row operations } = _{\mathbf{GL}(k)}\backslash \mathrm{Mat}^*(k,n).$$

where $\mathbf{GL}(k)$ is the group of $k \times k$ invertible matrices over $\mathbf{F}$, and $\mathrm{Mat}^*(k,n)$ is the set of $k \times n$ matrices over $\mathbf{F}$ with rank k.

The row picture is considering the row space of A (the original definition of $\mathbf{Gr}(k,n)$). The column picture is to take the columns of A: $\delta_1,\ldots,\delta_n \in \mathbf{F}^k$. Note that $\dim \mathbf{Gr}(k,n) = k(n-k)$.

Example 1.2. $k = 2$:

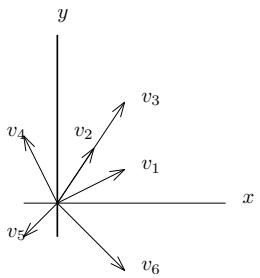

$\in \mathbf{Gr}(2, n)$.

$k = 3$

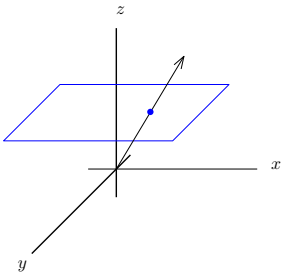

projective picture:

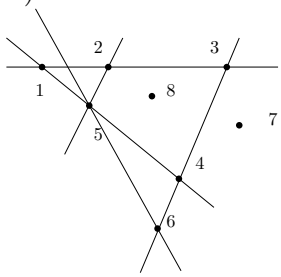

$\in \mathbf{Gr}(3, n)$. □

1.2 Plücker coordinates

Let $[n] = \{1, 2, \ldots, n\}$ and $\binom{[n]}{k} = \{I \subset [n] \mid \#I = k\}$. For a $k \times n$ matrix A and $I \subset \binom{[n]}{k}$ let $\Delta_I(A) = \det(k \times k \text{ submatrix in column set } I)$, i.e., $\Delta_I(A)$ is a maximal minor of A. Since A has rank k, at least one $\Delta_I(A) \neq 0$.

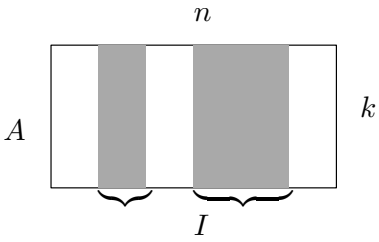

For $B \in \mathbf{GL}(k)$, $\Delta_I(B \cdot A) = \det(B) \cdot \Delta_I(A)$. Thus the $\binom{n}{k}$ minors $\Delta_I(A)$ for A in $\mathbf{Gr}(k, n)$ form projective coordinates on $\mathbf{Gr}(k, n)$.

The **Plücker embedding** is the map $\mathbf{Gr}(k, n) \mapsto \mathbb{P}^{\binom{n}{k}-1}$, $A \mapsto (\Delta_{I_1}(A) : \Delta_{I_2}(A) : \cdots)$.

Example 1.3. For $\mathbf{Gr}(2, 4)$, its dimension is $2 \cdot 4 - 2 \cdot 2 = 4$. $\mathbf{Gr}(2, 4) \to \mathbb{P}^5$, $A \mapsto (\Delta_{12} : \Delta_{13}, \Delta_{14} : \Delta_{23} : \Delta_{24} : \Delta_{34})$. Moreover, the maximal minors satisfy the following relation called a **Plücker relation**

$$\Delta_{13}\Delta_{24} = \Delta_{12}\Delta_{34} + \Delta_{14}\Delta_{23}.$$

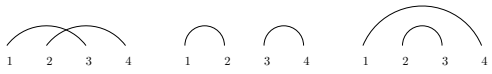

□

The Grassmannian has the following decomposition: $\mathbf{Gr}(k, n) = \coprod_{\lambda \subset k \times (n-k)} \Omega_\lambda$ where λ is a Young diagram contained in the $k \times (n-k)$ rectangle, and

$\Omega_I := \{A \in \mathbf{Gr}(k, n) \mid \Delta_I(A) \text{ is the lexicographically minimal nonzero Plücker coordinate}\}$.

This is the **Schubert decomposition** of $\mathbf{Gr}(k, n)$.

Example 1.4. In $\mathbf{Gr}(2,5)$ the matrix A

$$A = \begin{bmatrix} 0 & 1 & 2 & 1 & 3 \\ 0 & 1 & 2 & 2 & 3 \end{bmatrix} \quad \begin{bmatrix} 0 & 1 & 2 & 0 & 3 \\ 0 & 0 & 0 & 1 & 0 \end{bmatrix} \in \Omega_{\{2,4\}} = \Omega_{\ydiagram{2,1}},$$

since the second and fourth are the pivot columns. □

Identify $I \in \binom{[n]}{k}$ with the Young diagram $\lambda \subset k \times (n-k)$. The set I gives the labels of the vertical steps. Explicitly, $\lambda = (\lambda_1 \geq \lambda_2 \geq \cdots)$ is identified with the set $I = \{i_1 < i_2 < \cdots < i_k\}$ where $\lambda_j = n - k + j - i_j$.

Example 1.5. $k = 3, n = 9$, $\lambda = 532 \sim I = \{2, 5, 7\}$

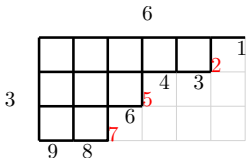

Figure 1: Illustration of correspondence between $\lambda \subset k \times (n-k)$ and set $I \in \binom{[n]}{k}$ for $k = 3$ and $n = 9$. The labels of the vertical steps of λ are the elements of I.

□

Schubert calculus is based on the following result.

Theorem 1.6. $\Omega_\lambda \cong \mathbf{F}^{|\lambda|}$ *where* $|\lambda|$ *is the number of boxes of* λ.

Theorem 1.7. *If* $\mathbf{F} = \mathbb{C}$ *then* $H^*(\mathbf{Gr}(k,n,\mathbb{C}))$ *has a linear basis* $[\overline{\Omega}_\lambda]$.

Example 1.8. $\mathbf{Gr}(1,3) = \{(x_1 : x_2 : x_3)\} = \underbrace{\{(1, x_2, x_3)\}}_{\Omega_{\ydiagram{2}}} \cup \underbrace{\{(0, 1, x_3)\}}_{\Omega_{\ydiagram{1}}} \cup \underbrace{\{(0, 0, 1)\}}_{\Omega_\varnothing}$ □

1.3 Matroid Stratification

[Gelfand-Serganova stratification]

For $\mathcal{M} \subset \binom{[n]}{k}$ a **stratum** is $S_\mathcal{M} = \{A \in \mathbf{Gr}(k,n) \mid \Delta_I \neq 0 \Leftrightarrow I \in \mathcal{M}\}$.

There is the following important axiom:

Exchange Axiom: For all $I, J \in \mathcal{M}$ and for all $i \in I$ there exists a $j \in J$ such that $(I \backslash \{i\}) \cup \{j\} \in \mathcal{M}$.

In fact the nonempty collection of subsets $\mathcal{M}$ that satisfy the exchange axiom are called **matroids**, the sets $I \in \mathcal{M}$ are called **bases** of $\mathcal{M}$, and k is the **rank** of the $\mathcal{M}$.

Lemma 1.9. *If* $\mathcal{M}$ *is not a matroid then* $S_\mathcal{M} = \varnothing$.

The best way to prove this Lemma is using the Plücker relations. The converse is not true.

A matroid $\mathcal{M}$ is a **realizable** matroid (over $\mathbf{F}$) if and only if $S_\mathcal{M} \neq \varnothing$. In general it is a hard question to characterize realizable matroids.

2 Lecture 2, 2/10/2012

Last time we saw $\mathbf{Gr}(k,n) = {}_{\mathbf{GL}(k)}\backslash \operatorname{Mat}^*(k,n)$, the Plücker coordinates $\Delta_I(A)$ for $I \in \binom{[n]}{k}$, and two stratifications: the Schubert and matroid stratifications.

$$\mathbf{Gr}(k,n) = \coprod_{\lambda} \Omega_\lambda = \coprod_{\mathcal{M}} S_{\mathcal{M}},$$

where the cells Ω_λ have a simple structure and the matroid strata $S_{\mathcal{M}}$ have a complicated structure.

2.1 Mnëv's Universality Theorem

The strata $S_{\mathcal{M}}$ can be as complicated as any algebraic variety (even for $k = 3$).

Example 2.1. For $k = 3$ and $n = 6$, consider the point of $\mathbf{Gr}(3,6)$ given by the projective picture in Figure 2.

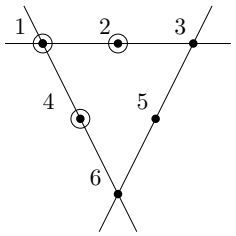

Figure 2: Projective picture of point in the cell $\Omega_{\{1,2,4\}}$ in $\mathbf{Gr}(3,6)$.

It is in $\Omega_{1,2,4} = \Omega$ 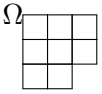 and $\mathcal{M} = \binom{[6]}{3} \setminus \{\{1,2,3\},\{1,4,6\},\{3,5,6\}\}$. □

Any system of algebraic equations can be realized by a configuration like the one in Figure 2.

One of the main topics of this course will be to give a third decomposition of $\mathbf{Gr}(k,n)$ called the *Positroid decomposition* (see Section 11.3) that sits between the Schubert decomposition and the matroid decomposition.

2.2 Schubert decomposition

Recall the Schubert decomposition $\mathbf{Gr}(k,n) = \coprod_{\lambda \subset k\times(n-k)} \Omega_\lambda$, where $\Omega_\lambda = \Omega_I$. The set $I \in \binom{[n]}{k}$ indicates the columns in which the lattice path given by λ has vertical descents (see Figure 1).

Definition 2.2. There are several ways to define a Schubert cell:

1. Ω_λ consists of the elements of $\mathbf{Gr}(k,n)$ such that Δ_I is the lexicographic minimum non-zero Plücker coordinate.
2. A point in $\mathbf{Gr}(k,n)$ is in correspondence with a non-degenerate $k \times k$ matrix A modulo row operations. By Gaussian elimination such a matrix A has a canonical form: the *reduced row-echelon form* of the matrix. So Δ_I consists of the elements of $\mathbf{Gr}(k,n)$ with pivot set I.

□

Example 2.3.

$$A = \begin{bmatrix} 0 & \underline{1} & * & * & 0 & * & 0 & 0 & * \\ 0 & 0 & 0 & 0 & \underline{1} & * & 0 & 0 & * \\ 0 & 0 & 0 & 0 & 0 & 0 & \underline{1} & 0 & * \\ 0 & 0 & 0 & 0 & 0 & 0 & 0 & \underline{1} & * \end{bmatrix},$$

Let $I = \{2, 5, 7, 8\}$ be the set of the indices of the pivot columns (the pivots are underlined). □

Clearly $\Omega_I \cong \mathbf{F}^{\#*}$ and also clear that Δ_I, where I is the set of pivots, is the lexicographically minimum nonzero Plücker coordinates.

Definition 2.4. The **Gale order** is a partial order on $\binom{[n]}{k}$ given as follows: if $I = \{i_1 < i_2 < \cdots < i_k\}$ and $J = \{j_1 < j_2 < \cdots < j_k\}$, then $I \preceq J$ if and only if $i_1 \leq j_1, i_2 \leq j_2, \ldots, i_k \leq j_k$. □

Proposition 2.5. *For $A \in \Omega_I$, $\Delta_J(A) = 0$ unless $I \preceq J$.*

Proof. We use the reduced row echelon form. □

Corollary 2.6. *The set $\mathcal{M} := \{J \in \binom{[n]}{k} \mid \Delta_J(A) \neq 0\}$ has a unique minimal element with respect to the Gale order.*

Thus, we get another equivalent definition of a Schubert cell:

3. Ω_I consists of the elements of $\mathbf{Gr}(k, n)$ such that Δ_I is the *Gale order minimum* non-zero Plücker coordinate.

Theorem 2.7 ($\mathbf{F} = \mathbb{C}$ or $\mathbb{R}$)**.** $\overline{\Omega_I} \supset \Omega_J$ *if and only if* $I \preceq J$.

Proof. ($\Rightarrow$): For J such that $I \not\preceq J$ then by Proposition 2.5 $\Delta_J(A) = 0$ and so $A \in \Omega_I$. In the closure it still holds that $\Delta_I(A) = 0$ for $A \in \overline{\Omega_I}$. (Looking at the row echelon form, pivots can only jump to the right).

($\Leftarrow$): this is left as an exercise. □

From row echelon form, remove the k pivot columns to obtain a $k \times (n-k)$ matrix.

Example 2.8. Continuing with the matrix from Example 2.3, if we remove the pivot columns we obtain:

$$\begin{bmatrix} 0 & \underline{1} & * & * & 0 & * & 0 & 0 & * \\ 0 & 0 & 0 & 0 & \underline{1} & * & 0 & 0 & * \\ 0 & 0 & 0 & 0 & 0 & 0 & \underline{1} & 0 & * \\ 0 & 0 & 0 & 0 & 0 & 0 & 0 & \underline{1} & * \end{bmatrix} \mapsto \begin{bmatrix} 0 & * & * & * & * \\ 0 & 0 & 0 & * & * \\ 0 & 0 & 0 & 0 & * \\ 0 & 0 & 0 & 0 & * \end{bmatrix} \mapsto \text{mirror image of } \lambda = \ydiagram{4,2,1,1}.$$

Also note that λ corresponds to $I = \{2, 5, 7, 8\}$ (see Example 1.5 for illustration between shapes λ and sets I). □

Theorem 2.9. $\Omega_\lambda \cong \mathbf{F}^{|\lambda|}$.

2.3 Classical definition of Schubert cells

We think of $\mathbf{Gr}(k,n)$ as the space of k-dimensional subspaces $V \subset \mathbf{F}^n$. Fix the complete flag of subspaces:

$$\{0\} \subset V_1 \subset V_2 \subset \cdots \subset V_n = \mathbf{F}^n,$$

where $V_i =< e_n, e_{n-1}, \ldots, e_{n+1-i} >$ and $e_i = (0, \ldots, 0, 1, 0, \ldots, 0)$ is the ith elementary vector. Pick a sequence of integers $\mathbf{d} = (d_0, d_1, \ldots, d_n)$.

4. $\Omega_{\mathbf{d}} = \{V \in \mathbf{Gr}(k,n) \mid d_i = \dim(V \cap V_i) \text{ for } i = 0, \ldots, n\}$.

The conditions on $d_i \in \mathbb{Z}_{\geq 0}$ are:

$$\begin{cases} d_0 = 0, \quad d_{i+1} = d_i \text{ or } d_i + 1, \\ d_n = k. \end{cases}$$

Proof that Definition 4 of the Schubert cell is equivalent to Definition 3. We already have $\Omega_\lambda \leftrightarrow \Omega_I$. We show $\Omega_\lambda \leftrightarrow \Omega_{\mathbf{d}}$ and then show $\Omega_I \leftrightarrow \Omega_{\mathbf{d}}$.

Given $\lambda \subset k \times (n-k)$ we obtain $\mathbf{d}$ by doing the following: we start at the SW corner of the Young diagram and follow the border of the diagram until the NE corner. We label the horizontal and vertical steps, where we add 1 if we go north. See Example 2.11(a) for an illustration of this.

Given $I \subset \binom{[n]}{k}$ we obtain $\mathbf{d}$ by $d_i = \#(I \cap \{n-i+1, n-i+2, \ldots, n\})$. Note that this is precisely the dimension of the $rowspace(A) \cap V_i$ or equivalently the number of pivots in positions $n, n-1, \ldots, n-i+1$. □

Exercise 2.10. *Check that all these correspondences agree with each other.*

Example 2.11. For $k = 4$ and $n = 9$ let $\lambda = 3211$, from the labels of the Young diagram we get $\mathbf{d} = (0,1,2,2,3,3,3,4,4)$ (see Figure 3). And since $d_i = \#(I \cap \{n-i+1, n-i+2, \ldots, n\})$ we get that $I = \{2,5,7,8\}$.

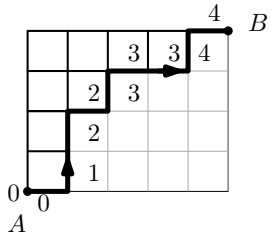

Figure 3: Illustration of correspondence between λ and $\mathbf{d}$.

□

2.4 Plücker embedding

Recall the definition of the Plücker map $\varphi : \mathbf{Gr}(k,n) \to \mathbb{P}^{N-1}$ where $N = \binom{n}{k}$ by $A \mapsto (\Delta_{I_1} : \Delta_{I_2} : \cdots : \Delta_{I_N})$.

Lemma 2.12. *The map φ is an embedding.*

Proof. We know that at least one Plücker coordinate is nonzero, without loss of generality say $\Delta_{12\dots k}(A) \neq 0$. Then by left $\mathbf{GL}_k$ action we can write A in the form

$$\widetilde{A} = [I_k \mid x_{ij}],$$

where (x_{ij}) is a $k \times (n-k)$ submatrix. From the minors we can reconstruct (x_{ij}). That is let $\Delta_I(\widetilde{A}) := \Delta_I(A)/\Delta_{12\dots k}(A)$ so that $\Delta_{12\dots k}(\widetilde{A}) = 1$. Then by the cofactor expansion $x_{ij} = \pm\Delta_{12\cdots i-1\, k+j\, i+1\dots k}(\widetilde{A})$. Thus a point in the image of φ determines the matrix A in $\mathbf{Gr}(n,k)$. □

3 Lecture 3, 2/15/2012

3.1 The Grassmannian $\mathbf{Gr}(n,k)$ over finite fields $\mathbf{F}_q$

Say $F = \mathbf{F}_q$ where $q = p^r$ is a power of a prime p. What can we say in this case about $\mathbf{Gr}(k,n,\mathbf{F}_q)$?

The first way is to view it as ${}_{\mathbf{GL}(k,\mathbf{F}_q)}\backslash \operatorname{Mat}^*(k,n,\mathbf{F}_q)$. Recall that:

$$\begin{aligned}\#\operatorname{Mat}^*(k,n,\mathbf{F}_q) &= (q^n-1)(q^n-q)(q^n-q^2)\cdots(q^n-q^{n-k+1}),\\ \#\mathbf{GL}(k,\mathbf{F}_q) &= (q^k-1)(q^k-q)\cdots(q^k-q^{k-1}).\end{aligned}$$

Then

$$\#\mathbf{Gr}(n,k,\mathbf{F}_q) = \frac{1-q^n}{1-q^k}\cdot\frac{1-q^{n-1}}{1-q^{k-1}}\cdots\frac{1-q^{n-k+1}}{1-q}.$$

We can write this more compactly using q-numbers: $[n]_q = 1+q+q^2+\cdots+q^{n-1} = \frac{1-q^n}{1-q}$, $[n]_q! = [1]_q[2]_q\cdots[n]_q$ and $\begin{bmatrix} n \\ k \end{bmatrix}_q = \frac{[n]_q!}{[k]_q![n-k]_q!}$. Then

Theorem 3.1. $\#\mathbf{Gr}(n,k,\mathbf{F}_q) = \begin{bmatrix} n \\ k \end{bmatrix}_q$.

The second way is to use the Schubert decomposition $\mathbf{Gr}(k,n,\mathbf{F}_q) = \coprod_{\lambda\subseteq k\times(n-k)} \Omega_\lambda$ which implies

$$\#\mathbf{Gr}(k,n,\mathbf{F}_q) = \sum_{\lambda\subseteq k\times(n-k)} q^{|\lambda|}.$$

Thus

Corollary 3.2. $\begin{bmatrix} n \\ k \end{bmatrix}_q = \sum_{\lambda\subseteq k\times(n-k)} q^{|\lambda|}$.

Example 3.3.

$$\begin{aligned}\mathbf{Gr}(2,4,\mathbf{F}_q) &= \frac{(1-q^4)(1-q^3)}{(1-q^2)(1-q)}\\ &= 1+q+2q^2+q^3+q^4\end{aligned}$$

$\varnothing$ 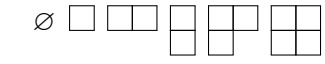

□

Problem 3.4. *Given a diagram $D \subseteq k\times(n-k)$, fix complement $\overline{D}$ to be 0. One obtains $X_D \subseteq \mathbf{Gr}(k,n,\mathbf{F}_q)$. For e.g. if D is a skew Young diagram. Find $\#X_D/\mathbf{F}_q$. Note that Ricky Liu [6] studied the combinatorics of related problems but not the # of points in $\mathbf{F}_q$.*

3.2 More on the Plücker embedding

Recall, the Plücker embedding $\varphi : \mathbf{Gr}(k,n) \mapsto \mathbb{P}^{\binom{n}{k}-1}$, $A \mapsto (\Delta_{I_1}(A) : \Delta_{I_2}(A) : \cdots)$. The **signed** Plücker coordinates are

$$\Delta_{i_1,i_2,\ldots,i_k} = \pm\Delta_{\{i_1,i_2,\ldots,i_k\}},$$

where the sign is positive if $i_1 < i_2 < \ldots < i_k$ and the sign changes whenever we switch two indices. Also $\Delta_{i-1,\ldots,i_k} = 0$ if the indices repeat. In terms of these signed coordinates the Plücker relations are: for any $i_1,\ldots,i_k,j_1,\ldots,j_k \in [n]$ and $r = 1,\ldots,k$:

$$\Delta_{i_1,\ldots,i_k,j_1,\ldots,j_k} = \sum \Delta_{i'_1,\ldots,i'_k}\Delta_{j'_1,\ldots,j'_k}, \tag{3.5}$$

where we sum over all indices $i_1,\ldots,i_k$ and $j'_1,\ldots,j'_k$ obtained from $i_1,\ldots,i_k$ and $j_1,\ldots,j_k$ by switching $i_{s_1}, i_{s_2},\ldots,i_{s_r}$ $(s_1 < s_2 < \ldots < s_r)$ with $j_1, j_2,\ldots,j_r$.

Example 3.6. For $n = 4, k = 3$ and $r = 1$ we have ($\Delta_{32} = -\Delta_{23}$)

$$\Delta_{12}\cdot\Delta_{34} = \Delta_{32}\cdot\Delta_{14} + \Delta_{13}\cdot\Delta_{24}.$$

□

Theorem 3.7 (Sylvester's Lemma)**.**

1. *The image of* $\mathbf{Gr}(k,n)$ *in* $\mathbb{P}^{\binom{n}{k}-1}$ *is the locus of common zeros of the ideal* I_{kn} *generated by the Plücker relations* (3.5) *in the polynomial ring* $\mathbb{C}[\Delta_I]$ *(where we treat* Δ_I *as formal variables).*
2. I_{kn} *is the ideal in* $\mathbb{C}[\Delta_I]$ *of all polynomials vanishing on the image of* $\mathbf{Gr}(k,n)$*.*
3. I_{kn} *is a prime ideal.*

We give the proof of the first part of this result. The full proof can be found in Fulton's book.

Proof. First we show that the coordinates Δ_I satisfy the Plücker relations (3.5). Given k-vectors $d_1,\ldots,d_k,w_1,\ldots,w_k$. Let $|v_1\ldots v_k| := \det(v_1,\ldots,v_k)$ then

$$|v_1\ldots v_k|\cdot|w_1\ldots w_k| = \sum |v'_1\ldots v'_k|\cdot|w'_1\ldots w'_k|$$

where the sum in the right hand side is obtained by switching r vectors from $v_1,\ldots,v_k$ with r vectors from $w_1,\ldots,w_k$. Let f be the difference between the left-hand side and the right-hand side (we want to show that $f = 0$). Note that (i) f is a multilinear function of $v_1,\ldots,v_k,w_k$ and (ii) f is an alternating function of $v_1,\ldots,v_k,w_k$.

Claim: If $v_i = v_{i+1}$ or $v_k = w_k$ then $f = 0$.

First we do the case $v_k = w_k$ where $r < k$ by induction on k.

$$f = |v_1\ldots v_k|\cdot|w_1\ldots v_k| - \sum |v'_1\ldots v_k|\cdot|w'_1\ldots v_k|$$

Assume that $v_k = [0\ldots01]^T = e_n$ and expand the determinants in the expression above with respect to the last column. We obtain the equation for f involving $k-1$ vectors. By induction we get $f = 0$.

Second, if $v_i = v_{i+1}$ the cancellation is easy to see as the following example shows.

Example 3.8. For $k = 3$ and $r = 1$ we get

$$\begin{aligned} f &= |v_1v_1v_3|\cdot|w_1w_2w_3| - (|w_1v_1v_3|\cdot|v_1w_2w_3| + |v_1w_1w_3|\cdot|v_1w_2w_3|) \\ &= 0 - (|w_1v_1v_3|\cdot|v_1w_2w_3| - |w_1v_1w_3|\cdot|v_1w_2w_3|) = 0. \end{aligned}$$

□

Now we prove part 1 of Sylvester's Lemma. We want to show that the image of $\varphi\mathbf{Gr}(k,n)$ in $\mathbb{P}^{\binom{n}{k}-1}$ is the zero locus of I_{kn}. Let $\{\Delta_I\}_{I\in\binom{[n]}{k}}$ be any point in $\mathbb{P}^{\binom{n}{k}-1}$ satisfying the Plücker relations. We need to find a $k\times n$ matrix A such that $\Delta_I=\Delta_I(A)$.

Suppose $\Delta_{12\dots k}\neq 0$. We can rescale the coordinates such that $\Delta_{12\dots k}=1$. Let A be the matrix $[I_k \mid x_{ij}]$ where $x_{ij}=\Delta_{1\,2\dots i-1\,j+k\,i+1\dots k}$. Let $\widetilde{\Delta}_I=\Delta_I(A)$. We want tot show that $\widetilde{\Delta}_I=\Delta_I$ for all $I\in\binom{[n]}{k}$.

We know the following:

1. $\Delta_{1\,2\dots\,k}=\widetilde{\Delta}_{1\,2\dots\,k}=1$,
2. For all I such that $|I\cap\{1,2,\dots,k\}|=k-1$ we have $\widetilde{\Delta}_I=x_{ij}$ for some j but by construction $x_{ij}=\Delta_I$,
3. Both $\widetilde{\Delta}_I$ and Δ_I satisfy the Plücker relations.

We claim that form the three observations above it follows that $\Delta_I=\widetilde{\Delta}_I$ for all $I\in\binom{[n]}{k}$. We show this for $r=1$ by induction on $p=|I\cap\{1,2,\dots,k\}|$. The base case is $p=k,k-1$.

We use the Plücker relations to expand $\Delta_{1\,2\dots\,k}\cdot\Delta_{i_1\dots i_k}$:

$$\begin{aligned}\Delta_{1\,2\dots\,k}\cdot\Delta_{i_1\dots i_k}&=\sum_{s=1}^{k}\Delta_{1\,2\dots\,s-1\,i\,s+1\dots k}\cdot\Delta_{s\,i_2\dots i_k},\\&=\sum\widetilde{\Delta}_{1\,2\dots\,s-1\,i\,s+1\dots k}\cdot\widetilde{\Delta}_{s\,i_2\dots i_k},\\&=\widetilde{\Delta}_{1\,2\dots\,k}\cdot\widetilde{\Delta}_{i_1\dots i_k},\end{aligned}$$

where $\Delta_{s\,i_2\dots i_k}=\widetilde{\Delta}_{s\,i_2\dots i_k}$ y induction on p.

At the end since $\Delta_{1\,2\dots\,k}=\widetilde{\Delta}_{1\,2\dots\,k}$ we obtain $\Delta_{i_1\dots i_k}=\widetilde{\Delta}_{i_1\dots i_k}$ as desired. □

Remark 3.9. Note that in the proof of Part 1 of Sylvester's Lemma we only used the Plücker relations for $r=1$. The radical ideal of the ideal generated by just these relations is I_{kn} (the ideal with the Plücker relations for all r). □

3.3 Matroids

Recall the notion of matroid $\mathcal{M}\subset\binom{[n]}{k}$. The elements of the matroid satisfy the **Exchange axiom**: For all $I,J\in\mathcal{M}$ and for all $i\in I$ there exists a $j\in J$ such that $(I\backslash\{i\})\cup\{j\}\in\mathcal{M}$.

Theorem 3.10. *Pick $A\in\mathbf{Gr}(k,n)$ and let $\mathcal{M}=\{I\in\binom{[n]}{k}\mid\Delta_I(A)\neq 0\}$. Then $\mathcal{M}$ is a matroid.*

Proof. Two sets I,J and in $\mathcal{M}$ if and only if $\Delta_J\cdot\Delta_I\neq 0$. But by the Plücker relations:

$$\Delta_J\cdot\Delta_I=\sum_{j\in J}\pm\Delta_{(J\backslash j)\cup i}\cdot\Delta_{(I\backslash i)\cup j}.$$

Thus there exists a $j\in J$ such that $\Delta_{(J\backslash j)\cup i}\cdot\Delta_{(I\backslash i)\cup j}\neq 0$ which implies the stronger condition that both $(J\backslash j)\cup i$ and $(I\backslash i)\cup j$ are in $\mathcal{M}$. □

We call the stronger condition implied by the proof the **strong exchange axiom**.

Exercise 3.11. *Is the strong exchange axiom equivalent to the exchange axiom?*

4 Lecture 4, 2/17/2012

Last time we saw the bf Stronger Exchange axiom: for all $i_1, \ldots, i_r \in I$ there exists $j_1, \ldots, j_r \in J$ such that $(I \backslash \{i_1, \ldots, i_r\}) \cup \{j_1, \ldots, j_r\} \in \mathcal{M}, (J \backslash \{j_1, \ldots, j_r\}) \cup \{i_1, \ldots, i_r\} \in \mathcal{M}$.

Example 4.1 (non-realizable matroid)**.** The **Fano plane** in $\binom{[7]}{3}$ which is illustrated in Figure 4.

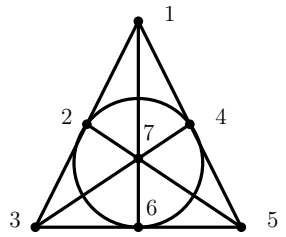

Figure 4: The Fano plane.

□

Exercise 4.2. *Check that the Fano matroid is not realizable over* $\mathbb{R}$.

4.1 Two definitions of matroids

Recall the Gale order: $\{i_1, \ldots, i_k\} \preceq \{j_1, \ldots, j_k\}$ if and only if $i_1 \leq j_1, \ldots, i_k \leq j_k$. A generalization of this order is obtained by picking a permutation $w = w_1 \cdots w_n$ in $\mathfrak{S}_n$, order the set $[n]$ by $w_1 < w_2 < \ldots < w_n$ and define a **permuted Gale order** $\preceq_w$ accordingly.

Definition 4.3. Let $\mathcal{M} \subseteq \binom{[n]}{k}$.

1. **Exchange Axiom:** for all $I, J \in \mathcal{M}$ and for all $i \in I$ there exists a $j \in J$ such that $(I \backslash \{i\}) \cup \{j\} \in \mathcal{M}$.
2. $\mathcal{M}$ is a matroid if for all w in $\mathfrak{S}_n$, $\mathcal{M}$ has a unique minimal element in $\subseteq_w$ (permuted Gale order $\subseteq_w$).

□

The second definition above is connected to the Grassmannian since in Lecture 2 we had seen that if we fix $A \in \mathbf{Gr}(n,k)$ then $\mathcal{M} := \{I \in \binom{[n]}{k} \mid \Delta_I(A) \neq 0\}$ has a unique minimal element with respect to the Gale order.

Another related result from Lecture 2 was the Schubert and matroid stratification of $\mathbf{Gr}(k,n)$:

$$\mathbf{Gr}(k,n) = \coprod_{\lambda \subseteq k \times (n-k)} \Omega_\lambda = \coprod_{\mathcal{M}} S_{\mathcal{M}},$$

where Ω_λ depends on an ordered basis but $S_{\mathcal{M}}$ depends on an unordered basis. Thus we really have $n!$-Schubert decompositions: for $w \in \mathfrak{S}_n$ we have $\mathbf{Gr}(k,n) = \coprod_{\lambda \subseteq k \times (n-k)} \Omega_\lambda^w$ where Ω_λ^w has the same definition as Γ_λ but with respect to the order $e_{w_1} < e_{w_2} < \ldots < e_{w_n}$. (We can also think of Ω_λ^w as $w^{-1}(\Gamma_\lambda)$ where $\mathfrak{S}_n$ acts on $\mathbb{C}^n$ by permuting coordinates according to w.

Theorem 4.4 (Gelfand-Goresky-MacPherson-Sergenova [2])**.** *Matroid stratification is the common refinement of* $n!$ *permuted Schubert decompositions.*

Proof. [⋆⋆⋆ pending ⋆⋆⋆] □

Example 4.5. For $k = 3$ and $n = 5$ consider the matroid $\mathcal{M}$ from Figure 5. The minimal basis with respect to the Gale order is $\{1, 2, 4\}$. For $w = 34512$ the minimal basis with respect to the w permuted Gale order is $\{3, 4, 1\}$. So $S_{\mathcal{M}} \in \Omega_{1,2,4} \cap \Omega_{3,4,1}^{34512} \cap \cdots$.

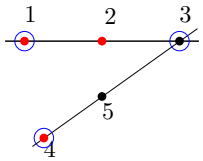

Figure 5: Matroid $\mathcal{M}$. The minimal basis with respect to the Gale order is $\{1, 2, 4\}$. For $w = 34512$ the minimal basis with respect to the w permuted Gale order is $\{3, 4, 1\}$.

□

4.2 Matroid polytopes and a third definition of matroids

We denote by $e_1, \ldots, e_n$ the coordinate vectors in $\mathbb{R}^n$. Given $I = \{i_1, \ldots, i_k\} \in \binom{[n]}{k}$ we denote by e_I the vector $e_{i_1} + e_{i_2} + \cdots + e_{i_k}$. Then for any $\mathcal{M} \subseteq \binom{[n]}{k}$ we obtain the following convex polytope

$$P_{\mathcal{M}} = \text{conv}(e_I \mid I \in \mathcal{M}) \subset \mathbb{R}^n,$$

where conv means the convex hull. Note that $P_{\mathcal{M}} \subset \{x_1 + x_2 + \cdots + x_n = k\}$ so $\dim P_{\mathcal{M}} \leq n - 1$.

Definition 4.6 (Gelfand-Serganova-M-S)**.** $P_{\mathcal{M}}$ is a **matroid polytope** if every edge of $P_{\mathcal{M}}$ is parallel to $e_j - e_i$, i.e. edges are of the form $[e_I, e_J]$ where $J = (I \backslash \{i\}) \cup \{j\}$. □

This gives us a third definition of a matroid.

Definition 4.7. 3. A matroid is a subset $\mathcal{M} \subseteq \binom{[n]}{k}$ such that $P_{\mathcal{M}}$ is a matroid polytope.

□

Theorem 4.8. *The three definitions of a matroid: 1. by the exchange axiom, 2. by the permuted Gale order, and 3. by matroid polytopes are equivalent.*

Exercise 4.9. *Prove this theorem.*

Example 4.10. If $\mathcal{M} = \binom{[n]}{k}$ is the uniform matroid then $P_{\mathcal{M}} = \text{conv}(e_I \mid I \in \binom{[n]}{k})$. This polytope is called the **hypersimplex** Δ_{kn}. The hypersimplex has the following property: All e_I for $I \in \binom{[n]}{k}$ are vertices of Δ_{kn} and these are all the lattice points of Δ_{kn}. □

Question 4.11. *What are the vertices of any $P_{\mathcal{M}}$?*

The answer is e_I where $I \in \mathcal{M}$ (basis of the matroid).

Example 4.12. For $k = 1$, $\Delta_{1n} = \text{conv}(e_1, e_2, \ldots, e_n)$ is the usual $(n-1)$-dimensional simplex. See Figure 6 for an illustration of Δ_{13}.

□

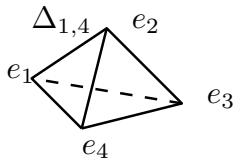

Figure 6: An illustration of Δ_{13}.

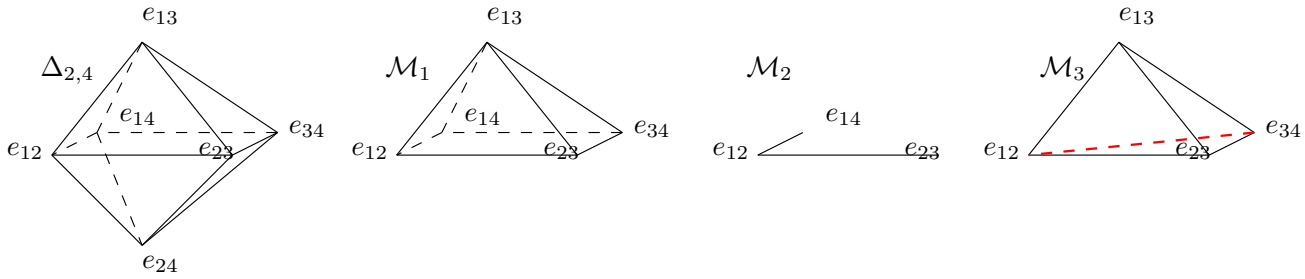

Figure 7: (a) the hypersimplex Δ_{24}, (b) three subpolytopes of Δ_{24} corresponding to $\mathcal{M}_1 = \{12, 13, 14, 23, 34\}, \mathcal{M}_2 = \{12, 14, 23\}$ and $\mathcal{M}_3 = \{12, 23, 34, 13\}$ the first two are matroid polytopes and the third one is not (it has a bad edge $[e_{12}, e_{34}]$, or in terms of $\mathcal{M}_3$ take $I = \{3, 4\}$, $J = \{1, 2\}$ and $i = 3$ then the Exchange Axiom fails).

Example 4.13. For $k = 2$ and $n = 4$ the hypersimplex Δ_{24} has six vertices $e_{12} = (1, 1, 0, 0), e_{13} = (1, 0, 1, 0), \ldots$ (see Figure 7(a)). The matroid polytopes are subpolytopes of Δ_{24} without new edges. In Figure 7(b) there are three subpolytopes associated with $\mathcal{M}_1 = \{12, 13, 14, 23, 34\}, \mathcal{M}_2 = \{12, 14, 23\}$ and $\mathcal{M}_3 = \{12, 23, 34, 13\}$ respectively. $\mathcal{M}_1$ and $\mathcal{M}_2$ are matroids but $\mathcal{M}_3$ is not (take $I = \{3, 4\}$, $J = \{1, 2\}$ and $i = 3$ then the Exchange Axiom fails).

□

Exercise 4.14. *Consider the subset S_{2468} of the Grassmannian $\mathbf{Gr}(4, 8, \mathbf{F}_q)$ that consists of the elements that can be represented by 4×8 matrices A with 0s outside the shape 2468. Find a combinatorial expression for the number $f_4(q)$ of elements of S_{2468} over $\mathbf{F}_q$. Calculate also $f_4(1), f_4(0)$ and $f_4(-1)$.*

5 Lecture 5, 2/20/2012

Last time we talked about matroid polytopes.

If $\mathcal{M} = \binom{[n]}{k}$ (uniform matroid) then the matroid polytope is the hypersimplex Δ_{kn}.

5.1 Moment Map

First we will talk about the moment map which is important in symplectic and toric geometry.

Let $T = (\mathbb{C}^*)^n$, it acts on $\mathbb{C}^n$ by $(t_1, \ldots, t_n) \cdot (x_1, \ldots, x_n) \mapsto (t_1 x_1, t_2 x_2, \ldots, t_n x_n)$. This induces a T-action on $\mathbf{Gr}(k, n, \mathbb{C})$.

Recall $\mathbf{Gr}(k, n) = {}_{\mathbf{GL}_k} \backslash Mat(k, n)$. We claim that T acts by right multiplication by $\mathrm{diag}(t_1, \ldots, t_n)$ (we rescale column i by t_i). In terms of Plücker coordinates: $(t_1, \ldots, t_n) \cdot \{\Delta_I\} \mapsto \{\prod_{i \in I} t_i \Delta_I\}$.

We define the **moment map**: $\mu : \mathbf{Gr}(k,n,\mathbb{C}) \to \mathbb{R}^n, A \mapsto (y_1,\ldots,y_n)$ where $y_i = \frac{\sum_{I \ni i} |\Delta_I|^2}{\sum_I |\Delta_I|^2}$.

Example 5.1. $k=2$ and $n=4$, $\mathbf{Gr}(2,4) \to \mathbb{R}^4$, $A \mapsto (y_1,y_2,y_3,y_4)$ where for instance $y_1 = \dfrac{|\Delta_{12}|^2+|\Delta_{13}|^2+|\Delta_{14}|^2}{\sum_I |\Delta_I|^2}$. □

Theorem 5.2 (Atiyah-Guillemin-Sternberg)**.** *(1) Image of μ is a convex polytope.*

(2) Moreover, pick any point $A \in S_{\mathcal{M}} \subset \mathbf{Gr}(k,n)$, then $\mu(T \cdot A)$ is a convex polytope (A is fixed, $T \cdot A$ is a set of matrices).

Exercise proof this case of convexity theorem.
Claim:

(1) $\mu(\mathbf{Gr}(k,n)) = \begin{pmatrix}[n]\\ k\end{pmatrix}$.

(2) $\mu(\overline{T \cdot A}) = P_{\mathcal{M}}$ is a matroid polytope.

Idea proof of Claim.
(1) Clearly $0 \le y_i \le 1$, also $y_1 + \cdots + y_n = k$. This means that $\mu(\mathbf{Gr}(k,n)) \subseteq \Delta_{kn}$. (Recall that $\Delta_{kn} = \{(y_1,\ldots,y_n) \mid 0 \le y_i \le 1, y_1+\cdots+y_n = k\}$.)

Pick A_I to be the 0-1 matrix whose $k \times k$ submatrix indexed by I is the identity matrix, and the other columns are 0. This is a fixed point of T in $\mathbf{Gr}(k,n)$. Actually this is the form of all the fixed points. Thus there are $\binom{n}{k}$ such fixed points (one for each set $I \in \begin{pmatrix}[n]\\ k\end{pmatrix}$).

Now $\Delta_J(A_I) = \delta_{I,J}$. Then $\mu(A_I) = e_I = \sum_{i \in I} e_i$ and this is a vertex of Δ_{kn}. From the convexity theorem, μ is a convex polytope, this together with the fact that $\mu(A_I) = e_I$ forces $\mu(\mathbf{Gr}(k,n))$ to be Δ_{kn}. □

Remark 5.3. To prove the convexity result we have to show that if

$$A \overset{\text{Plücker}}{\to} \{\Delta_I\} \overset{\mu}{\to} y = (y_1,\ldots,y_n),$$
$$A \cdot \mathrm{diag}(t_1,\ldots,t_n) \overset{\text{Plücker}}{\to} \{\prod_{i \in I} t_i \Delta_I\} \overset{\text{Plücker}}{\to} y' = (y'_1,\ldots,y'_n),$$

then y and y' are connected by a line where every point in the line corresponds to an image of μ. □

5.2 Normalized Volumes

$P \subset \mathbb{R}^n$, polytope with integer vertices in $\mathbb{Z}^n$. Let $d = \dim(P)$ and let V be a d-dimensional affine subspace containing P (it may or may not contain the origin). Let $L = V \cap \mathbb{Z}^n = \ell_0 + <\ell_1,\ldots,\ell_d>_{\mathbb{Z}}$, where $<\ell_1,\ldots,\ell_d>_{\mathbb{Z}}$ is the set of all linear $\mathbb{Z}$-combinations of $\{\ell_1,\ldots,\ell_d\}$.

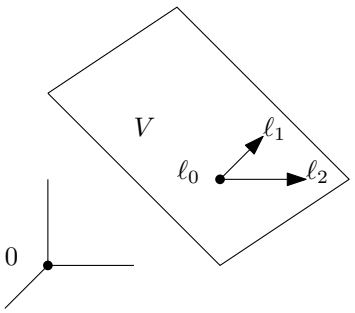

Define $\mathrm{Vol}(\cdot)$: volume form of V such that $\mathrm{Vol}(\ell_0 + \Pi(\ell_1, \ldots, \ell_d)) = 1$ where $\Pi(\ell_1, \ldots, \ell_d)$ is the parallelepiped spanned by $\{\ell_1, \ldots, \ell_d\}$.

Also we define **normalized volume** $\widetilde{\mathrm{Vol}} := d!\,\mathrm{Vol}$. Claim $\widetilde{\mathrm{Vol}}P \in \mathbb{Z}$ and $\widetilde{\mathrm{Vol}}$ of the standard coordinate simplex is 1.

Example 5.4. For the lines A and B, $\widetilde{\mathrm{Vol}}(A) = 2$ but $\widetilde{\mathrm{Vol}}(B) = 1$.

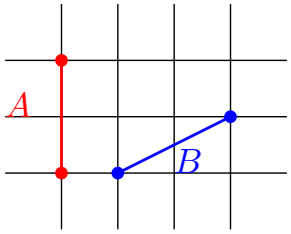

□

The following result justifies why normalized volumes are interesting.

Theorem 5.5. *The degree of a torus orbit $T \cdot A$ is the normalized volume of $\mu(\overline{T \cdot A}) = P_{\mathcal{M}}$.*

Example 5.6. For $\mathbf{Gr}(2, 4)$:

$$\begin{aligned} \alpha_1 t_1 t_2 + \alpha_2 t_1 t_3 + \cdots + \alpha_6 t_3 t_4 &= 0 \\ \beta_1 t_1 t_2 + \beta_2 t_1 t_3 + \cdots + \beta_6 t_3 t_4 &= 0 \\ \gamma_1 t_1 t_2 + \gamma_2 t_1 t_3 + \cdots + \gamma_6 t_3 t_4 &= 0. \end{aligned}$$

The number of solutions of this system is $\widetilde{\mathrm{Vol}}(\Delta_{24})$. We can calculate this volume by showing that we can divide Δ_{24} into four simplices of normalized volume 1. Thus $\widetilde{\mathrm{Vol}}(\Delta_{24}) = 4$. □

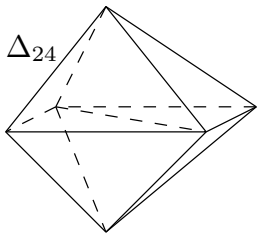

This motivates calculating the normalized volume of the hypersimplex. In general the normalized volume of Δ_{kn} is given by the **Eulerian number** $A_{k-1,n-1}$, where $A_{k,n} = \#\{w \in S_n \mid \mathrm{des}(w) = k\}$ where $\mathrm{des}(w)$ is the number of descents of w ($\#\{i \mid w_i > w_{i+1}\}$).

Theorem 5.7. $\widetilde{\mathrm{Vol}}(\Delta_{kn}) = A_{k-1,n-1}$.

Example 5.8.

permutations	$A_{k-1,n-1}$	$\widetilde{\mathrm{Vol}}(\Delta_{kn})$
123	$A_{0,3} = 1$	$\widetilde{\mathrm{Vol}}(\Delta_{14}) = 1$
213, 132 312, 231	$A_{1,3} = 4$	$\widetilde{\mathrm{Vol}}(\Delta_{24}) = 4$
321	$A_{23} = 1$	$\widetilde{\mathrm{Vol}}(\Delta_{34}) = 1$

□

Euler knew the following:

$$\begin{aligned} 1 + x + x^2 + x^3 + \cdots &= \frac{1}{1-x} \\ x + 2x^2 + 3x^3 + 4x^4 + \cdots &= \frac{x}{(1-x)^2} \\ 1^2x + 2^2x^2 + 3^2x^3 + 4^2x^4 + \cdots &= \frac{x + x^2}{(1-x)^3} \\ 1^3x + 2^3x^2 + 3^3x^3 + \cdots &= \frac{x + 4x^2 + x^3}{(1-x)^4}. \end{aligned}$$

And in general:

Proposition 5.9.

$$\sum_{r=1}^{\infty} r^n x^r = \frac{\sum_{k=0}^{n} A_{k,n} x^{k+1}}{(1-x)^{n+1}},$$

or equivalently, $A_{k-1,n-1} = [x^k](1-x)^n \sum_{r \geq 1} r^{n-1} x^r$.

We think of the hypersimplex in two ways: as a section of the n-hypercube:

$$\Delta_{kn} = [0,1]^n \cap \{x_1 + \cdots + x_n = k\},$$

or equivalently as a slice of the $(n-1)$-hypercube:

$$\Delta_{kn} = [0,1]^{n-1} \cap \{k - 1 \leq x_1 + \cdots + x_{n-1} \leq k\}.$$

Example 5.10. We divide $[0,1]^3$ into Δ_{14}, Δ_{24} and Δ_{34}.

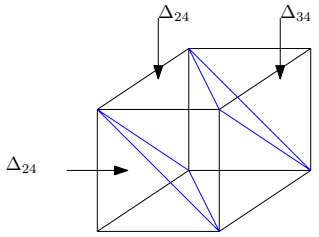

$\widetilde{\mathrm{Vol}} A = 2$ but $\widetilde{\mathrm{Vol}}(B) = 1$.

□

Proof. First let us take the first interpretation.

Take the positive octant $(\mathbb{R}_{\geq 0})^n$. Define $k\Delta = (\mathbb{R}_{\geq 0})^n \cap \{x_1 + \cdots + x_n = k\}$, this is a k-dilated $(n-1)$-simplex. So $\widetilde{\mathrm{Vol}}(k\Delta) = k^{n-1}$.

By inclusion-exclusion we can decompose the n-hypercube as

$$[0,1]^n = (\mathbb{R}_{>0})^n - \sum_i (e_i + (\mathbb{R}_{\geq 0})^n) + \sum_{i<j} (e_i + e_j + (\mathbb{R}_{\geq 0})^n) - \cdots$$

This is really an identity for characteristic functions of subsets (modulo set of measure 0)

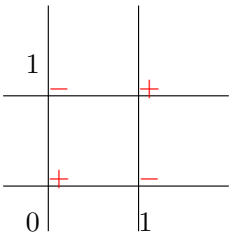

Then the volume of Δ_{kn} (using the first interpretation)

$$\begin{aligned}\widetilde{\mathrm{Vol}}(\Delta_{kn}) &= \widetilde{\mathrm{Vol}}(k\Delta) - \sum_i \widetilde{\mathrm{Vol}}((k-1)\Delta) + \sum_{i<j} \widetilde{\mathrm{Vol}}((k-2)\Delta) - \cdots \\ &= k^{n-1} - n(k-1)^{n-1} + \binom{n}{2}(k-2)^{n-1} - \cdots + (-1)^k \binom{n}{k-1}.\end{aligned}$$

From the expression $A_{k-1,n-1} = [x^k](1-x)^n \sum_{r\geq 1} r^{n-1}x^r$ from Proposition 5.9 one can show this expression above gives $A_{k-1,n-1}$. □

Stanley's proof. We use the interpretation of $\Delta_{kn} = [0,1]^{n-1} \cap \{k-1 \leq x_1 + \cdots + x_{n-1} \leq k\}$. For $w \in S_{n-1}$, there is a simple triangulation of $[0,1]^{n-1}$ into $\Delta_w = \{0 < x_{w_1} < x_{w_2} < \ldots < x_{w_n} < 1\}$ of $(n-1)!$ simplices.

This is not exactly the triangulation we need, it is not compatible with the slicing of the hypercube:

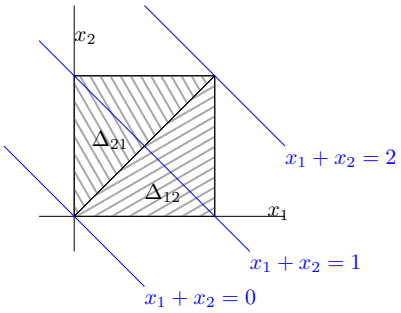

Instead define $S : [0,1]^{n-1} \to [0,1]^{n-1}$ to be the following piecewise-linear volume preserving map. $(x_1, \ldots, x_{n-1}) \mapsto (y_1, \ldots, y_{n-1})$ where $x_i = \{y_1 + \cdots + y_i\} = y_1 + \cdots + y_i - \lfloor y_1 + \cdots + y_i \rfloor$ (where $\{x\}$ is the fractional part of x). The forward map is:

$$y_i = \begin{cases} x_i - x_{i-1} \text{ if } x_i \geq x_{i-1} \\ x_i - x_{i-1} + 1 \text{ if } x_i < x_{i-1}, \end{cases}$$

where we assume $x_0 = 0$. The maps S is piecewise linear map and volume preserving.

We had a trivial triangulation $\Delta_{w^{-1}} := \{0 < x_{w^{-1}(1)} < \cdots < x_{w^{-1}(n-1)} < 1\}$. We get $(n-1)!$ simplices. Then $x_{i-1} < x_i \Leftrightarrow w_{i-1} > w_i \Leftrightarrow (i-1)$ is a descent of $\widetilde{w} = 0w_1w_2\ldots w_{n-1}$. Thus if $\mathrm{Des}(\widetilde{w})$ is the st of descents of $\widetilde{w}$ then

$$y_i = \begin{cases} x_i - x_{i-1} & \text{if } i-1 \notin \mathrm{Des}(\widetilde{w}), \\ x_i - x_{i-1} + 1 & \text{if } i-1 \in \mathrm{Des}(\widetilde{w}) \end{cases}$$

Then $y_1 + y_2 + \cdots y_{n-1} = x_{n-1} - x_0 + \mathrm{des}(w)$, and so $\mathrm{des}(w) \leq y_1 + y_2 + \cdots + y_{n-1} \leq \mathrm{des}(w) + 1$.

So $S(\Delta_{w^{-1}})$ is in the kth slice of the $(n-1)$-cube where $k = \mathrm{des}(w) + 1$. And $S(\Delta_{w^{-1}})$ is a triangulation of the $(n-1)$-cube with exactly $A_{k-1,n-1}$ simplices in the kth slice. □

6 Lecture 6, 2/24/2012

We digress a bit from the Grassmannian to talk about Matroids.

Problem 6.1. *For any matroid $\mathcal{M}$, what is the integer $\widetilde{\mathrm{Vol}}P_{\mathcal{M}}$?*

The **dual matroid** if $\mathcal{M}^* := \{[n]\backslash I \mid I \in \mathcal{M}\}$. Clearly, $P_{\mathcal{M}^*} \cong P_{\mathcal{M}}$ by the map $(x_1, \ldots, x_n) \mapsto (1 - x_1, \ldots, 1 - x_n)$.

6.1 Graphical Matroids $\mathcal{M}_G$

If G is a graph with labelled edges $\{1, 2, \ldots, n\}$, the bases of $\mathcal{M}_G$ are the set of edges corresponding spanning trees of G. We denote by G^* the dual graph of G (when G is planar).

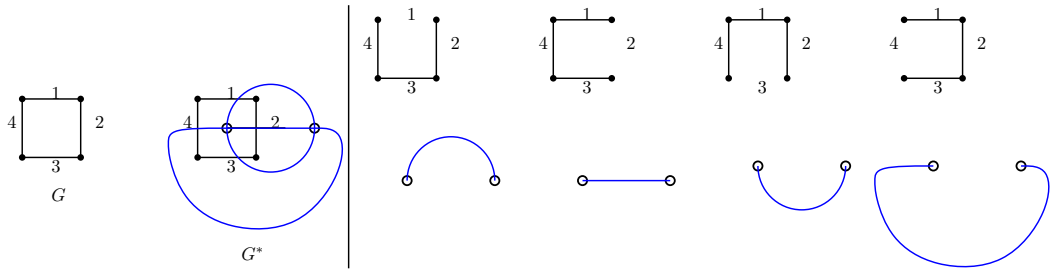

Figure 8: A graph G, its dual G^* and the spanning trees of G and of G^*.

Exercise 6.2. *1. Check exchange axiom on spanning trees of G.*

2. If G is a planar graph, $\mathcal{M}_{G^*} = (\mathcal{M}_G)^*$.

Example 6.3. If G is an n-cycle then $\mathcal{M}_G \cong \Delta^{n-1}$ is an $(n-1)$-simplex. □

Example 6.4. If G is an $(r+1)$-cycle glued at a vertex with a $(s+1)$-cycle then $P_{\mathcal{M}_G} = \Delta^r \times \Delta^s$. And $\widetilde{\mathrm{Vol}}(P_{\mathcal{M}_G}) = \binom{r+s}{r}$

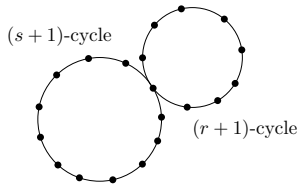

□

Proposition 6.5. *In full dimensions $\mathrm{Vol}(A \times B) = \mathrm{Vol}(A) \cdot \mathrm{Vol}(B)$, if A is r-dimensional and B is s-dimensional then $\widetilde{\mathrm{Vol}}(A \times B) = \binom{r+s}{r}\widetilde{\mathrm{Vol}}(A)\widetilde{\mathrm{Vol}}(B)$.*

Problem 6.6. *What is $\widetilde{\mathrm{Vol}}(P_{\mathcal{M}_G}) =$? or give families of graphs G with nice formulas for $\widetilde{\mathrm{Vol}}(P_{\mathcal{M}_G}) =$?.*

6.2 Generalization of Matroid polytopes

A **generalized permutahedron** is a polytope $P \subset \mathbb{R}^n$ such that any edge of P is parallel to $e_i - e_j$ for some $i \neq j$. (such a permutahedron has dimension $n-1$)

Example 6.7. $n = 3$, the lengths of the sides satisfy the following *hexagon equation*: $a+f = c+d$, $e+f = b+c$, and $a+b = c+d$.

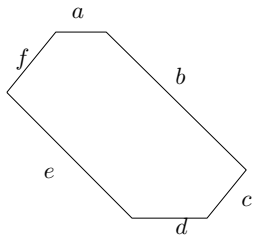

□

Example 6.8. The usual **permutahedron** P_n with $n!$ vertices $(w_1, \ldots, w_n)$ for all $w \in S_n$.

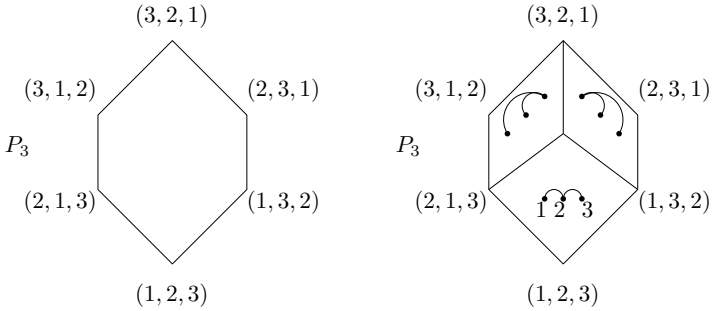

Figure 9: The permutahedron P_3, and tiling of P_3 illustrating why $\mathrm{Vol}(P_n)$ is n^{n-2}, the number of Cayley trees with n vertices.

□

Exercise 6.9. *Check that P_n is a generalized permutahedron.*

Exercise 6.10. $\mathrm{Vol}(P_n) = n^{n-2}$ *or equivalently* $\widetilde{\mathrm{Vol}}(P_n) = (n-1)!n^{n-2}$. *This is Cayley's formula for the number of trees with n labelled vertices.*

case $k = 3$. □

6.3 Graphical Zonotopes

The **Minkowski sum** $A + B = \{x + y \mid x \in A, y \in B\}$.

A **zonotope** is a Minkowski sum of line segments. In the plane you get n-gons whose opposite sides have same length and are parallel. From the examples above, in the plane only the square is a zonotope.

If G is a graph on n vertices labelled $1, 2, \ldots, n$, the **graphical zonotope** is $Z_G = \sum_{(i,j)\in E(G)}[e_i, e_j] \cong \sum_{(i,j)\in E(G)}[0, e_j - e_i]$. In the last equation you pick an orientation of edges, however the zonotope does not depend on the orientation.

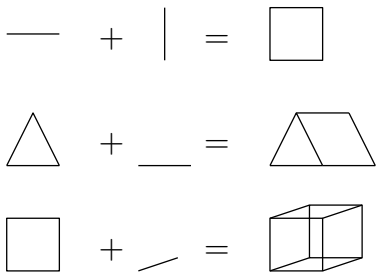

Figure 10: Examples of Minkowski sums.

Proposition 6.11. *For the complete graph, the zonotope is the permutahedron $Z_{K_n} = P_n$.*

A **Newton polytope** of $f \in \mathbb{C}[x_1, x_2, \ldots, x_n]$, then we can write $f = \sum c_{a_1,\ldots,a_n} x_1^{a_1} \cdots x_n^{a_n}$. Then $\mathrm{New}(f) = \mathrm{conv}(\{(a_1, \ldots, a_n) \mid c_{a_1,\ldots,a_n} \neq 0\})$

Example 6.12. $\mathrm{New}(x^2y^3 + x + 27y^2) = \mathrm{conv}((2,3),(1,0),(0,2))$.

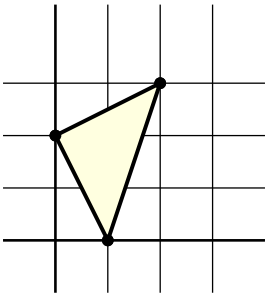

Figure 11: The newton polytope of $x^2y^3 + x + 27y^2$.

□

One of the most important features of the Newton polytope is the following property than says that we can view $\mathrm{New}(\cdot)$ as a generalized logarithm.

Proposition 6.13. $\mathrm{New}(f \cdot g) = \mathrm{New}(f) + \mathrm{New}(g)$.

Proof. The non-trivial point of this proof is that vertices are not cancelled. □

Proposition 6.14. *Z_G is a generalized permutahedron.*

using Newton polytopes. Recall the Vandermonde determinant

$$\begin{bmatrix} 1 & 1 & \ldots & 1 \\ x_1 & x_2 & \ldots & x_n \\ x_1^2 & x_2^2 & \ldots & x_n^2 \\ \vdots & \vdots & \ddots & \vdots \\ x_1^{n-1} & x_2^{n-1} & \cdots & x_n^{n-1} \end{bmatrix} = \sum_{w \in S_n} (-1)^{\mathrm{sgn}(w)} x_1^{w_1-1} x_2^{w_2-1} \cdots x_n^{w_n-1} = \prod_{i<j} (x_j - x_i).$$

If we take the Newton polytope of both sides and use Property [], $\mathrm{New}(LHS) = \mathrm{conv}((w_1 - 1, \ldots, w_n - 1)) = P_n$ and $\mathrm{New}(RHS) = \sum [e_i, e_j] = Z_{K_n}$. □

Theorem 6.15. $\mathrm{Vol}(Z_G) = \#\{\textit{spanning trees in } G\}$.

Proof. We prove it by induction on the number of edges of G. Let $t(G) = \#\{\text{spanning trees in } G\}$, this numbers satisfy the following deletion-contraction relation

$$t(G) = t(G\backslash e) + t(G/e).$$

Where $G\backslash e$ is graph G with edge e deleted and G/e is the graph G with edge e contracted. One can then show that Z_G also satisfies the same relation. □

6.4 Chromatic polynomial of G

$\chi_G(t) = \#\{\text{proper } t\text{-colorings of vertices of } G\}$, a proper coloring is one where the vertices of any edge of G have different colors.

Theorem 6.16. *$\chi_G(t)$ is a polynomial in t.*

Proof. $\chi_G(t)$ satisfies a deletion-contraction relation $\chi_G = \chi_{G\backslash e} - \chi_{G/e}$, and show $\chi_G(t) = t^n$ if G consists of just n vertices with no edges. □

Problem 6.17 (open)**.** *Is there a polytope such that some statistic gives $T_G(x, y)$. Is there a polytopal realization of the Tutte polynomial.*

7 Lecture 7, 2/29/2012

7.1 Schubert Calculus

We start with basic facts about (co) homology: Let X be a topological space and $H_i(X)$ is the ith homology of X which is some vector space over $\mathbb{C}$. Its dual $H^i(X) := (H_i(X))^*$ is the cohomology of X. These are both topological invariant of X.

The **Betti number** is $\beta_i(X) = \dim H^i(X)$. If $H^*(X) = H^0 \oplus H^1 \oplus \cdots$, this space has a multiplicative structure (cup-product).

Suppose that X is a nonsingular complex algebraic variety and $\dim_{\mathbb{C}} X = N$ then the homology and cohomology only live in even dimension:

$$H_*(X) = H_0 \oplus H_2 \oplus \cdots \oplus H_{2N}$$
$$H^*(X) = H^0 \oplus H^2 \oplus \cdots \oplus H^{2N}.$$

The fundamental class $[X]$ is the canonical generator of H_{2N}.

We also consider Poincaré duality that says $H^i(X) \cong H_{2N-i}(X)$, or equivalently $H^i(X) \cong (H^{2N-i}(X))^*$. If $Y \subset X$ is an algebraic subvariety with $\dim_{\mathbb{C}} Y = m$ then $[Y] \in H_{2m}(X) \cong H^{2N-2m}(X)$ (it has codimension $2m$). If $X = \coprod_{i\in I} Y_i$ then we say that X has a cell decomposition (CW-complex), where $Y_i \cong \mathbb{C}^{m_i}$ and $\overline{Y_i}$ is an algebraic subvariety and $\overline{Y_i}\backslash Y_i$ is a union of smaller dimensional Ys.

Claim 1: Cohomology classes of $[\overline{Y_i}]$ are in $H^{2N-2m_i}(X)$ so they form a linear basis of $H^*(X)$. In particular $H^0(X)$ is spanned by $[X]$. And $H^{2N}(X)$ is spanned by [point].

Claim 2: If Y and Y' are algebraic subvarieties of X and $Y \cap Y' = Z_1 \cup \cdots \cup Z_r$ where

(i) $\mathrm{codim}\, Y + \mathrm{codim}\, Y' = \mathrm{codim}\, Z_i$ for all i (proper intersection)

(ii) For every generic point $z \in Z_i$, $T_z Z_i = T_z Y \cap T_z Y'$ where T_z is the *tangent space* (transversal intersection)

Then

$$[Y] \cdot [Y'] = \sum [Z_i].$$

Figure 12: Example of transversal and non-transversal intersections. In the first example the intersection of the tangent spaces at the points where the varieties meet is a point. In the second example, the tangent spaces are the same.

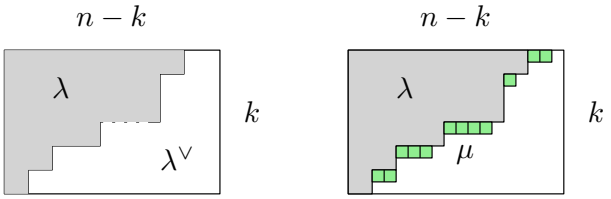

Figure 13: (a) Example of a partition λ and its complement $\lambda^\vee$, and (b) example of partitions obtained in Pieri rule.

7.2 Cohomology of $\mathbf{Gr}(k, n, \mathbb{C})$

$$\mathbf{Gr}(k,n) = \coprod_{\lambda \subseteq k\times(n-k)} \Omega_\lambda,$$

where $\Omega_\lambda \cong \mathbb{C}^{|\lambda|}$ is a Schubert cell. Let $X_\lambda := \overline{\Omega}_{\lambda^\vee}$ where $\lambda^\vee = (n-k-\lambda_k, \cdots, n-k-\lambda_1)$ is the complement of λ in $k \times (n-k)$.

Denote by $\sigma_\lambda = [X_\lambda] \in H^{2|\lambda|}(\mathbf{Gr}(k,n,\mathbb{C}))$, these are the Schubert classes. The Schubert classes do not depend on the choice of basis, just on the partition.

Theorem 7.1. *The Schubert classes σ_λ for $\lambda \subseteq k \times (n-k)$ form a linear basis of $H^*(\mathbf{Gr}(k,n,\mathbb{C}))$.*

Example 7.2. $\sigma_\varnothing = [\mathbf{Gr}(k,n)]$ and $\sigma_{k\times(n-k)} = [\text{point}]$. □

Remarks 7.3 (Special feature of this basis)**.** This basis is self-dual with respect to Poincaré duality. This means:

(i) $B = \{\sigma_\lambda \mid |\lambda| = i\}$ basis of $H^{2i}(\mathbf{Gr}(k,n))$,

(ii) $B^* = \{\sigma_{|\mu|} \mid |\mu| = k(n-k) - i\}$ basis of $H^{2k(n-k)-2i}(\mathbf{Gr}(k,n))$. B and B^* are dual basis (the dual map is $\sigma_\lambda \mapsto \sigma_{\lambda^\vee}$).

Let $c \in \mathbb{C}$, for $\sigma \in H^{2k(n-k)}(\mathbf{Gr}(k,n))$ where $\sigma = c \cdot [\text{point}]$ then $< \sigma >:= c$.

Theorem 7.4 (Duality Theorem)**.** *For partitions λ, μ such that $|\lambda| + |\mu| = k(n-k)$ then $< \sigma_\lambda \cdot \sigma_\mu >= \delta_{\lambda,\mu^\vee}\sigma_{k\times(n-k)}$. Where the product of Schubert classes is in the cup product.*

Theorem 7.5 (Pieri Formula)**.** *Let $\sigma_r = \sigma_{\square\square\cdots\square}$ (k boxes) then*

$$\sigma_\lambda \cdot \sigma_r = \sum_\mu \sigma_\mu,$$

where the sum is over μ such that μ/λ is a horizontal r-strip.

In terms of coordinates the partitions are interlaced $n-k \geq \mu_1 \geq \lambda_1 \leq \mu_2 \geq \lambda_2 \geq \cdots \geq \mu_k \geq \lambda_k$ and $\sum(\mu_i - \lambda_i) = r$.

Example 7.6. □

7.3 Note on proofs

Consider $\sigma_\lambda \cdot \sigma_\mu = [X_\lambda] \cdot [X_\mu]$. We work with $X_\lambda \cap \widetilde{X}_\mu$ where X_λ corresponds to standard Schubert decomposition (ordering basis with permutation $12\cdots n$) and $\widetilde{X}_\mu$ corresponds to the opposite ordering of the coordinates (permutation $n\, n-1 \cdots 21$). We do this choice of basis to obtain a transversal intersection and then use Claim 2.

If $|\lambda|+|\mu| = k(n-k)$ and $\lambda = \mu^\vee$ then we get a point. Otherwise you can show that $X_\lambda \cap \widetilde{X}_\mu = \varnothing$.

Pieri formula uniquely defines the multiplicative structure of the Schubert cells.

$$\sigma_\lambda \cdot \sigma_\mu = \sum_{\nu, |\nu|=|\lambda|+|\mu|} c^\nu_{\lambda\mu} \sigma_\nu,$$

where $c^\nu_{\lambda\mu}$ are the *Littlewood Richardson coefficients*. By the duality theorem $c^\nu_{\lambda\mu} =< \sigma_\lambda \cdot \sigma_\mu \cdot \sigma_{\nu^\vee} >$, i.e. $c_{\lambda\mu\nu} := c^{\nu^\vee}_{\lambda\mu} = \#\{X_\lambda \cap \widetilde{X}_\mu \cap \widetilde{\widetilde{X}}_\nu\}$. Then $c_{\lambda\mu\nu} \in \mathbb{Z}_{\geq 0}$ and these coefficients have S_3-symmetry.

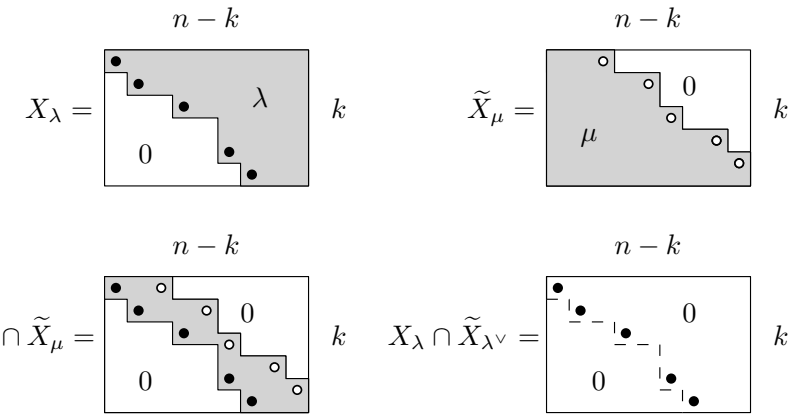

7.4 Honeycomb version of the Littlewood Richardson rule

This version was done by Knutson-Tao [5], it is a reformulation of a rule by Bernstein-Zelevinsky.

We work in the plane $\mathbb{R}^2 = \{(x,y,z) \in \mathbb{R}^3 \mid x+y+z = 0\}$. In this plane there are three types of lines $(a,*,*), (*,b,*)$ and $(*,*,c)$ where $a,b,c \in \mathbb{Z}$.

Theorem 7.7. $c^\nu_{\lambda\mu} = \#\{$*integer honeycomb with fixed boundary rays*$\}$.

If we know the rational lengths ℓ_i of the internal edges we can reconstruct the honeycomb.

We can rescale the honeycomb such that $\ell_i \in \mathbb{Z}_{\geq 0}$ and also $\lambda_1 + \lambda_2 = \lambda_1 - \lambda_2$ and the lengths on a hexagon should satisfy the *hexagon condition*

8 Lecture 8, 3/2/2012

Recall from last time that $H^*(\mathbf{Gr}(k,n,\mathbb{C}))$ has a linear basis of Schubert classes Ω_λ. In this lecture we will mention the relation between $H^*(\mathbf{Gr}(k,n,\mathbb{C}))$ and symmetric functions.

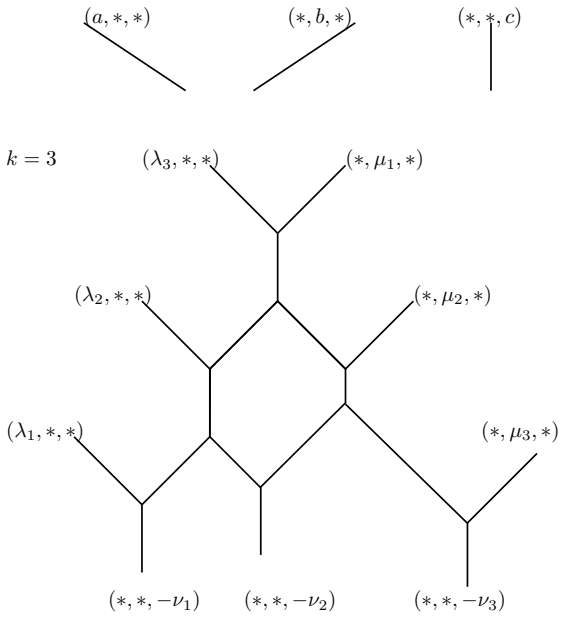

8.1 Symmetric functions

Let Λ be the ring of symmetric functions. We build this ring in the following way: let $\Lambda_k = \mathbb{C}[x_1,\ldots,x_n]^{\mathfrak{S}_k}$, the symmetric polynomials with k variables and let $\Lambda = \varprojlim \Lambda_k$.

- $e_r = \sum_{1\le i_1<i_2<\cdots<i_r} x_{i_1}x_{i_2}\cdots x_{i_r}$ (elementary symmetric functions)
- $h_r = \sum_{1\le j_1\le j_2\le\cdots\le j_r} x_{j_1}\cdots x_{j_r}$ (complete symmetric functions)

Theorem 8.1 (Fundamental theorem of symmetric functions)**.** $\Lambda = \mathbb{C}[e_1,e_2,\ldots] = \mathbb{C}[h_1,h_2,\ldots]$.

Another well known fact about Λ is it has a linear basis of Schur functions s_λ where λ is a partition $\lambda =$ 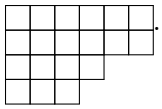 .

Definition 8.2. We give two equivalent definitions of the Schur functions.

- Given a partition $\lambda = (\lambda_1,\ldots,\lambda_k)$ let $\alpha = (\alpha_1,\ldots,\alpha_k) = (\lambda_1+k-1, \lambda_2+k-2,\ldots,\lambda_k+0)$.

$$s_\lambda(x_1,\ldots,x_k) = \begin{vmatrix} x_1^{\alpha_1} & x_2^{\alpha_1} & \cdots & x_k^{\alpha_1} \\ x_1^{\alpha_2} & x_2^{\alpha_2} & \cdots & \\ \vdots & \vdots & \ddots & \vdots \\ x_1^{\alpha_k} & x_2^{\alpha_k} & \cdots & x_k^{\alpha_k} \end{vmatrix} / \det(x_j^{k-i})$$

  then $s_\lambda = \lim_{k\to\infty} s_\lambda(x_1,\ldots,x_k)$.
- $s_\lambda = \sum_{T\in SSYT(\lambda)} x^T$ where $SSYT(\lambda)$ is the set of semistandard Young tableaux

$$T = \begin{array}{|c|c|c|c|c|c|c|}\hline 1&1&1&2&2&2\\\hline 2&2&3&3&4&7\\\hline 3&4&4&6\\\cline{1-4} 5&5&5\\\cline{1-3}\end{array}, \qquad x^T = x_1^3x_2^5x_3^3x_4^3x_5^3x_6x_7.$$

  In particular $e_r = s_{1^r}$ and $h_r = s_{(r)}$.

□

From the second definition of s_λ it is easy to see the following rule.

Theorem 8.3 (Pieri formula for s_λ)**.**

$$h_r \cdot s_\lambda = \sum_\mu s_\mu.$$

where μ are partitions such that μ/λ is a horizontal r-strip.

Equivalently $e_r \cdot s_\lambda = \sum_\mu s_\mu$ where μ/λ is a vertical r-strip.

Lemma 8.4. *Suppose that we have an associative bilinear operation $*$ on Λ such that $s_r * s_\lambda = \sum_\mu s_\mu$ where μ/λ is a horizontal r-strip, then $(\Lambda, *) \cong (\Lambda, \cdot)$.*

Proof. By the fundamental theorem we know that $(\Lambda, \cdot) = \mathbb{C}[h_1, h_2, \ldots]$, since $s_r = h_r$, the Pieri-type formula essentially says that $(\Lambda, *)$ has the same product of by the algebraically independent generators h_r as $(\Lambda, \cdot)$. □

Definition 8.5. Let $\Lambda_{k,n} = \Lambda / I_{k,n}$ where $I_{k,n} :=< s_\lambda \mid \lambda \not\subset k \times (n-k) >$. □

Exercise 8.6. *Show that $I_{n,k} =< e_i, h_j \mid i > k, j > n-k >$. Show that $s_\lambda \not\subset k \times (n-k)$ form a linear basis of $I_{n,k}$.*

Theorem 8.7. $H^*(\mathbf{Gr}(k,n)) \cong \Lambda_{k,n}$.

Proof. Define the map $\sigma_\lambda \mapsto s_\lambda$, $s_\lambda \cdot s_\mu = \sum_\nu c^\nu_{\lambda\mu} s_\nu$. □

8.2 Gleizer-Postnikov web diagrams

The Gleizer-Postnikov diagrams (GP-diagrams) defined in [3] involve four directions instead of the three directions of the Knutson-Tao puzzles. In the latter λ, μ and ν have k parts, and in the former λ and μ have k parts and ν has $k+\ell$ parts. Note that by convention $s_{(\lambda_1,\ldots,\lambda_k,0))} = s_{(\lambda_1,\ldots,\lambda_k)}$ and $s_\lambda = 0$ if some $\lambda_i < 0$.

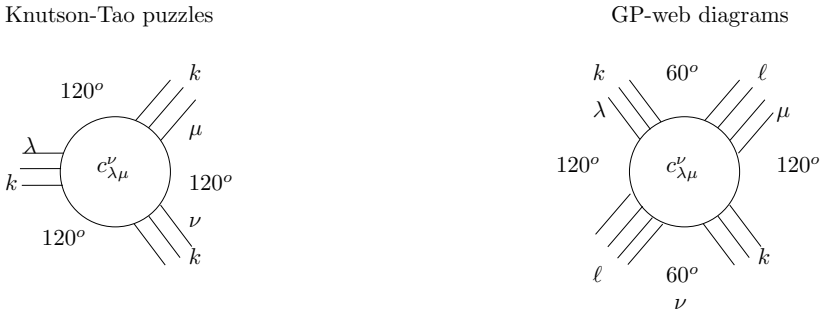

Figure 14: Schematic comparison of Knutson-Tao puzzles and Gleizer-Postnikov web diagrams.

The horizontal edge at a height c from the x-axis is labelled $c = 2h/\sqrt{3}$. The edges going from NW-SE and from NE-SW are labelled according to their x-intercepts. See Figure 15.

Example 8.8 ($k = \ell = 1$)**.** $s_r \cdot s_s = \sum_{c \geq r-s} s_{s+c, r-c}$. We have a conservation law: a flow of $r+s$ is coming in and coming out. See Figure 16.

□

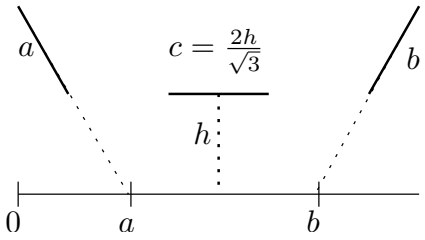

Figure 15: How to label the edges of a GP-web diagram.

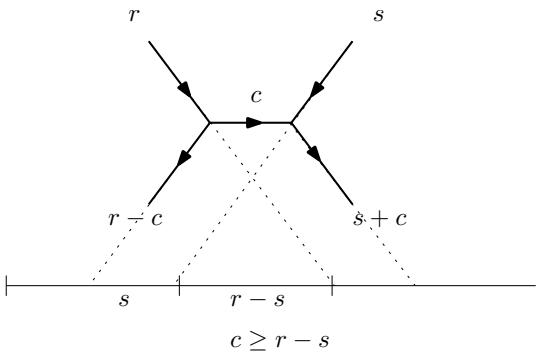

Figure 16: Example of GP-web diagrams for $k = \ell = 1$.

Theorem 8.9. *The Littlewood-Richardson coefficient $c^{\nu}_{\lambda\mu}$ is the number of web diagrams of type λ, μ and ν.*

Proof. Define $*$ product on Λ by $s_\lambda * s_\mu = \sum_\nu \#\{\text{web diagrams type } \lambda, \mu, \nu\} s_\nu$. Next we prove the Pieri rule for $*$-product.

For $\ell = 1$ we get interlacing $\nu_1 \geq \lambda_1 \geq \lambda_2 \geq \cdots \geq \nu_k \geq \lambda_k \geq \nu_{k+1}$ (see Figure 17). By conservation law $|\lambda| + \mu_1 = |\nu|$. This is equivalent to saying that ν/λ is a horizontal μ_1-strip. Conversely, given ν such that ν/λ is a horizontal μ_1-strip we can build a unique web diagram. The non-trivial part showing it is associative.

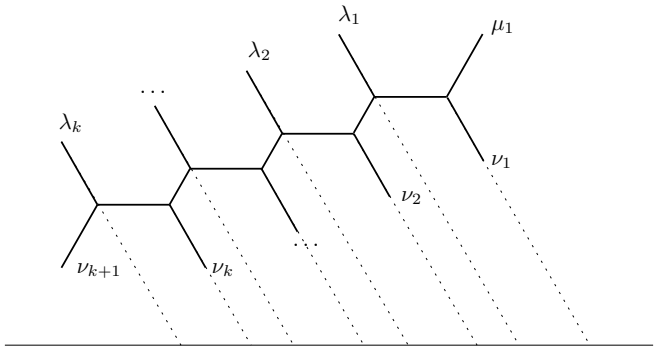

Figure 17: Illustration of the Pieri-rule for GP-web diagrams

□

Example 8.10. Let's verify that $c^{631}_{21,52} = 2$. See Figure 18

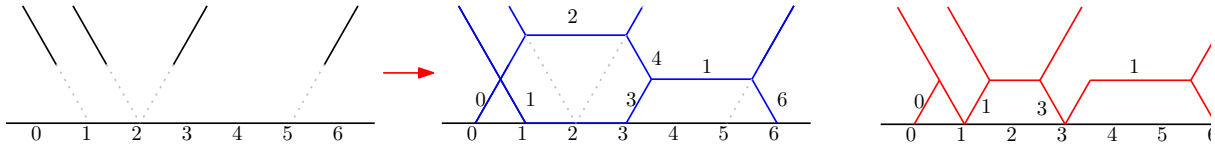

Figure 18: Example showing the two GP web diagrams when $\lambda = 21, \mu = 52$ and $\nu = 6310$.

□

Problem 8.11. *(Open) The GP-web diagrams with six directions are infinite. However with five directions the diagrams are finite. In this case, what is the analogue of the Littlewood-Richardson coefficients.*

9 Lecture 9, 3/7/2012

A permutation w is a bijection between $[n] \to [n]$. We multiply permutations from right to left. A simple transposition is a permutation $s_i = (i, i+1)$. We can write any w as a product of simple transpositions. A *reduced decomposition* is an expression of w as a product $s_{i_1} s_{i_2} \cdots s_{i_\ell}$ of simple transpositions of minimum possible length ℓ. The reduced decompositions of w are related by certain *moves*

$$s_i s_j = s_j s_i \quad |i-j| \geq 2, \text{(2-move)}$$
$$s_i s_{i+1} s_i = s_{i+1} s_i s_{i+1} \text{(3-move)}$$

9.1 Wiring diagrams

$$w = \begin{pmatrix} 1 & 2 & 3 & 4 & 5 \\ 3 & 2 & 5 & 1 & 4 \end{pmatrix}, \quad w = s_4 \underline{s_2 s_1 s_2} s_3.$$

We do not allow *triple intersections* and intersections occur at different heights.

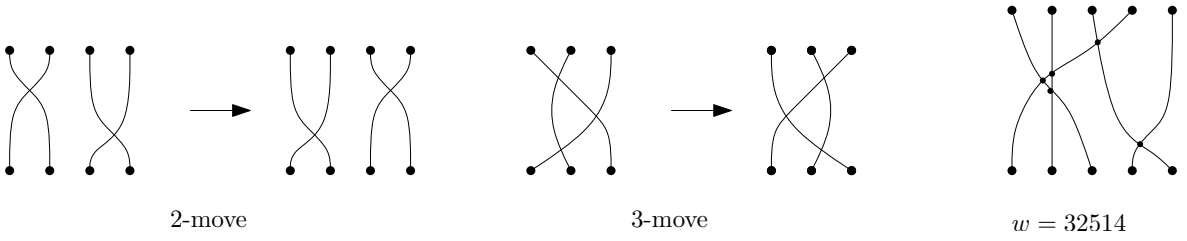

Figure 19: Illustration of 2 and 3-moves and of the wiring diagram of $w = 32514 = s_4 s_2 s_1 s_2 s_3$.

We want to transform the GP-web diagrams into wiring diagrams.
The number of such plane partitions are the Littlewood-Richardson rule.

Exercise 9.1. *Show that the classical Littlewood-Richardson rule corresponds to this rule in terms of plane partitions.*

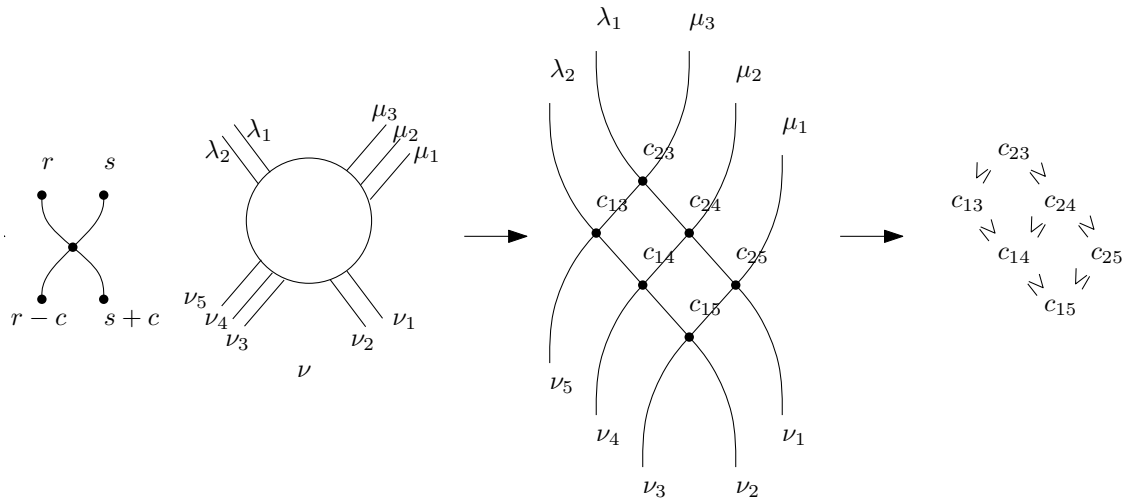

Figure 20: Illustration of how to transform a GP-web diagram into a wiring diagram.

If V is a vector space with basis $e_0, e_1, e_2, \ldots$ a **Scattering matrix** (R-matrix)

$$R(c) : V \otimes V \to V \otimes V, e_r \otimes e_s = \begin{cases} e_{s+c} \otimes e_{r-c} & \text{if } c \geq r - s, \\ 0 & \text{otherwise.} \end{cases}$$

where $e_{-i} = 0$ for $i > 0$. This corresponds to picture. (e_i are levels of excitement of particles and $R(c)$ describes how they interact)

Given a partition $\lambda = (\lambda_1, \ldots, \lambda_k)$ we map $s_\lambda \mapsto e_{\lambda_k} \otimes e_{\lambda_{k-1}} \otimes \cdots \otimes e_{\lambda_1} \in V^{\otimes k}$.

We define an operator $M_{k,\ell} : V^{\otimes k} \otimes V^{\otimes \ell} \to V^{\otimes (k+\ell)}$. Then $R_{ij}(c)$ is the operator on $V^{\otimes m}$ that acts as $R(c)$ on the ith and jth copies of V. Clearly $R_{ij}(c)$ commutes with $R_{\hat{i}\hat{j}}(c)$ if $\#\{i, j, \hat{i}, \hat{j}\} = 4$ (they act on four different copies of V).

Definition 9.2.

$$M_{k,\ell} = \sum_{(c_{ij})} \prod_{i=1,\ldots,k} \prod_{j=k+\ell,k+\ell-1,\ldots,k+1} R_{ij}(c_{ij}),$$

where the sum is over (c_{ij}) such that $c_{ij} \geq c_{i'j'} \geq 0$ whenever $i' \leq i < j \leq j'$. □

For example $M_{23} = \sum R_{15}(c_{15})R_{14}(c_{14})R_{13}(c_{13})R_{25}(c_{25})R_{24}(c_{24})R_{23}(c_{23})$ (you can choose any linear extension of the poset - such number is the number of Young Tableaux on the rectangle)

Theorem 9.3 (LR-rule: R-matrix version)**.** *Given $\lambda = (\lambda_1, \ldots, \lambda_k)$ and $\mu = (\mu_1, \ldots, \mu_\ell)$ then*

$$M_{k,\ell}(e_\lambda \otimes e_\mu) = \sum_{\nu=(\nu_1,\ldots,\nu_{k+\ell})} c^\nu_{\lambda,\mu} e_\nu.$$

The Pieri-rule is easy, the hard part is to show associativity: if $W = V^{\otimes k} \otimes V^{\otimes \ell} \otimes V^{\otimes m}$

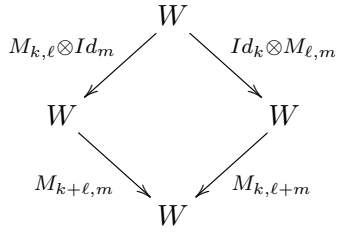

Proposition 9.4.

$$M_{k+\ell,m} \circ (M_{k,\ell} \otimes Id_m) = M_{k,\ell+m} \otimes (Id_k \otimes M_{\ell,m}).$$

R-matrices satisfy the **Yang-Baxter Equation** which depends on two parameters α, β:

$$R_{23}(\beta)R_{13}(\alpha+\beta)R_{12}(\alpha) = R_{12}(\alpha)R_{13}(\alpha+\beta)R_{23}(\beta).$$

These diagrams satisfy a generalized Yang-Baxter equation that depends on three parameters.

Proposition 9.5 (Generalized Yang-Baxter equation)**.**

$$R_{23}(c_{23})R_{13}(c_{13})R_{12}(c_{12}) = R_{12}(c'_{12})R_{13}(c'_{13})R_{23}(c'_{23}),$$

where

$$\begin{cases} c'_{12} = \min(c_{12}, c_{13} - c_{12}) \\ c'_{13} = c_{12} + c_{23} \\ c'_{23} = \min(c_{23}, c_{13} - c_{12}). \end{cases}$$

when $c_{13} = \alpha + \beta$ it reduces to the classical Yang-Baxter equation.

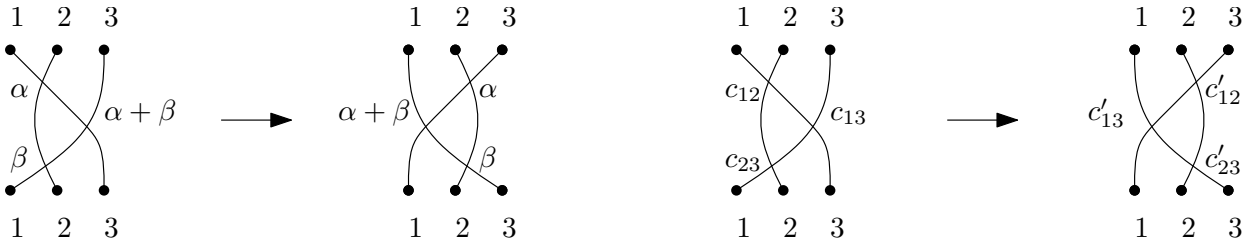

Yang-Baxter equation

Generalized Yang-Baxter equation

Figure 21: Illustration of the Yang Baxter equation and the generalized Yang Baxter equation.

Exercise 9.6. *Prove this generalized Yang-Baxter equation.*

This Generalized Yang-Baxter takes the wiring diagram with c_{ij} to an expression with c'_{ij}. The important point is to show that the inequalities on c_{ij} get translated to the inequalities on c'_{ij}.

To finish this prove we need to generalize this transformation of inequalities to arbitrary wiring diagrams.

9.2 String cone

[$\star\star\star$ This part needs polishing $\star\star\star$]

Let D be any wiring diagram for some reduced decomposition $w = s_{i_1} \cdots s_{i_\ell}$.

Example 9.7. We start from a wiring diagram of $w = 4213 = s_2 s_3 s_2 s_1$ and obtain a bipartite graph (see Figure 22). □

We switch directions of some edges such that strands $L_1, L_2, \ldots, L_i$ are directed down and $L_{i+1}, \ldots, L_n$ are directed up.

$G_{D,i}$ look at directed path P from L_{i+1} to L_i, each path gives an inequality: sum of weights of edges in graph ≥ 0.

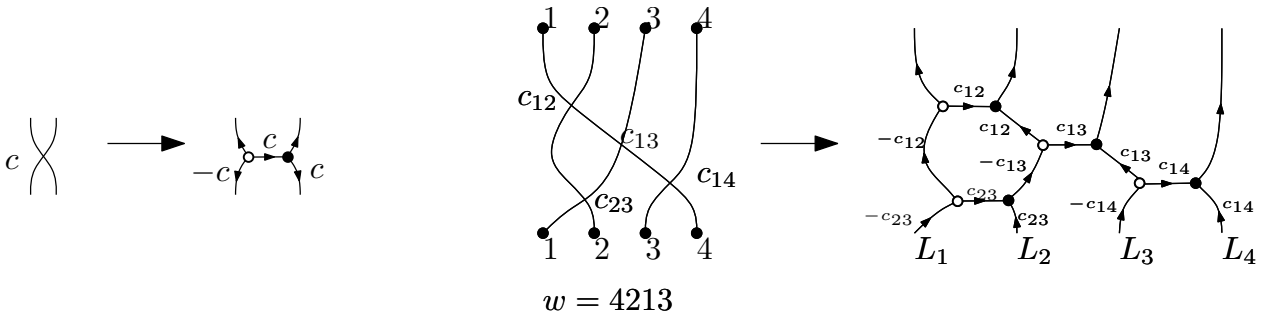

Figure 22: Illustration of how to obtain a bipartite graph from a wiring diagram of $w = 4213$.

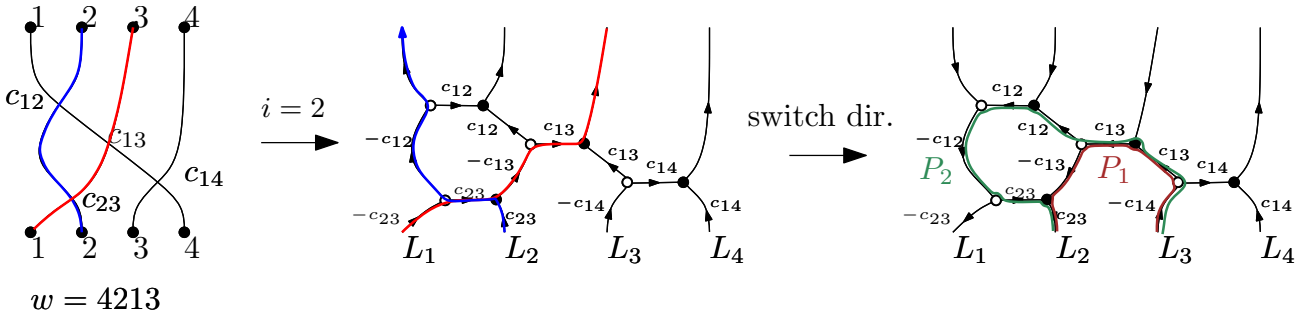

Figure 23: (a) In the bipartite graph obtained from a wiring diagram of $w = 4213$ we switch the directions of the edges of the strands L_1 and L_2 so that they are directed down and L_3 and L_4 are directed up. (b) Paths from L_3 to L_2 in the bipartite graph obtained from a wiring diagram of $w = 4213$ after switching directions of the strands L_1 and L_2.

Example 9.8. Continuing from Example 9.7. For $i = 2$, there are two paths $P : L_3 \to L_2$ with the convention that $c_{ij} = -c_{ji}$. See Figure 23.

From the first path P_1, we obtain the inequality $c_{41} + (c_{13} - c_{13} + c_{13}) - c_{23} \geq 0$ which simplifies to $c_{41} + c_{13} + c_{32} \geq 0$. Form the second path P_2, we obtain the inequality $c_{41} + (c_{13} - c_{13}) + (c_{12} - c_{12} + c_{12}) + (c_{23} - c_{23}) \geq 0$ which simplifies to $c_{41} + c_{12} \geq 0$. □

Claim This cone is what we really need. Every time we apply a 3-move and transform parameters by the Generalized Yang-Baxter equation then the cone for one diagram transforms to the cone of the diagram we obtain ... transform as needed. (piecewise linear continuous map)

If we have a wiring diagram for the associativity these inequalities become very simple (we get the plane partition inequalities)

10 Lecture 10, 3/9/2012

How about showing $*$-product is commutative. We know that associativity with Pieri rule shows that $*$-product of Schur functions is equivalent to normal product of Schur functions (which are commutative). Surprisingly, there is no direct way to see commutativity from the $*$-product picture.

10.1 Symmetries of Littlewood-Richardson coefficients

$c^{\nu}_{\lambda\mu} := c_{\lambda\mu\nu^\vee}$ has S_3 symmetry. It is not clear how to see this symmetry from the KT honeycomb.

Also $c^{\nu}_{\lambda\mu} = c^{\nu'}_{\lambda'\mu'}$ where λ' is the conjugate partition. There is a reformulation of KT honeycombs in terms of puzzles that makes this symmetry explicit.

Also $c^{\nu}_{\lambda\mu} = c^{\nu}_{\mu\lambda}$ and this is related to the *Schützenberger involution*. An interesting open question is to understand this symmetry in the $*$-product setting (using Yang-Baxter equation...).

10.2 Total positivity

An $m \times n$ matrix is called **totally positive** or **TP** (**totally nonnegative** or **TNN** respectively) if every minor is > 0 (≥ 0 respectively).

Example 10.1.

$$\begin{bmatrix} a & b \\ c & d \end{bmatrix}, a, b, c, d \geq 0, ad - bc > 0.$$

□

The following Lemma relates total positivity with combinatorics.

Lemma 10.2 (Lindström Lemma)**.** *Let G be a finite acyclic directed graph with weights x_e on edges and selected vertices: $A_1, \ldots, A_n, B_1, \ldots, B_n$. Define $M = (M_{ij})$ where $M_{ij} = \sum_{p:A_i \to B_j} \prod_{e \in P} x_e$. Then*

$$\det(M) = \sum_{(P_1,\ldots,P_n), P_i : A_i \to B_{w(i)}} (-1)^{sgn(w)} \prod_{i=1}^{n} \prod_{e \in P_i} x_e,$$

where $(P_1, \ldots, P_n)$ are families of non-crossing *paths connection the As and Bs. Where non-crossing means that no pair of paths P_i and P_j have a common vertex.*

Remark 10.3. If we sum over all paths without the restriction that they are non-crossing we just get a restatement of the definition of the determinant. □

Example 10.4.

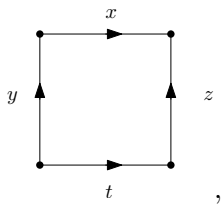

$$, \qquad M = \begin{bmatrix} x + ytz & yt \\ tz & t \end{bmatrix}, \quad \det(M) = (x + ytz)t - yt \cdot tz = xt.$$

□

Proof.

$$\det(M) = \sum_{w \in \mathfrak{S}} (-1)^{sgn(w)} \prod_i M_{i,w(i)} = \sum_{(P_1,\ldots,P_n), P_i : A_i \to B_{w(i)}} (-1)^{sgn(w)} \prod_{i=1}^{n} \prod_{e \in P_i} x_e,$$

for any family of paths connecting As with Bs. Next we use the *Involution principle*. We build a sign-reversing involution φ on families $(P_1, \ldots, P_n)$ with a crossing. Find the min. P_i that intersects a path and find first point c on P_i that intersects a path. On that path find the minimal P_j that passes through c.

We claim that this map is an involution, it preserves the weight of the path but reverses sign. □

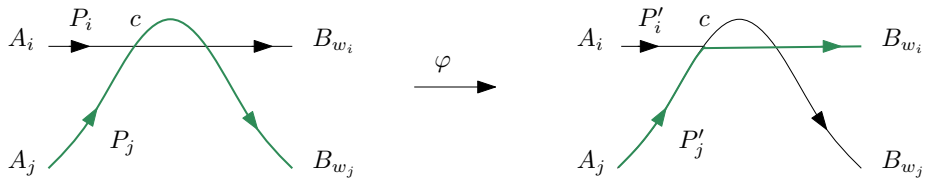

Figure 24: Illustration of sign reversing involution φ in the proof of Lindström Lemma.

A special case of this Lemma is related to positivity.

Corollary 10.5. *If G is a plane graph (embedded in a disk, see Figure 25) $A_1, \ldots, A_m$ are on the left-hand side of the boundary of the disk and $B_1, \ldots, B_n$ are on the right-hand side (ordered from top to bottom). Assume edge weights $x_e > 0$, then the matrix $M = (M_{ij})$ is totally nonnegative.*

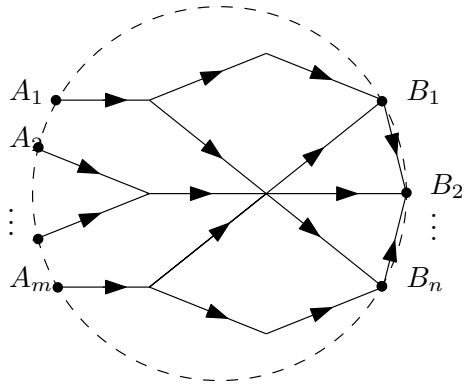

Figure 25: Plane graph G. If $x_e > 0$, then the matrix M of Lindström's Lemma is TNN.

Proof. Lindström Lemma implies that any minor is given by a nonnegative expression. That is, if graph is planar all signs associated to noncrossing paths are positive. □

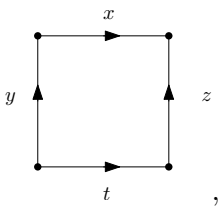

, $\quad M = \begin{bmatrix} x+ytz & yt \\ tz & t \end{bmatrix}, \quad x, y, t, z > 0 \quad \det(M) = (x+ytz)t - yt \cdot tz = xt > 0.$

Thus M is totally positive. Moreover, all 2×2 totally positive matrix can be written uniquely in this way.

Claim: Any TNN matrix has this form (but not in a unique way).

The following is based on the work of Bernstein-Fomin-Zelevinsky related to previous results by Lusztig. Assume that $m = n$ and that $M \in \mathbf{GL}_n$. Recall the LUD-decomposition $M = LUD$ where L is lower triangular with ones on the diagonal, D is a diagonal matrix, and U is upper triangular with ones on the diagonal.

It is well known that M is TNN if and only if L, U, D are TNN. So our first goal is to understand TNN upper triangular matrices. Let U_n be upper-triangular unipotent subgroup of $\mathbf{GL}_n$. The strata of the TNN part of U_n correspond to permutations $w \in S_n$.

Example 10.6. $n = 2$, $\begin{bmatrix} 1 & x \\ 0 & 1 \end{bmatrix}$ where $x \geq 0$. There are two possibilities: $x = 0$ in which case we get the identity. If $x > 0$ we get the matrix $\begin{bmatrix} 1 & x \\ 0 & 1 \end{bmatrix}$. Given w, we write its wiring diagram (now drawn from left to right). See Figure 26 for an example of this correspondence for $\mathfrak{S}_2$ (in this case we are not using the fact that the graph we obtain from the wiring diagram is bipartite, this property will be important later).

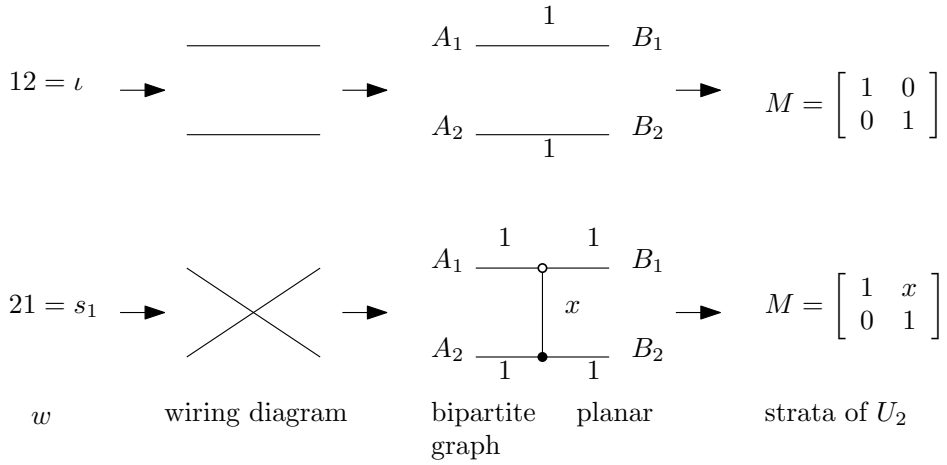

Figure 26: How permutations in S_2 correspond to strata of the TNN part of U_2.

□

For $w \in S_n$ pick any reduced decomposition $w = s_{i_1} \cdots s_{i_\ell}$. Next we decompose M into a product of certain elementary matrices. We illustrate this with an example.

Example 10.7. For $w = \begin{pmatrix} 1 & 2 & 3 & 4 \\ 4 & 2 & 1 & 3 \end{pmatrix} = s_1 s_3 s_2 s_1$, we have

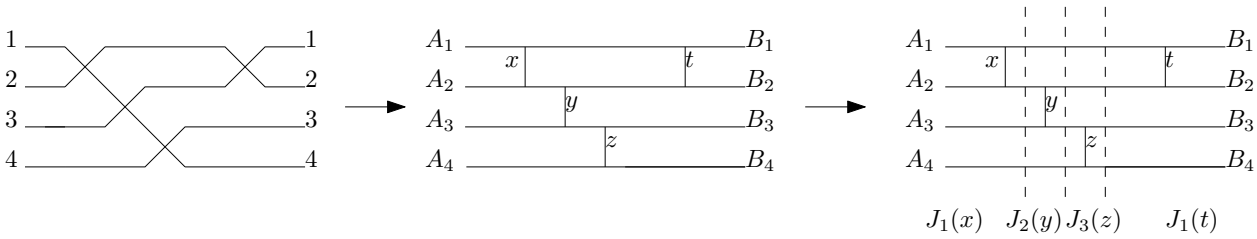

Figure 27: Example of Bruhat cell.

$$M = J_1(x)J_2(y)J_3(z)J_1(t) = \begin{bmatrix} 1 & x & & \\ & 1 & & \\ & & 1 & \\ & & & 1 \end{bmatrix} \begin{bmatrix} 1 & & & \\ & 1 & y & \\ & & 1 & \\ & & & 1 \end{bmatrix} \begin{bmatrix} 1 & & & \\ & 1 & & \\ & & 1 & z \\ & & & 1 \end{bmatrix} \begin{bmatrix} 1 & t & & \\ & 1 & & \\ & & 1 & \\ & & & 1 \end{bmatrix}$$

The matrices $J_i(x)$ are called **elementary Jacobi matrices**. □

Lemma 10.8. *If $s_{i_1} \cdots s_{i_\ell}$ is a reduced decomposition of w, the set of matrices $\{J_{i_1}(x_1) \cdots J_{i_\ell}(x_\ell) \mid x_1, \ldots, x_\ell > 0\}$ depend only on the permutation w.*

Proof. Seeing that the set of matrices does not change under a 2-move is easy. For 3-moves (see Figure 28) we do the following:

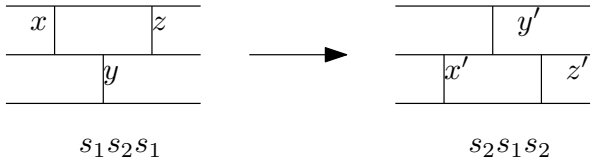

Figure 28: 3-move.

$$M = J_1(x)J_2(y)J_1(z) = \begin{bmatrix} 1 & x+z & xy \\ 0 & 1 & y \\ 0 & 0 & 1 \end{bmatrix} = \begin{bmatrix} 1 & y' & y'z' \\ 0 & 1 & x'+z' \\ 0 & 0 & 1 \end{bmatrix}$$

Thus we obtain the system of equations

$$\begin{array}{ccc} y' & = x+z & \\ x'+z' & = y & \Rightarrow \\ y'z' & = xy & \end{array} \quad \begin{array}{ll} y' & = x+z \\ z' & = \frac{xy}{x+z} \\ x'' & = y - \frac{xy}{x+z} = \frac{yz}{x+z}. \end{array}$$

Note that the solutions are *subtraction-free*. This means that for positive x, y, z we obtain a unique positive solution x', y', z'.

□

11 Lecture 11, 3/14/12

Question 11.1. *What is the number of potential nonzero minors of an upper triangular matrices (including the "empty" minor)? Why is it the Catalan numbers $C_n = \frac{1}{n+1}\binom{2n}{n}$.*

Example 11.2. For $n = 1$ there are 2 minors, for $n = 2$ there are five minors, for $n = 3$ there are 14 such minors. □

Exercise 11.3. *Answer the question above and explain what is the refinement of Catalan numbers you get when you restrict to the size of the minor.*

Pick a reduced decomposition of $w = s_{i_1} \cdots s_{i_\ell}$. Then the **Bruhat cell** is $B_w = \{J_{i_1}(x_1)J_{i_2}(x_2) \cdots J_{i_\ell}(x_\ell) \mid x_1, \ldots, x_\ell > 0\}$ where $J_i(x)$ is the $n \times n$ upper triangular matrix with ones on the diagonal, the $(i, i+1)$ entry is x and the other entries are 0.

$$J_i(x) = \begin{bmatrix} 1 & & & & \\ & 1 & & x & \\ & & \ddots & & \\ & & & 1 & \end{bmatrix}$$

See Figure 27 for an Example of a Bruhat cell. We also showed:

Lemma 11.4. *B_w depends only on w (not on its reduced decomposition).*

11.1 Bruhat order

Definition 11.5. The **(strong) Bruhat order** on $\mathfrak{S}_n$ is the partial order on permutations with covering relations $u \lessdot w$ such that

1. $u = w(i,j)$
2. $\ell(u) + 1 = \ell(w)$.

Equivalently, $u \leq w$ if any (or *some* for another equivalent definition) reduced decomposition for $w = s_{i_1} \cdots s_{i_\ell}$ contains a subword $s_{j_1} \cdots s_{j_r}$ which is a reduced decomposition for u. □

Note that it is not true that you can pick a reduced decomposition of u and add reflections to obtain a reduced decomposition of w. [⋆ ⋆ ⋆ give an example of this ⋆ ⋆ ⋆] See Figure 29 for the Hasse diagram of the Bruhat order in $\mathfrak{S}_3$.

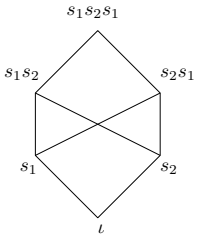

Figure 29: The strong Bruhat order in $\mathfrak{S}_3$.

Theorem 11.6 (Bernstein-Fomin-Zelevinsky)**.**

1. *The TNN of U_n decompose as $\coprod_{w \in \mathfrak{S}_n} B_w$,*
2. *$B_w \cong \mathbb{R}^\ell_{>0}$ where $\ell = \ell(w)$, and the isomorphism is $J_{i_1}(x_1) \cdots J_{i_\ell}(x_\ell) \mapsto (x_1, x_2, \ldots, x_\ell)$.*
3. *The closure $\overline{B}_u \subseteq \overline{B}_v$ if and only if $u \leq w$ in the strong Bruhat order.*

Remark 11.7. To start seeing why part 2. of the theorem above is related to the Bruhat order if $x_i = 0$ then $J_{i_j}(0) = I$ is the identity matrix. This is analogous to considering subwords (one has to check that in the closure we get $x_i \geq 0$). □

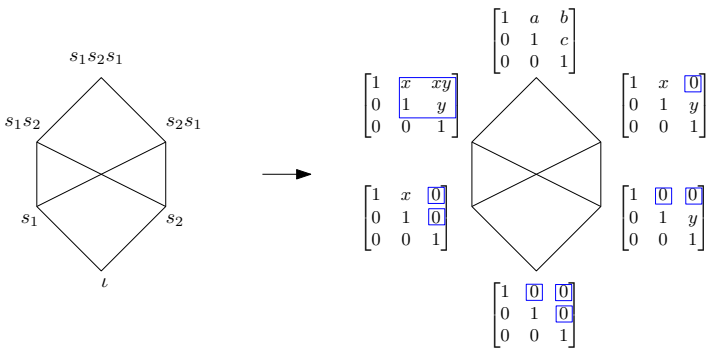

Figure 30: Illustration of correspondence between w in the Bruhat order of $\mathfrak{S}_3$ and TNN upper-triangular matrices. The zero minors are in a blue square.

Question 11.8. *How about the whole of* $\mathbf{GL}_n$*?*

11.2 Fomin-Zelevinsky double wiring diagrams and double Bruhat cells

We take two permutations u and w and *shuffle* two reduced decompositions of these permutations.

Example 11.9. $u^{-1} = s_1 s_2$ and $w^{-1} = s_2 s_3 s_1$.

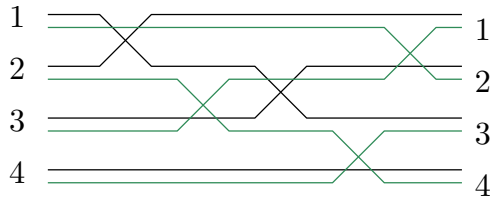

Figure 31: Example of double wiring diagram.

□

We can convert these double wiring diagrams into **trivalent graphs** as shown in Figure 32.

We have two types of Jacobi matrices $J_i(x)$ (x on the $(i, i+1)$ entry) as before and $J_{\bar{i}}(x)$ which is the identity matrix and x on the $(i+1, i)$ entry. We get an analogous decomposition as in the case of single Bruhat cells.

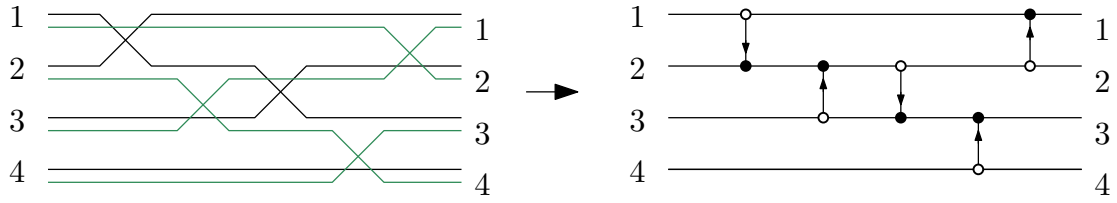

Figure 32: Going from double wiring diagram to trivalent graph.

Example 11.10. Continuing from Example 11.9, $M = J_1(x_1)J_{\bar{2}}(x_2)J_2(x_3)J_{\bar{3}}(x_4)J_{\bar{1}}(x_5)$. □

Definition 11.11. For $u, w \in \mathfrak{S}_n$ with reduced decompositions $u = s_{i_1} s_{i_2} \cdots s_{i_{\ell(u)}}$ and $w = s_{j_1} s_{j_2} \cdots s_{j_{\ell(w)}}$ the **double Bruhat cell** is

$$B_{u,w} = \{J_{i_1}(x_1)J_{\overline{j_1}}(t_1)J_{i_1}(x_2)J_{\overline{j_1}} \cdots \operatorname{diag}(t_1, t_2, \ldots, t_n) \mid x_1, x_2, \ldots, x_{\ell(u)}, t_1, t_2, \ldots, t_{\ell(w)} > 0\}$$

. □

Theorem 11.12 (Lusztig, Fomin-Zelevinsky)**.**

1. *The TNN of* $\mathbf{GL}_n$ *decompose as* $\coprod_{u,w \in \mathfrak{S}_n} B_{u,w}$,
2. $B_{u,w} \cong \mathbb{R}_{>0}^{\ell(u)+\ell(w)+n}$, *and the isomorphism is* $J_{i_1}(x_1) \cdots J_{i_\ell}(x_\ell) \mapsto (x_1, x_2, \ldots, x_{\ell(u)}, t_1, t_2, \ldots, t_{\ell(w)})$.
3. *The closure* $\overline{B}_{u,w} \subseteq \overline{B}_{v,z}$ *if and only if* $u \leq v$ *and* $w \leq z$ *in the strong Bruhat order.*

11.3 Totally nonnegative Grassmannian

Definition 11.13. $\mathbf{Gr}_{\geq 0}(k, n, \mathbb{R})$ are the elements in $\mathbf{Gr}(k, n, \mathbb{R})$ such that all Plücker coordinates $\Delta_I \geq 0$ (we use only maximal minors). □

In this setting the matroid strata are

$$S_{\mathcal{M}}^{>0} = \{A \in \mathbf{Gr}(k,n) \mid \Delta_I(A) > 0 \text{ for } I \in \mathcal{M}, \Delta_J(A) = 0 \text{ for } J \notin \mathcal{M}\}.$$

We also have that $\mathbf{Gr}_{\geq 0}(k,n) = \coprod_{\mathcal{M}} S_{\mathcal{M}}^{>0}$.

Recall that for $\mathbf{Gr}(k,n)$ the matroid stratification can get complicated (recall Lecture 2, Mnëv's Universality Theorem,...) but the TNN Grassmannian has a "nice" stratification.

11.4 Relation to classical total positivity

Let B be a $k \times (n-k)$ matrix. From this matrix we obtain a $k \times n$ matrix A such that there is a one-to-one correspondence between minors of B (of all sizes) and maximal minors of A (and with the same sign).

$$B = \begin{bmatrix} b_{11} & \cdots & b_{1\,n-k} \\ \vdots & & \vdots \\ b_{k1} & \cdots & b_{k\,n-k} \end{bmatrix}, \quad A = \left[\begin{array}{ccccc|cccc} 1 & & & & & \pm b_{k1} & \pm b_{k2} & \cdots & \pm b_{k\,n-k} \\ & \ddots & & & & & & \cdots & \\ & & 1 & & & b_{31} & b_{32} & \cdots & b_{3\,n-k} \\ & & & 1 & & -b_{21} & -b_{22} & \cdots & -b_{2\,n-k} \\ & & & & 1 & b_{11} & b_{12} & \cdots & b_{1\,n-k} \end{array}\right]$$

So the classical total positivity embeds on the TNN Grassmannian. Moreover, there is a symmetry feature in the latter (take first column and place it at the end and change sign by $(-1)^{k-1}$. This operation does not change the TNN Grassmannian. There is no such operation in the classical setting.

12 Lecture 12, 3/16/2012

$\mathbf{GL}_k^{\geq 0}$ embeds to a part of $\mathbf{Gr}_{\geq 0}(k,2k)$ where $\Delta_{12\ldots k} > 0$ and $\Delta_{k+1,\ldots,2k} > 0$. A double Bruhat cell $B_{u,v}$ in $\mathbf{GL}_k^{\geq 0}$ corresponds to some special cells $S_{\mathcal{M}}^{>0}$ that we will soon see.

Proposition 12.1 (cyclic symmetry)**.** *Given a matrix $A = [v_1, \ldots, v_n]$ that represents a point in $\mathbf{Gr}(k,n)$, if $\widetilde{A} = [v_2, \ldots, v_n, (-1)^{k-1}v_1]$ then the maximal minors of the latter are the same (and with the same sign) as the maximal minors of A. That is, $A \in \mathbf{Gr}_{\geq 0}(k,n) \Leftrightarrow \widetilde{A} \in \mathbf{Gr}_{\geq 0}(k,n)$. So there is an action of the cyclic group $\mathbb{Z}/n\mathbb{Z}$ on $\mathbf{Gr}_{\geq 0}(k,n)$.*

Example 12.2. $\mathbf{Gr}(1,n) \cong \mathbb{P}^{n-1} = \{(a_1 : \cdots : a_n)\}$. Then $\mathbf{Gr}_{\geq 0}(1,n) = \{(a_1 : \ldots, : a_n) \mid a_i \geq 0\}$. See Figure 33 for a picture of $\mathbf{Gr}_{\geq 0}(1,3)$. $\mathbf{Gr}_{\geq 0}(1,n)$ is equivalent to the $n-1$ simplex. □

Example 12.3. For $k = 2$, For $\mathbf{Gr}_{\geq 0}(2,n)$ viewed in $\mathbb{R}^2$, we need $\Delta_{i\,i+1} = \det([v_i, v_{i+1}]) > 0$ so v_{i+1} is after v_i in counterclockwise order. So $\mathbf{Gr}_{\geq 0}(2,n)$ consists of vectors $v_1, \ldots, v_n$ ordered counterclockwise (see Figure 34). □

If $v_1 \parallel v_3$ then either $v_1 \parallel v_2 \parallel v_3$ or $v_1 \parallel v_4 \parallel v_3$ or $v_1 = 0$ or $v_3 = 0$. We represent these as point on the circle. If two vectors are parallel then we superimpose two points in a circle. If $v_i = 0$ we delete the point. We obtain a poset structure. The covering relation is either merging consecutive groups (which means we have two groups of vectors, the vectors in each group are parallel, we merge these two groups to be all parallel) or removing an element from a group that has more than one element (we have two or more vectors parallel in a group, we make any of these vectors equal to 0). The minimal elements are circles with two elements. So the poset of $\mathbf{Gr}_{\geq 0}(2,4)$ has six minimal elements and one maximal element. In general these posets have $\binom{n}{k}$ minimal elements. See Figure 35 for an example of part of the poset for $\mathbf{Gr}_{\geq 0}(2,4)$.

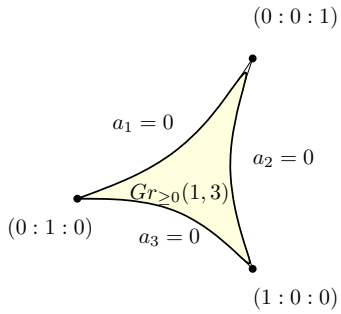

Figure 33: A picture of $\mathbf{Gr}_{\geq 0}(1,3)$.

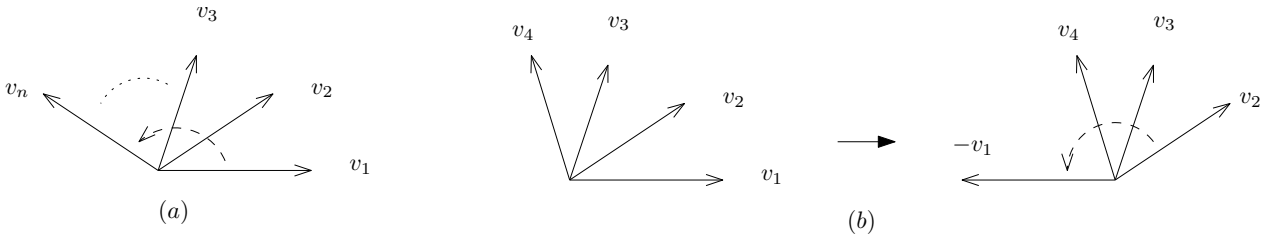

Figure 34: (a) Illustration of $\mathbf{Gr}_{\geq 0}(2,n)$. (b) cyclic symmetry of $\mathbf{Gr}_{\geq 0}(2,n)$.

12.1 Planar networks

We want to generalize the setup of double Bruhat cells for $\mathbf{GL}_n$. Let G be any directed graph drawn inside a disk with n boundary vertices (of degree 1) $b_1, \ldots, b_n$ on the boundary of the disk (sources or sinks) and with positive weights x_e on the edges. k is the number of boundary sources.

Example 12.4. Let G be the planar graph in Figure 36. The k-set of boundary sources is $I = \{1,2,3,6,7\}$, its complement $\overline{I} = \{4,5,8\}$ is the set of boundary sinks. □

We want to define boundary measurements M_{ij} for $i \in I$ and $j \in \overline{I}$ so that M_{ij} is the weighted sum over directed paths from b_i to b_j.

Example 12.5. Consider the planar network in Figure 37. The first guess for such a weighted sum would to weight each path as the product of the weights of the edges and take a sum of all such contributions.

$$M_{12}\text{"} = \text{"}xyzu + xyztyzu + xyztyztyzu + \cdots = \frac{xyzu}{1-yzt}$$

We could have a problem whenever $yzt = 1$. Instead we do an alternating sum

$$M_{12} = xyzu - xyztyzu + xyztyztyzu - \cdots = \frac{xyzu}{1+yzt}$$

Now we can pick any positive values of the parameters x, y, z, t, u. For instance, if $x = z = t = 1$ and $y = u = 2$ we get $M_{12} = \frac{1 \cdot 2 \cdot 1 \cdot 2}{1+2} = \frac{4}{3}$.

□

We count paths P with the sign $(-1)^{\#\text{loops in } P}$ where a loop means a closed directed path without self intersection. But how do we define such loops to count them? In the planar case we

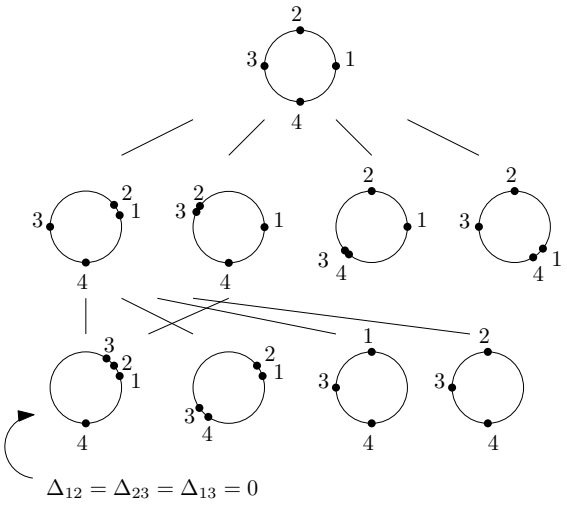

Figure 35: Part of the poset of $\mathbf{Gr}_{\geq 0}(2,4)$. The covering relation is either merging consecutive groups or removing an element from a group that has more than one element.

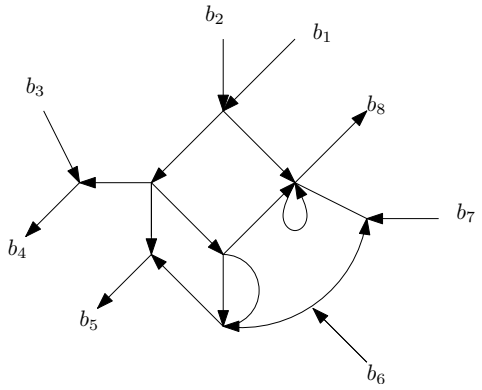

Figure 36: Example of planar network.

can define the **winded index** wind(P) to be the number of full turns of the tangent vector to P (counterclockwise is positive). Then wind(P) is the number of counterclockwise loops minus the number of clockwise loops.

Example 12.6. For the path P in Figure 38, the winded index $\text{wind}(P) = -1$. □

Exercise 12.7. *Is it true for any graph that the number of erased loops* (mod 2) *is a well defined?*

Definition 12.8 (Formal boundary meassurement)**.** Given formal variables x_e assigned to the edges $M_{ij}^{\text{form}} = \sum_{P:b_i \to b_j} (-1)^{\text{wind}(P)} \prod_{e \in P} x_e$. □

Lemma 12.9. *M_{ij}^{form} adds to a subtraction-free rational expression.*

Proof. Idea of the proof is to use *loop erased walks*, which is a deterministic way of erasing walks: we traverse the path and every time we self intersect we remove the loop from the path and continue. The path we end up with has no loops and we denote it by P' and call it the loop erased part

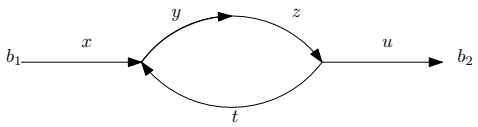

Figure 37: Illustration of path.

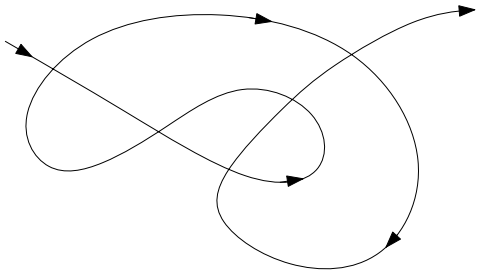

Figure 38: Path with winded index -1.

of P. The erased loops are $L_1, \ldots, L_r$ and we denote by $\mathrm{el}(P)$ the number of erased loops in this procedure. See Figure 39 for an example.

From $P \to P'$ where P' is the loop erased part of P where $L_1, \ldots, L_r$ are the erased loops. We denote by $\mathrm{el}(P)$ the number of erased loops in this procedure.

Now let G be any graph and select two vertices A and B

$$M_{AB}^G = \sum_{P:A\to B} (-1)^{\mathrm{el}(P)} \prod_{e\in P} x_e.$$

Lemma 12.10. *For any finite graph M_{AB} is a subtraction-free rational expression.*

□

Definition 12.11. The weighted sums M_{ij} are specializations of these subtraction-free expression to positive values of x_e. □

13 Lecture 13, 3/21/12

13.1 Loop-erased walks

Recall that by a *loop* we mean a closed directed path without self intersections. Recall also the notion of *loop-erased walk*. Let P be any directed path in any directed graph, the path P reduces to a loop erased path P', without self intersections, and loops $L_1, \ldots, L_r$. See Figure 39 for an example. Recall that $\mathrm{el}(P)$ is the number of erased loops.

Remark 13.1. Physicists think of undirected graphs and normally grids. There is a model called Loop-Erased-Random-Walk (LERW) model which gives same distribution as uniform random tree distribution (take a uniform random tree and pick two vertices, get unique path between them). □

Remark 13.2. In the planar case we defined $\mathrm{wind}(P)$ to be the number of counter-clockwise loops minus the number of clockwise loops. $\mathrm{wind}(P) \pmod{\mathrm{el}}(P) \pmod 2$ so $(-1)^{\mathrm{wind}(P)} = (-1)^{\mathrm{el}(P)}$. □

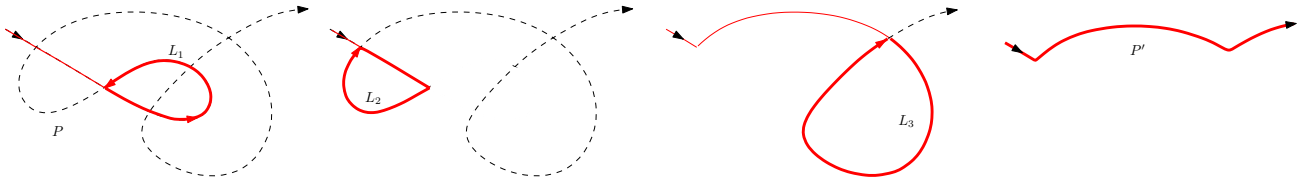

Figure 39: Example of loop erased walks.

Given a path P' without self intersections we want to describe all paths Ps with loop-erased part P'. We need to insert loops $L_r, L_{r-1}, \dots$ back. See Figure 40. The loop L'_1 we insert cannot intersect the path before A_1 and so on.

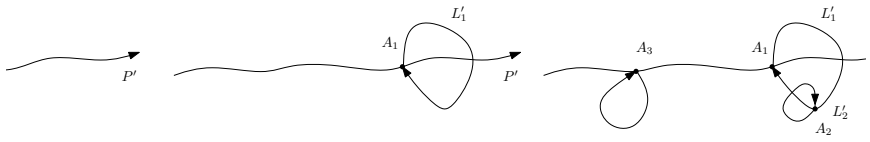

Figure 40: Illustration of how to insert loops to a path P' without self intersections.

To do this more systematically, given a path $P' = (v_1, \dots, v_{\mathrm{el}})$ without self intersections at each vertex vertex v_r we insert a closed path C_i from v_i to v_i that does not pass through $v_1, \dots, v_{i-1}$ (C_i can be empty, or have many self intersections). At the end we obtain a path P with $\mathrm{el}(P) = \sum \mathrm{el}(C_i)$.

Lemma 13.3. *Let G be any finite directed graph with formal edge variables x_e. For two vertices A and B of G we define*

$$M^G_{AB} := \sum_{P:A\to B} (-1)^{\mathrm{el}(P)} x_P,$$

where $x_P = \prod_{e\in P} x_e$ and the sum is over directed paths P from A to B. Then M^G_{AB} is a subtraction-free rational expression.

Proof. Assume G is connected. We will proceed by induction on $\#E(G) - \#V(G)$. The base case is -1 for trees which is easy to prove.

For the general case we first assume that is $A \neq B$

$$\begin{aligned} M^G_{AB} &= \sum_{P':A\to B} x_{P'} \prod_{i=1}^{\ell} \Big(\sum_{C_i} (-1)^{\mathrm{el}(C_i)} x_{C_i}\Big), \\ &= \sum_{P':A\to B} x_{P'} \prod_{i=1}^{\ell} M^{G_i}_{v_i,v_i}, \end{aligned}$$

where the sum is over directed paths $P' = (v_1, \dots, v_\ell)$ without self-intersections and $G_i = G\backslash\{v_1, \dots, v_{i-1}\}$. From this equation we see that the problem reduces to the case when $A = B$. For the inductive step we split the graph at vertex A. See Figure 41.

Note that $M^G_{AA} = 1 - M^{G'}_{A'B'} + (M^{G'}_{A'B'}) - \cdots = \frac{1}{1+M^{G'}_{A'B'}}$ where 1 comes from the empty path and the sign comes from the change of parity since when $A = B$ we get an additional loop. By induction $M^{G'}_{A'B'}$ is subtraction-free rational expression ($\#E(G') = \#E(G)$ but $\#V(G') = \#V(G) + 1$). $\square$

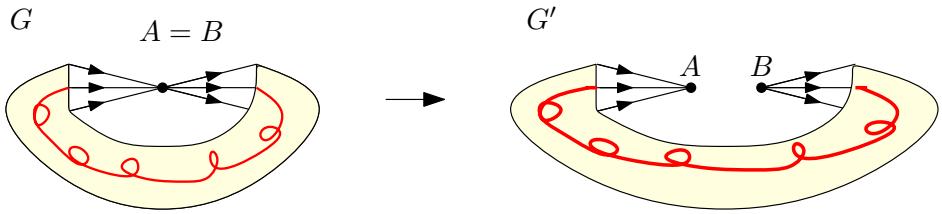

Figure 41: Illustration of Inductive step for proof of Lemma 13.3

Example 13.4. Let G be the graph with vertices A, B, C and D in Figure 42. Then

$$M^G_{AB} = x \cdot 1 \cdot M^{G_2}_{BB} + yz \cdot 1 \cdot M^{G_2}_{CC} \cdot M^{G_3}_{BB},$$

where $G_2 = G\backslash\{A\}$ and $G_3 = G\backslash\{A, C\}$. Now $M^{G_3}_{BB} = 1 - v + v^2 - \cdots = \frac{1}{1+v}$.

To calculate $M^{G_2}_{CC}$ we split G_2 at vertex C and obtain graph G'_2 and we obtain $M^{G'_2}_{C'_1C'_2} = z\frac{1}{1+v}tu$ and so $M^{G_2}_{CC} = 1/(1 + z\frac{1}{1+v}tu)$. To calculate $M^{G_2}_{BB}$ we split G_2 at vertex B and obtain graph $G''_2$and we obtain $M^{G''_2}_{B'_1B'_2} = v + tuz$ and so $M^G_{BB} = 1/(1 + v + tuz)$.

Putting everything together

$$M^G_{AB} = \frac{x}{1 + v + tuz} + \frac{yz}{1 + z\frac{1}{1+v}tu} \cdot \frac{1}{1+v},$$

which is a subtraction-free rational expression.

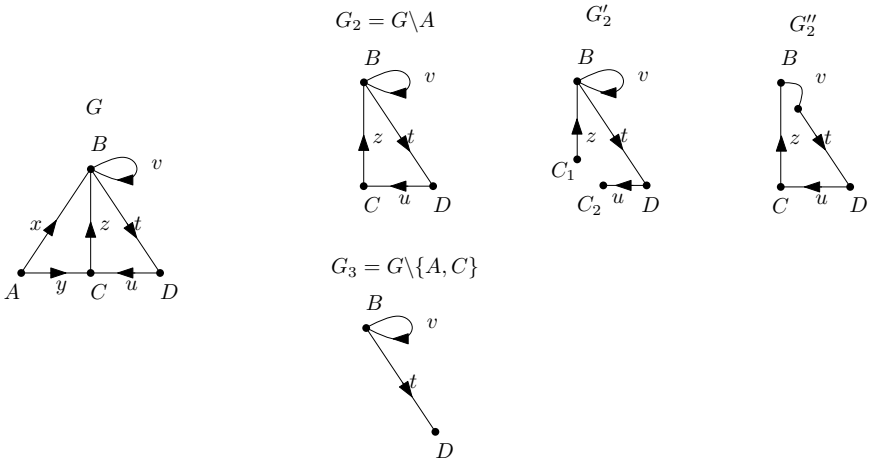

Figure 42: Example of how to calculate M^G_{AB}.

□

13.2 Boundary measurement map to $\mathbf{Gr}_{\geq 0}(k, n)$

Let G be a planar graph whose boundary vertices are $v_1, \ldots, v_n$. We let $I \subset [n]$ be the set of indices of the sources (v_i for $i \in I$ are sources) and $\overline{I}$ is the set of indices of sinks. We define M_{ij} is the signed sum over paths from v_i to v_j for $i \in I$ and $j \in \overline{I}$. This gives a $k \times (n-k)$ matrix.

We consider the following $k \times n$ matrix A: the $k \times k$ submatrix with columns indexed by I is the identity matrix. The rest of the entries are $\pm M_{ij}$ so that $\Delta_I(A) = 1$ and $\Delta_{(I\setminus i)\cup j}(A) = M_{ij}$. More explicitly, $I = \{i_1 < i_2 < \ldots < i_k\}$ where $A_{rj} = (-1)^t M_{i_r j}$ where t is the number of elements of I between i_r and j.

Example 13.5. For $n = 4$ and $k = 2$, let G be the graph illustrated in Figure 43. Then $I = \{1, 3\}$ and $\Delta_{12} = M_{32}, \Delta_{23} = M_{12}, \Delta_{14} = M_{34}, \Delta_{34} = M_{14}$. The matrix is

$$A = \begin{bmatrix} 1 & M_{12} & 0 & -M_{14} \\ 0 & M_{32} & 1 & M_{34} \end{bmatrix}.$$

□

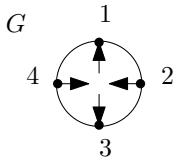

Figure 43: Illustration of planar graph with four boundary vertices two of which are sources.

The matrix A defines a point in $\mathbf{Gr}(k, n)$. We do not lose information about the boundary measurements M_{ij} since $M_{ij} = \frac{\Delta_{(I\setminus i)\cup j}}{\Delta_I}$ (the numerator does not make sense as a function in $\mathbf{Gr}(k, n)$ but rescaling it by Δ_I makes it work).

13.3 Boundary measurement map

The **boundary measurement map** is the map $M : \{\mathrm{G}\} \to \mathbf{Gr}(k, n)$ where G is a planar graph with k boundary sources, $n - k$ boundary sinks and positive edge weights x_e.

Theorem 13.6. *1. Image of M is $\mathbf{Gr}_{\geq 0}(k, n)$.*

2. Fix a graph G and think of M_G as the function that takes the edge weights $\mathbb{R}_{>0}^{\#E(G)}$ and maps it to $\mathbf{Gr}(k, n)$. $M_G : \cdot\mathbb{R}_{\geq 0}^{\#E(G)} \to \mathbf{Gr}(k, n)$. The image of M_G is a cell in $\mathbf{Gr}_{\geq 0}(k, n)$.

We can do the following simplifications that do not change the measurements M_{ij}:

1. We can remove all internal sources and sinks (the do not contribute to the measurements. So we can assume G has no such sources and sinks.
2. We can transform G into a 3-valent graph without changing M'_{ij}s

Can reduce to graphs with black and white vertices, the ones we got from the wiring diagrams. See Figure 44.

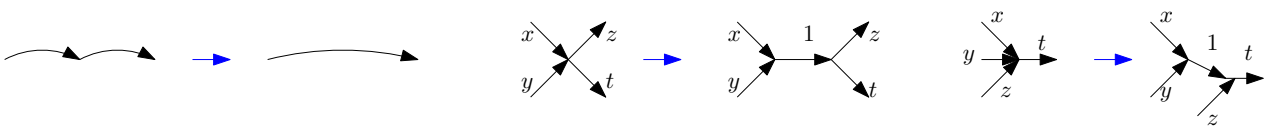

Figure 44: Illustration of simplifications.

14 Lecture 14, 3/23/2012

We continue with the simplification. Given a vertex of degree four we can transform it to a trivalent planar graph with the same measurements. In general you double weights of outgoing edges. See Figure 45. One obtains the same measurements, for example if we do the measurement from b_1 to b_2 in the degree four vertex we get xy. On the modified trivalent graph we obtain:

$$x(x_1 - x_1x_2x_3x_4x_1 + \cdots)2y = \left.\frac{x \cdot x1 \cdot 2y}{1 + x_1x_2x_3x_4}\right|_{x_1=x_2=x_3=x_4=1} = xy.$$

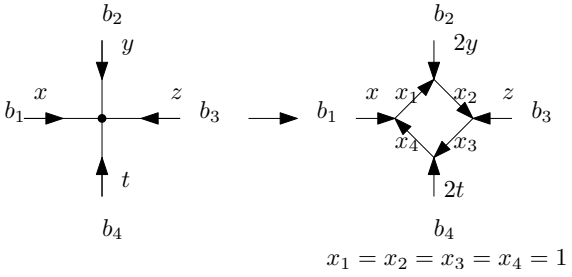

Figure 45: Illustration of how to simplify a 4-vertex.

Claim: we can transform any graph in to a planar trivalent graph.

We then color the vertices **white** if they have two outgoing edges and one incoming edge, and **black** if they have two incoming edges and one outgoing: 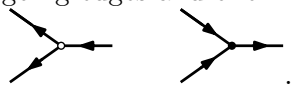 .

We can switch directions of some edges following the rules:

1. Switch direction and reverse the sign of weight.
2. Colors of vertices should not change.

Denote the graph you obtain by G'.

The next result states that even though the graph changes, the image under the map M in $\mathbf{Gr}(k, n)$ does not change.

Theorem 14.1. *$M(G) = M(G')$, that is we get the same point of $\mathbf{Gr}(k, n)$.*

Example 14.2. Consider the graphs G_1 and G_2 in Figure 46. For G_1 we get the matrix $A = [1\ x{+}y]$ ($I = \{1\}$). For G_1' we obtain $A' = [\frac{1}{x+y}\ 1]$ ($I' = \{2\}$) $M_{21} = x^{-1} - x^{-1}yx^{-1} + x^{-1}yx^{-1}yx^{-1} - \cdots = \frac{x^{-1}}{1+yx^{-1}}$. And A and A' are the same point of $\mathbf{Gr}(2, 1)$ (the signs are crucial).

For G_2, $I = \{1, 2\}$

$$A = \begin{bmatrix} 1 & 0 & -xzt & -xzy \\ 0 & 1 & yzt & yzu \end{bmatrix}$$

$\Delta_{13} = M_{23}, \Delta_{23} = M_{13}$. We choose a path from b_2 to b_3 and reverse to edges to obtain graph G_2'

$$A' = \begin{bmatrix} 1 & \frac{x}{y} & 0 & 0 \\ 0 & \frac{1}{tzy} & 1 & \frac{y}{t} \end{bmatrix}$$

A and A' represents the same point in $\mathbf{Gr}(2, 4)$.

□

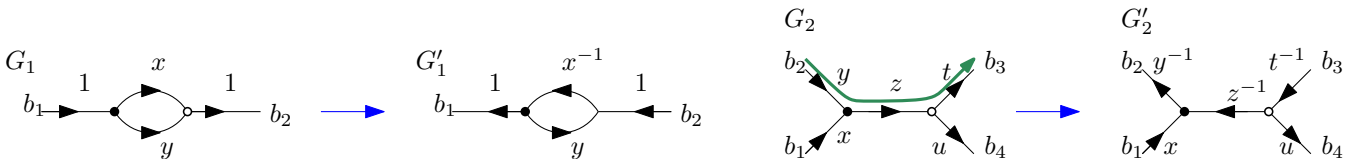

Figure 46: Planar graphs G_1 and G_2 and the graphs G_1' and G_2' obtained by reversing the directions of the edges of a path.

14.1 Plabic Graphs

Because of the previous theorem we do not care about the direction of the trivalent edges with solid and empty vertices. We consider such graphs.

A **plabic graph** (plabic is an abbreviation of planar bicolored graph) is an undirected graph with vertices colored in 2 colors. A **perfect orientation** is an orientation of edges such that the empty vertices have two outgoing edges and one incoming edge, and the solid vertices have two incoming edges and one outgoing. A plabic graph is **perfectly orientable** if the graph has a perfect orientation. See Figure 47 for examples.

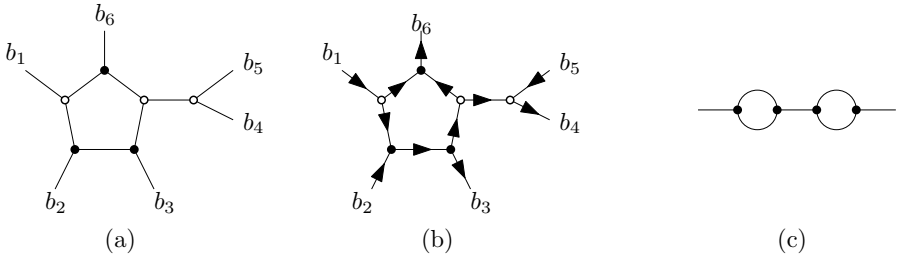

Figure 47: Examples of plabic graphs. (a) a perfectly orientable, (b) the perfect orientation of the graph in (a), and (c) a graph that is not perfectly orientable.

Now we prove that a perfectly orientable plabic graph corresponds to a cell in $\mathbf{Gr}(k,n)$ where n is the number of boundary vertices and we obtain k from the following relation.

Exercise 14.3. *Prove that if we have a perfectly orientable graph and pick one of its perfect orientations then* $k-(n-k) = \#$ *black vertices* $-\#$ *white vertices.*

There are necessary and sufficient conditions for a plabic graph to be perfectly orientable: for all induced subgraphs H of G we have $1 \leq \frac{\#V_\bullet(H)-\#V_\circ(H)}{2} \leq n$, where $\#V_\bullet$ and $\#V_\circ$ are the number of black and white vertices of the graph.

14.2 Gauge transformations

We can rescale the edge variables so that measurements don not change. We call these **gauge transformations** of the edge variables.

The number of essential parameters is $\#V(G) - \#E(G)$ the difference between the number of edges and the number of vertices. We know this is $\#F(G)-1$ where $\#F(G)$ is the number of faces of G. This indicates that it might be beneficial to have **face variables** and assign weights to these.

$f = xy^{-1}ztu^{-1}v$.

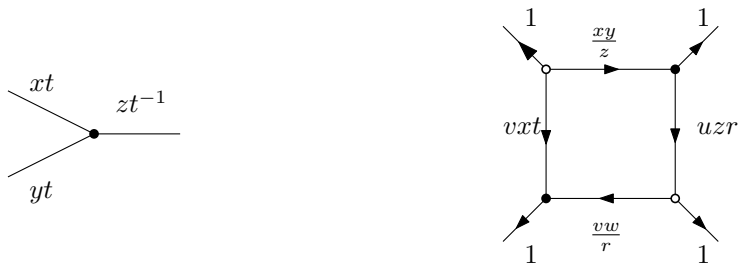

Figure 48: Illustration of Gauge transformations on directed planar graphs.

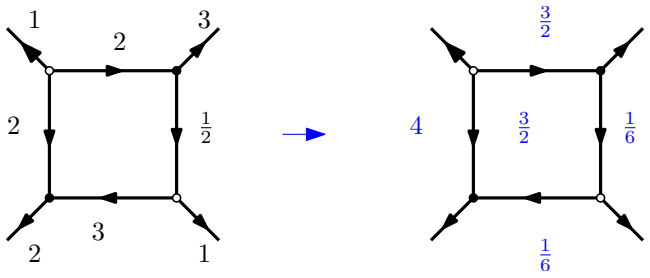

Figure 49: The edge and face variables of a graph.

Example 14.4. For the graph in Figure 49 we go from edge weights to face weights. □

Since each edge is in two faces with opposite orientation then the face variables satisfy the following relation $\prod_{\text{faces}} f = 1$.

Lemma 14.5. *One can reconstruct edge variables modulo the gauge transformations from the face variables modulo the relation* $\prod f = 1$.

From this Lemma we can redefine the map $M_G : \mathbb{R}_{>0}^{\#E(G)} \to \mathbf{Gr}(k,n)$ to a map $\widetilde{M}_{G'} : \mathbb{R}_{>0}^{\#F(G)-1} \to \mathbf{Gr}(k,n)$ where G' is a perfectly orientable plabic graph.

[⋆⋆⋆ something about top dimensional cells ⋆⋆⋆]

Example 14.6. If G is trivalent graph with one white vertex, it corresponds to $\mathbf{Gr}_{>0}(1,3)$ is 2-dimensional $\#F(G) - 1$. If H is the trivalent graph with one black vertex, it corresponds to $\mathbf{Gr}_{>0}(2,3)$ also 2-dimensional. For the graph G in Figure 48(b) corresponds to $\mathbf{Gr}_{>0}(2,4)$ it has dimension $k(n-k) = 4 = \#F(G) - 1$. □

15 Lecture 15, 4/6/2012

Recall the notions of a plabic graph G and a perfect orientation of such graphs. If G has n vertices and k is given by $k - (n-k) = \#V_\bullet - \#V_\circ$.

Exercise 15.1. *For any perfect orientation k is the number of boundary sources.*

Given a plabic graph with a perfect orientation we can build a boundary measurement map from G with variables $x_e > 0$ on the edges to a $k \times n$ matrix A that represents a point in $\mathbf{Gr}(k,n)$.

Also we can rescale the variables at each vertex such that the number of essential variables is $\#E(G) - \#V(G) = \#F(G) - 1$ where $\#F(G)$ is the number of faces of G. Sometimes it is more useful to work with face variables.

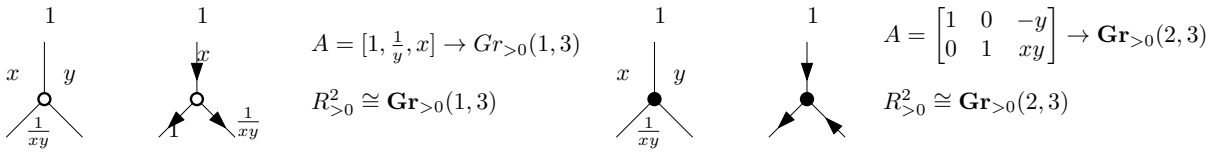

Figure 50: Example of a plabic graph G with a perfect orientation. We get a map between R^n to $\mathbf{Gr}(n,k)$ where n is the number of boundary vertices and $k-(n-k) = \#V_\bullet(G) - \#V_\circ(G)$.

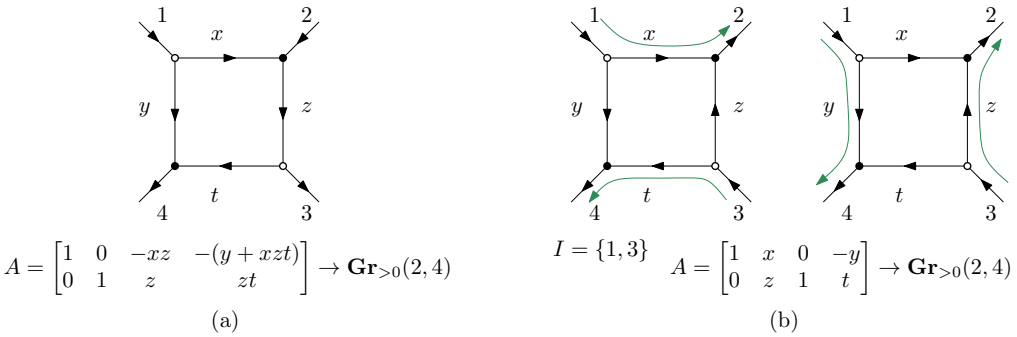

Figure 51: Example of a plabic graph G with a perfect orientation. We get a map between R^n to $\mathbf{Gr}(n,k)$ where n is the number of boundary vertices and $k-(n-k) = \#V_\bullet(G) - \#V_\circ(G)$.

Example 15.2. Let G be the plabic graph with a perfect orientation in Figure 51(a). We claim that the map $(x,y,z,t) \mapsto A$ is a bijection between $\mathbb{R}^4$ and $\mathbf{Gr}_>(2,4)$. We look at the minors: $\Delta_{12} = 1, \Delta_{13} = M_{23} = z, \Delta_{23} = M_{13} = xz, \Delta_{14} = M_{24} = zt, \Delta_{24} = M_{14} = y + xzt, \Delta_{34} = \begin{vmatrix} -xz & -(y+xzt) \\ z & zt \end{vmatrix} = -xz^2t + (y+xzt)z = yz$. We see all the minors are nonnegative. We will interpret $\Delta_{34} = yz$ as the product of nonintersecting paths.

□

Theorem 15.3. *Assume that G is acyclic let I be the set of boundary sources then A is a $k \times n$ matrix such that the columns indexed by I is an identity matrix and the other entries are $\pm M_{ij}$ such that $\Delta_{(I\setminus i)\cup j} = M_{ij}$. For any $J = (I\setminus\{i_1,\ldots,i_r\}) \cup \{j_1,\ldots,j_r\}$ we have that*

$$\Delta_J(A) = \sum \prod_{P_i} weight(P_i),$$

where the sum is over r noncrossing paths P_i connecting $b_{i_1},\ldots,b_{i_r}$ with $b_{j_1},\ldots,b_{j_r}$ (but not in that specified order).

Example 15.4. Let G be the plabic graph with a perfect orientation in Figure 51(b). The nontrivial minor is $\Delta_{24} = xt + yz$ and these correspond to paths between $I\setminus J$ with $J\setminus I$ (paths in green in Figure 51). □

Theorem 15.5. *For all plabic graphs G, $\Delta_J(A)$ is given by subtraction-free rational expression (a quotient of two positive polynomials) in the edge (or face) variables.*

For $\Delta_{(I\setminus i)\cup j} = M_{ij}$ we already know it is true. For any minor one can prove it by induction, however we will use Kelly Talaska's [8] simpler formula for $\Delta_J(A)$.

A **conservative flow** in G is a collection of vertex-disjoint directed cycles (w/o self crossings). We include in this definition the empty collection. See Figure 52(a) for an example.

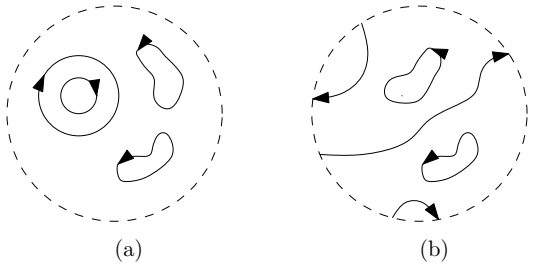

Figure 52: (a) Example of conservative flow in G, (b) example of a collection of vertex disjoint cycles and paths (without self-crossings).

A flow from $I\setminus J$ to $J\setminus I$ is a collection of vertex disjoint cycles and paths (w/o self crossings), that connect each source in $I\setminus J$ with a sink in $J\setminus I$. See Figure 52(b) for an example.

Theorem 15.6 (Talaska's formula)**.** *Fix I (set of boundary sources), for any J the corresponding minor $\Delta_J(A) = f/g$ such that f is the sum of weights of all flows from $I\setminus J$ to $J\setminus I$ and g is the sum of weights of all conservative flows.*

We give two examples of this result.

Example 15.7. Consider the graph G with $n = 6$ vertices in Figure 53 with a perfect orientation, then the set of boundary sources is $I = \{2, 3, 6\}$ so $k = 3$. This graph has $\#F(G) - 1 = 6$ essential parameters x, y, z, t, u, v (after rescaling). We obtain a 3×6 matrix A. If $J = \{1, 3, 5\}$ we compute $\Delta_{135}(A) = f/g$ where

$$g = 1 + xy$$

conservative flow in red. To compute f notes that $I\setminus J = \{2, 6\}$ and $J\setminus I = \{1, 5\}$. So $f = xzyt$ (paths in green in Figure 53). So $\Delta_{135} = \frac{xzyt}{1+xy}$.

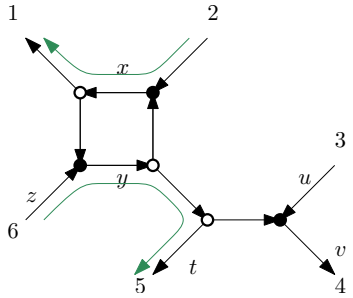

Figure 53: Example of Theorem 15.6.

□

Example 15.8. Consider the graph G with $n = 6$ vertices in Figure 54. Then the set of boundary vertices is $I = \{1, 4\}$. Fix $J = \{1, 5\}$. Then $\Delta_{15}(A) = f/g$. For the conservative flows (see conservative flows in green in Figure 54(a)).

$$g = 1 + xy + zyt + u + wt + xy \cdot u + xy \cdot wt + uwt + xy \cdot u \cdot wt + wvut + wvut \cdot xy.$$

Next we calculate f (see flows in blue and green in Figure 54(b)).

$$f = rwvus + rwvusxy + rwtzyus + rwvus \cdot zyt$$

□

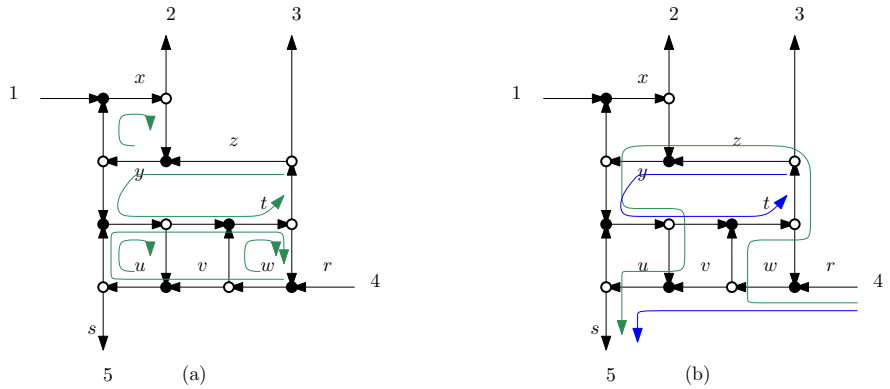

Figure 54: Example of Theorem 15.6. (a) the conservative flows in green, (b) flows from $I\backslash J$ to $J\backslash I$ where $I = \{1, 4\}$ and $J = \{1, 5\}$.

The proof of the theorem uses ideas similar to Lindström Lemma.

Proposition 15.9.

$$\Delta_J(A) = \sum_{\pi: I\backslash J \to J\backslash I} (-1)^{xing(\pi)} \prod_{i \in I\backslash J} M_{i,\pi(i)}$$

where the $xing(\pi)$ is the crossing number.

Example 15.10. $I\backslash J = \{i_1, i_2, i_3\}$ and $J\backslash I = \{j_1, j_2, j_3\}$ $\pi : i_1 \mapsto j_2, i_2 \mapsto j_3, i_3 \mapsto j_1$. $xing(\pi) = 2$

□

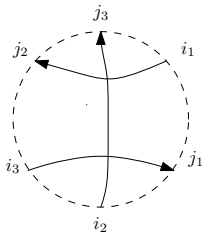

Figure 55: Example of Proposition 15.9.

The idea of the proof of Talaska's formula is $g \cdot \Delta_J(A) = f$

16 Lecture 16, 4/11/2012

16.1 An aside: weighted Catalan numbers

Let $C_n = \frac{1}{n+1}\binom{2n}{n}$ be the nth Catalan number. When is C_n odd? The answer is C_n is odd if and only if $n = 2^k - 1$. A more refined question is the following,

Theorem 16.1. *Let $\Psi(m)$ be the max power of 2 that divides m. Let $s(m)$ be the sum of the binary digits of m. Then $\Psi(C_n) = s(n+1) + 1$.*

Example 16.2. $C_4 = 14$ but $\Psi(C_4) = 1$ and the binary expression of 5 is 101. □

There is a proof of this theorem by Deutsch and Sagan [1]. The method they use is the following: C_n is the number of binary trees on n vertices (see Figure 56(a)). We define an action on such trees that switches the left and right child of a vertex. The size of any orbit is 2^s where $s \geq s(n+1) - 1$. Also the minimal number of orbits of size $2^{s(n+1)-1}$ is $(2s-1)!!$ which is an odd number.

This method can be generalized to **weighted Catalan numbers**, for weights $b_0, b_1, \ldots in \mathbb{Z}_{\geq 0}$, we associate to a Dyck path P the weight $wt(P) = b_{h_1} \cdots b_{h_n}$ where h_i is the height of the ith ascent of P. Let $C_n^{\mathbf{b}} = \sum_P wt(P)$. For example for $n = 3$: $C_n^{\mathbf{b}} = b_0^3 + 2b_0^2 b_1 + b_1^2 b_0 + b_0 b_1 b_2$ (see Figure 56(b)).

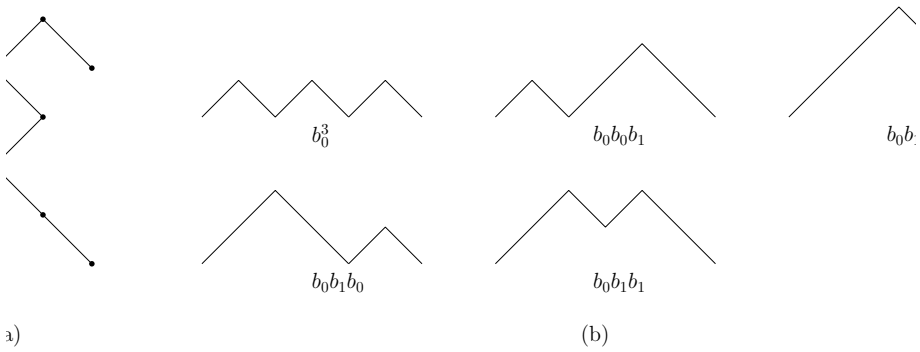

Figure 56: (a) Example of binary tree with $n = 12$ vertices, (b) weighted Dyck paths with $2 \cdot n$ steps for $n = 3$. In this case $C_n^{\mathbf{b}} = b_0^3 + 2b_0^2 b_1 + b_1^2 b_0 + b_0 b_1 b_2$.

These weighted Catalan numbers have a nice continued fraction: $\sum_n C_n^{\mathbf{b}} x^n = \cfrac{1}{1 - \cfrac{b_0 x}{1 - \cfrac{b_1 x}{1 - \cfrac{b_2 x}{1 - \ddots}}}}$. If $b_i = q^i$ then $C_n^{\mathbf{b}}$ becomes the q-Catalan numbers. For instance $C_3(q) = 1 + 2q + q^2 + q^3$.

Theorem 16.3 (Postnikov-Sagan)**.** *Let $\Delta f(x) := f(x+1) - f(x)$ be the divided difference operator. If $\mathbf{b} : \mathbb{Z}_{\geq 0} \to \mathbb{Z}$ such that (i) b_0 is odd, (ii) $\Delta^n(\mathbf{b})(x)$ is divisible by 2^{n+1} for all $n \geq 1$ and for all x. Then $\Psi(C_n^{\mathbf{b}}) = \Psi(C_n) = s(n+1) - 1$.*

Such a condition holds for q-Catalan numbers if $q = 1 + 4k$. For instance $b(x) = q^x$ for all $x \in \mathbb{Z}_{\geq 0}$, then $\Delta b = q^{x+1} - q^x = q^x(q-1)$ and in general $\Delta^n b = q^x(1-q)^n$. If $q = 4k+1$ then $\Delta^n b = (4k+1)^x (4k)^n$ so $\Delta^n b$ is divisible by 2^{n+1}.

16.2 Idea of proof of Talaska's Formula

We continue with the proof of Talaska's formula.

One can show from the definition of the determinant and moving negative signs the following expression:

$$\Delta_J(A) = \sum_{\pi: I\setminus J \to J\setminus I, \text{ bijection}} (-1)^{xing(\pi)} \prod_{i\in I\setminus J} \sum_{P_i: b_i \to b_{\pi(i)}} (-1)^{wind(P_i)} weight(P_i)$$

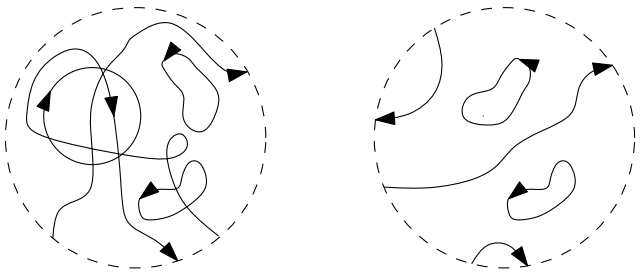

Figure 57: Conceptually what the equation $g \cdot \Delta_J(A) = f$ represents.

We want to show that $g \cdot \Delta_J(A) = f$. The LHS and RHS of this equation in terms of paths are represented in Figure 57. The sign is $(-1)^{xing(A)+\sum wind(P_i)}$. We build a sign-reversing involution φ (this is a generalization of Lindström's Lemma).

Description of φ: Find the smallest $i \in I\setminus J$ such that P_i has a common vertex with some P_j, $j > i$ or with a cycle in a conservative flow, or a self-intersection. Let x be the first intersection point on P_i. There are two cases:

Case 1. If there exists another path P_j that passes through x. Pick such P_j with minimal j and swap the tails of P_i and P_j.

Case 2. Otherwise, find the first point on P_i where we can move a loop in P_i to the flow or vice versa and move this loop.

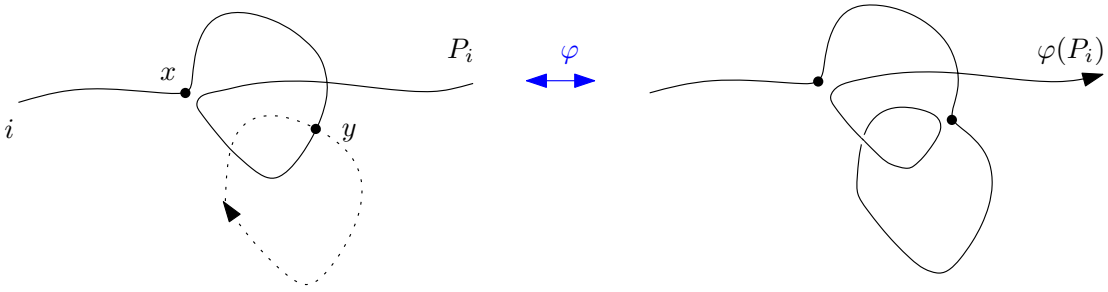

Figure 58: The sign reversing involution φ.

Our next goal is to prove the following theorem.

Theorem 16.4. *Given the map M : {plabic graph with positive edge weights} $\to$ $\mathbf{Gr}(k,n)$, Then $Image(M) = \mathbf{Gr}_{\geq 0}(k,n)$.*

Proof. From Theorem 15.6 we have shown that $Image(M) \subseteq \mathbf{Gr}_{\geq 0}(k,n)$. The converse is the hard direction. □

Example 16.5. $k = 2$ $\mathbf{Gr}_{\geq 0}(2,n)$ $v_1, v_2, \ldots, v_n \in \mathbb{R}^2$.. Given a configuration Figure 59(a) we want to build a graph with two boundary sources. See Figure 59(b) for examples of the inverse image of M in $\mathbf{Gr}_{>0}(2,3)$ and $\mathbf{Gr}_{>0}(2,4)$.

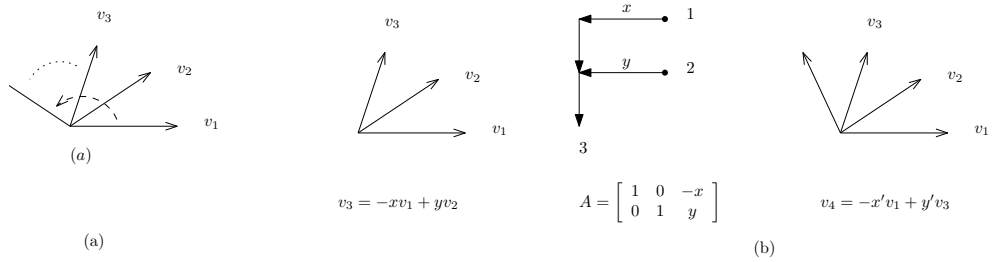

Figure 59: Example of reverse map, from point in $\mathbf{Gr}(2,n)$ to a plabic graph G with positive edge weights.

Claim: This type of graphs are the preimage of M of $\mathbf{Gr}_{>0}(2,n)$. □

The previous example shows how one generalizes the construction for all k. See Figure 60.

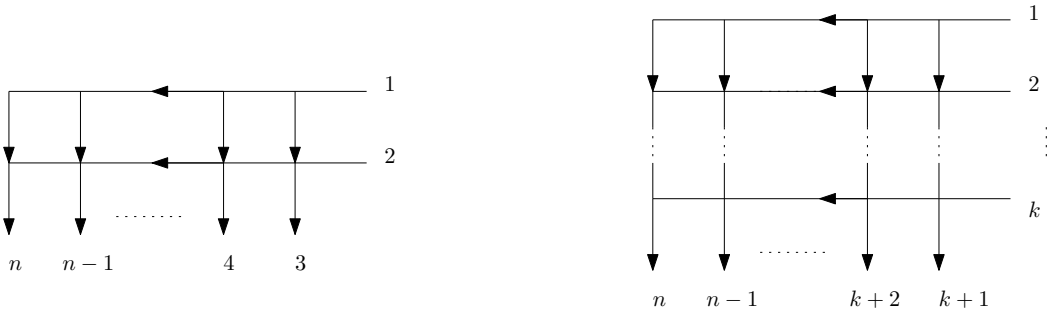

Figure 60: Examples of plabic graphs that are inverse images of $\mathbf{Gr}_{>0}(2,n)$ and more generally $\mathbf{Gr}_{>0}(k,n)$.

Theorem 16.6. *The $k \times (n-k)$ grid with positive edge weights gives exactly $\mathbf{Gr}_{>0}(k,n)$.*

We also want to describe the degenerate case (we want $\mathbf{Gr}_{\geq 0}(k,n)$).

Example 16.7. For $k = 2$ and $n = 4$, $v_3 = -xv_1 + yv_2$ $x, y \geq 0$ and $v_4 = -x'v_1 + y'v_3$. There are two cases $x = 0$, $y = 0$. □

17 Lecture 17, 4/13/2012

17.1 Degenerate cases

Given linearly independent vectors v_1 and v_2. Let $v_3 = -xv_1 + yv_2$, $v_4 = -x'v_1 + y'v_3 = -x''v_1 + y''v_4$.

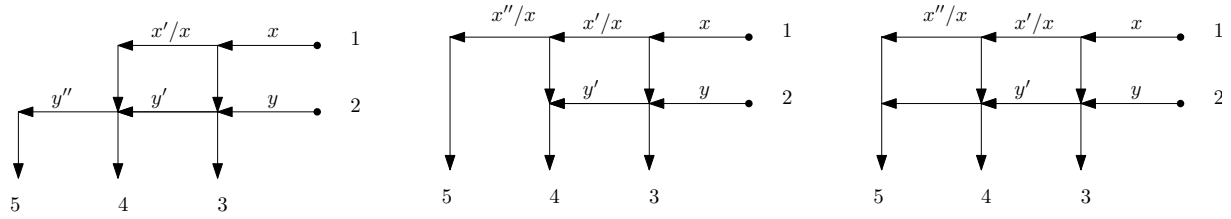

Figure 61: Example degenerate cases.

We consider three degenerate cases illustrated in Figure 61 **case 1.** $x'' = 0$ and $y'' > 0$, **case 2.** $x'' > 0$ and $y'' = 0$, and **case 3.** $x'' = y'' = 0$.

case 2 is special because all things have to the parallel to v_5. Once we skip a horizontal edge it has to remain like that.

Example 17.1. $k = 2$

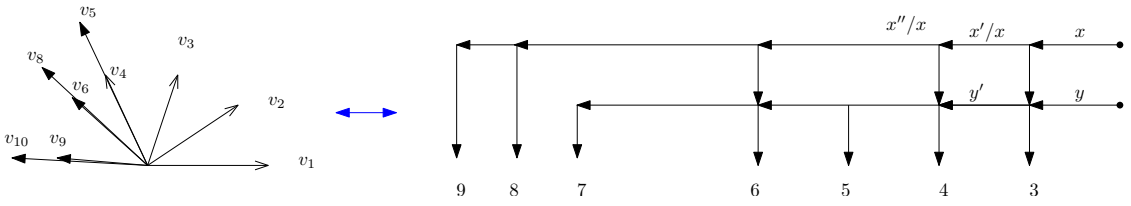

Figure 62: Example degenerate case $k = 2$.

and $k = 3$ column picture in $\mathbb{P}^2$.

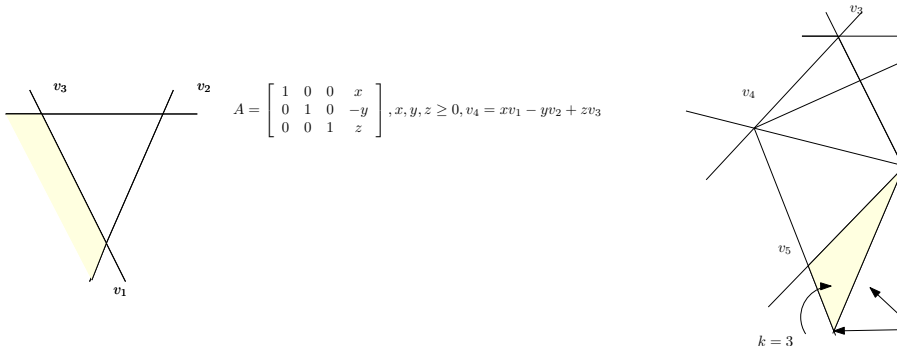

Figure 63: Example degenerate case $k = 3$.

□

17.2 General construction

A is a $k \times n$ matrix which is a point in $\mathbf{Gr}_{\geq 0}(k, n)$, assume A is in row echelon form with pivot column set I. We will obtain a filling of a Young diagram λ with nonnegative real numbers (see Figure 64) .

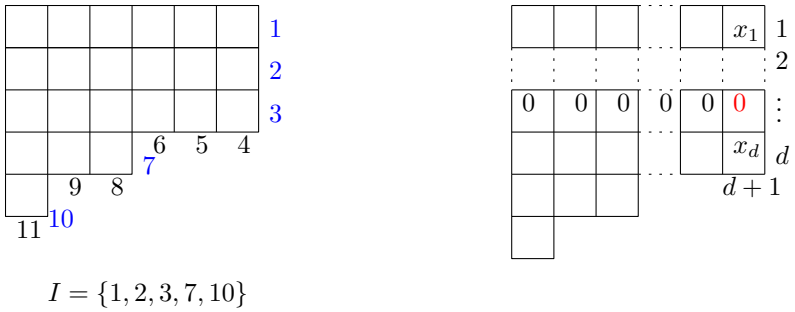

Figure 64: Tableaux with a blocked zero in red.

Let d be size of last column in λ, $v_1, \ldots, v_d$ are linearly independent. Say $v_{d+1} = (-1)^{d-1}x_1v_1 + \cdots + x_{d-2}v_{d-2} - x_{d-1}v_{d-1} + x_dv_d$.

Lemma 17.2. *$x_1, \ldots, x_d \geq 0$, $\Delta_I = 1$ and $\Delta_{(I\setminus i)\cup\{d+1\}} = x_i \geq 0$.*

We say that $x_r = 0$ is a **blocked** zero if there exists $i < r$ such that $x_i > 0$.

Lemma 17.3. *If $x_r = 0$ is a blocked zero then the rth row of A is zero (except $a_{rr} = 1$).*

Proof. Look at minors of A. □

Example 17.4. $A = \begin{bmatrix} 1 & 0 & -3 & -10 \\ 0 & 1 & \mathbf{0} & 0 \end{bmatrix}$

The entry in red is a blocked zero if the $(2, 4)$ entry is nonzero then we have a problem with a minor. [⋆⋆⋆ ask ⋆⋆⋆] □

Lemma 17.5. *If r is a blocked zero let B be the $(k-1) \times (n-1)$ matrix obtained from A by removing rth row and rth column and changing signs of nonpivot entries in first $r-1$ rows. Then $A \in \mathbf{Gr}_{\geq 0}(k, n)$ if and only if $B \in \mathbf{Gr}_{\geq 0}(k-1, n-1)$.*

Proof. Minors of A are the same as the minors of B. □

Example 17.6. $A = \begin{bmatrix} 1 & 0 & -3 & -10 \\ 0 & 1 & \mathbf{0} & 0 \end{bmatrix} \to B = [1\ 3\ 10]$. □

By this Lemma we can remove the blocked zeros.

Back to filling of Young diagram. If we have a blocked zero we set to zero the entries in the row of the diagram. The nontrivial case is when we have no blocked zeros.

Lemma 17.7. *Assume that there are no blocked zeroes (that is $x_1 = x_2 = \cdots = x_s = 0, x_{s+1}, \ldots, x_d > 0$). Let C be $k \times (n-1)$ matrix such that first d columns are the coordinate vectors $e_1, \ldots, e_d$ and the remaining entries are*

$$c_{i,j-1} = \begin{cases} a_{ij} & \text{if } i \in \{1, 2, \ldots, s\} \cup \{d+1, \ldots, k\} \\ \frac{a_{ij}}{x_i} + \frac{a_{i+1,j}}{x_{i+1}} & \text{if } i \in \{s+1, \ldots, d-1\} \\ \frac{a_{dj}}{x_d} & \text{if } i = d. \end{cases}$$

Then $A \in \mathbf{Gr}_{\geq 0}(k, d)$ if and only if $C \in \mathbf{Gr}_{\geq 0}(k, n)$.

In this case there is a nontrivial transformation of minors.

Example 17.8. $A = \begin{bmatrix} 1 & 0 & -x_1 & y \\ 0 & 1 & x_2 & z \end{bmatrix}$, $x_1, x_2 > 0$ to $C = \begin{bmatrix} 1 & 0 & \frac{y}{x_1} + \frac{z}{x_2} \\ 0 & 1 & \frac{z}{x_2} \end{bmatrix}$ Let $\Delta_J := \Delta_J(A)$ and $\widetilde{\Delta}_J := \Delta_J(C)$. We want to show we can obtain one minor from the other by a subtraction-free rational expression.

$\widetilde{\Delta}_{12} = 1, \widetilde{\Delta}_{13} = \frac{\Delta_{14}}{x_2}, \widetilde{\Delta}_{23} = \frac{\Delta_{24}}{x_1 x_2}$. $\Delta_{12} = 1, \Delta_{13} = x_2, \Delta_{23} = x_1, \Delta_{14} = x_2\widetilde{\Delta}_{13}, \Delta_{34} = x_1 x_2 \widetilde{\Delta}_{23}$, $\Delta_{24} = x_1(\widetilde{\Delta}_{13} + \widetilde{\Delta}_{23})$. □

Putting everything together

Start with A, find first linear dependence $v_{d+1} = x_d v_d - x_{d-1} v_{d-1} + x_{d-2} v_{d-2} - \cdots$, fill in zeros if you have blocked zeros (do the same with matrix A). Then change matrix to C (can have smaller number of columns), find first linear dependence $v'_{d'} = x'_{d'} w_{d'} - \cdots$, used these coefficients $x'_{d'}$ in the second column.

What type of diagrams do we obtain? We have fillings on Young diagrams with nonnegative entries. You are not allowed to have two nonzero entries $(i, j), (k, \ell)$ with $i < k$ and $\ell < j$ and a zero at (k, j).

18 Lecture 18, 4/18/2012

Last time we showed how to obtain from a matrix A in $\mathbf{Gr}_{\geq 0}(k, n)$ a Young diagram filled with numbers ≥ 0 with the following forbidden patterns:

These are called **Le-diagrams** (or L-diagrams) or **hook-diagrams**.

Example 18.1. For the hook-diagram $\begin{array}{|c|c|c|c|c|} \hline & x & y & & z \\ \hline t & u & v & & \\ \hline & w & & & \\ \hline \end{array}$ we obtain its hook-graph and associated plabic graph (see Figure 65).

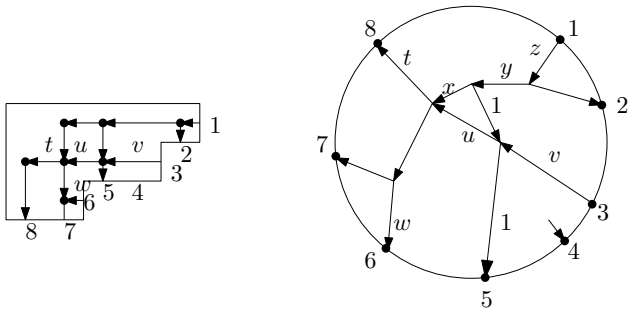

Figure 65: Example of hook graph and associated plabic graph.

□

Theorem 18.2. *$A \in \mathbf{Gr}_{\geq 0}(k, n)$ obtain hook diagram and hook graph G. Then A is a the boundary measurement matrix corresponding to G.*

Example 18.3. For the matrix

$$A = \begin{bmatrix} \underline{1} & 1 & 0 & 0 & 2 & 6 \\ 0 & 0 & \underline{1} & 0 & -2 & -2 \\ 0 & 0 & 0 & \underline{1} & 0 & 0 \end{bmatrix},$$

the set of pivot columns is $I = \{1, 3, 4\}$. From this set we obtain a Young shape $\lambda =$  . Next, we find the first linear dependence of the columns $v_2 = 1 \cdot v_1$  We remove the second column of A (corresponding to v_2) and obtain the matrix

$$A' = \begin{bmatrix} 1 & 0 & 0 & 2 & 6 \\ 0 & 1 & 0 & -2 & -2 \\ 0 & 0 & 1 & 0 & 0 \end{bmatrix}.$$

Next we find the first linear dependence $v_4 = 2v_1 - 2v_2 + 0v_3$  Since we have a blocked zero we get rid of the last row of A' and the third column and change signs to obtain

$$A'' = \begin{bmatrix} 1 & 0 & -2 & -6 \\ 0 & 1 & 2 & 2 \end{bmatrix}$$

where $a = -6, b = 2, x_1 = 2, x_2 = 2$ $A''' = \begin{bmatrix} 1 & 0 & a/x_1 + b/x_2 \\ 0 & 1 & b/x_2 \end{bmatrix} = \begin{bmatrix} 1 & 0 & -2 \\ 0 & 1 & 1 \end{bmatrix}$. We find the first linear dependence: $v_3 = -2v_1 + 1v_2$ and from it obtain the diagram  . From this hook-diagram we obtain the hook-graph G in Figure 66(a). By tallying the paths in G one can check that we get back matrix A. □

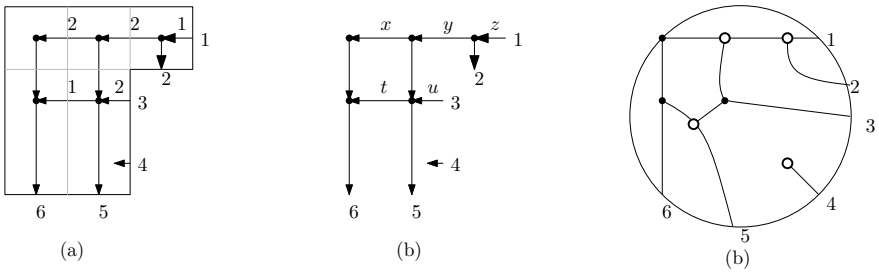

Figure 66: (a) Hook graph obtained in Example 18.3. (b) Hook graph with parameters x, y, z, t, u. By Theorem 18.4(2) this parametrizes a five dimensional cell of $\mathbf{Gr}_{\geq 0}(3, 6)$. (c) Associated graph with white and black lollipops.

Theorem 18.4. *1. Cells in $\mathbf{Gr}_{\geq 0}(k, n)$ are in bijection with hook diagrams that fit inside a $k \times (n-k)$ rectangle.*

2. The dimension of a cell equals the number of $*$s in the corresponding hook diagram.

3. The boundary measurement map $M_G : \mathbb{R}^d_{>0} \to \mathbf{Gr}(k, n)$ where G is a hook graph and d is the number of $*$s. This map is a bijection between $\mathbb{R}^d_{>0}$ and the corresponding cell.

Example 18.5. The hook graph in Figure 66(b) gives all points in the cell of $\mathbf{Gr}_{\geq 0}(3, 6)$: $A = \begin{bmatrix} 1 & z & 0 & 0 & yz & (x+t)yz \\ 0 & 0 & 1 & 0 & u & tu \\ 0 & 0 & 0 & 1 & 0 & 0 \end{bmatrix}$. □

We can view the hook graph as a plabic graph with certain white and black edges incident to edges called **lollipops**. See Figure 66(c). Such graphs can have two types of lollipops $\circ-$, corresponding to empty rows of hook diagram and $\bullet-$, corresponding to empty columns of hook diagram.

Example 18.6. □

Question 18.7. *What are the zero dimensional cells?*

The answer is $\binom{n}{k}$ since this is the number of Young diagrams that fit in $k \times (n-k)$ (choices of set I). This corresponds to a plabic graph

The map between hook graphs and cells is not a bijection since there are more graphs. However, there is a set of transformation of graphs that do not change the corresponding cell and one can use such transformations to go between two graphs that correspond to the same cell. These are analogues of Coxeter moves in wiring diagrams. (Graphs and cells analogues of wiring diagrams and permutations respectively).

Example 18.8. The hook-graphs and plabic graphs that correspond to the top cell in $\mathbf{Gr}_{\geq 0}(2,4)$ are represented in Figure 67.

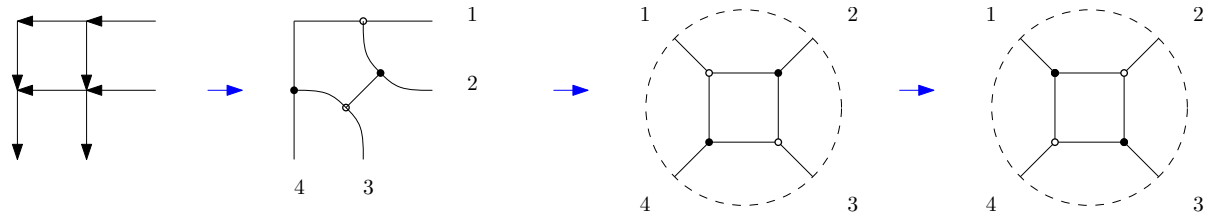

Figure 67: Example of hook-graphs and plabic graphs in top dimensional cell of $\mathbf{Gr}_{\geq 0}(2,4)$.

□

18.1 Undirected plabic graphs

In this section we consider plabic graphs with vertices of any degree. We will work with face variables. We orient the edges and we say a **perfect orientation** is one where the white vertices have indegree 1 and the black vertices have outdegree 1.

We have the following transformations of plabic graphs.

M1. Unicolored edge construction/deconstruction.

If we collapse all unicolored vertices we obtain a bipartite graph. Sometimes it is better to uncollapse a vertex to obtain trivalent vertices. See Figure 68 for an illustration.

Remark 18.9. The number of ways of uncollapsing a vertex into trivalent graphs is the Catalan numbers. So the number of ways of uncollapsing a graph is a product of Catalan numbers. □

M2. Square move: If you have four vertices forming a square, all vertices are trivalent and the colors alternate, then we switch the colors of the vertices. See Figure 69 for an illustration.

Question 18.10. *How are these transformations related to Coxeter moves to wiring diagrams?*

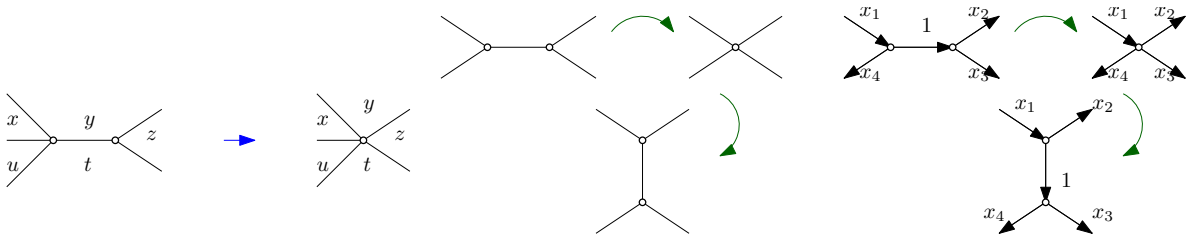

Figure 68: Illustration of M1. Unicolored edge construction/deconstruction.

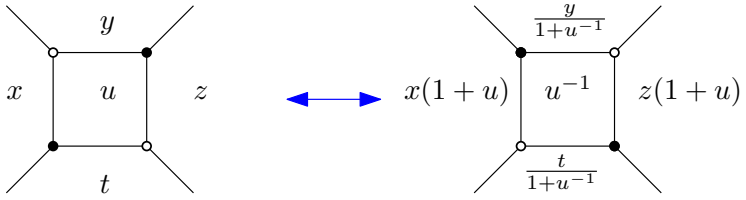

Figure 69: Illustration of M2. Square move.

19 Lecture 19, 4/20/2012

19.1 Moves on plabic graphs

We gave two moves on plabic graphs **M1 unicolored edge contraction/deconstruction**, and **M2 square move** (see Figure 68 and Figure 69). There is also a directed version of square move with edge variables. However, it is easier to do the square move with face variables.

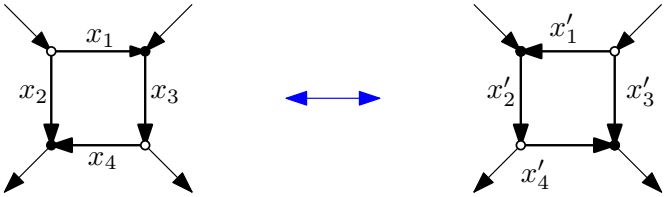

Figure 70: $x_1' = \frac{x_3x_4}{x_2+x_1x_3x_4}, x_2' = x_2 + x_1x_3x_4, x_3' = \frac{x_2x_3}{x_2+x_1x_3x_4}, x_4' = \frac{x_1x_3}{x_2+x_1x_3x_4}$.

The next reduction rules simplify the structure of the graph. They are illustrated in Figure 71.

- **R1. vertex removal**
- **R2. parallel edge reduction**
  $x = Au^{-1}, y = uv^{-1}, z = Bv$, $x' = \frac{A}{u+v}, z' = B(u+v)$ can solve for x' and z' and obtain $x/(1+y^{-1})$ and $z(1+y)$.
- **R3. leaf reduction**
- **R4. dipole reduction**

Once we have a leaf, using (R3) and (M1) (see Figure 72 we create an *avalanche of reductions*.

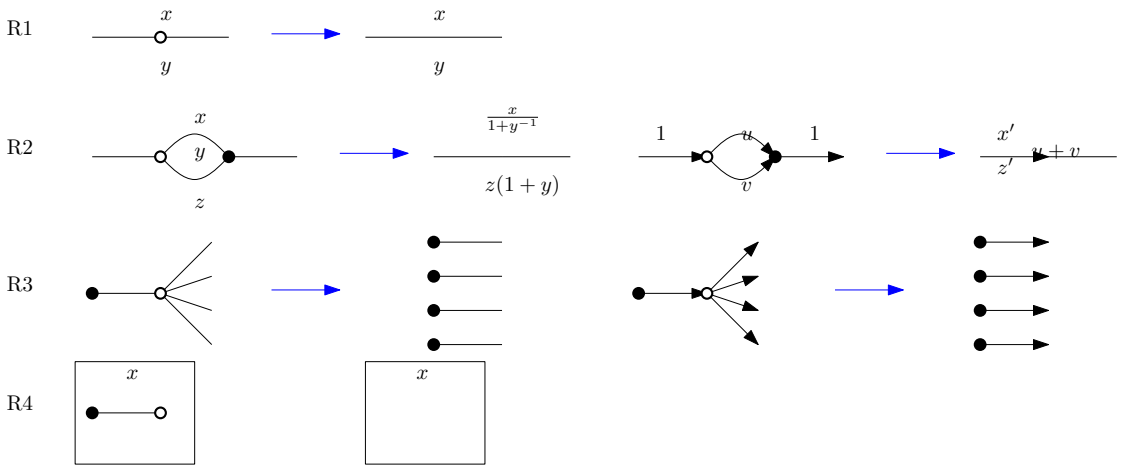

Figure 71: Illustration of reduction rules: R1. vertex removal, R2. parallel edge reduction, R3. leaf reduction and R4. dipole reduction.

Figure 72: Moves on leaves using (M1).

Definition 19.1. Two graphs are **move equivalent** $G_1 \cong G_2$ if they can be obtained from each other by the moves described above. □

Theorem 19.2. *1. Two perfectly orientable undirected graphs (with weights) map to the same point of* $\mathbf{Gr}_{\geq 0}(k,n)$ *if and only if they are move equivalent.*
2. Cells in $\mathbf{Gr}_{\geq 0}(k,n)$ *correspond to move equivalence classes of graphs (without weights)*

Definition 19.3. A plabic graph is **reduced** if it is impossible to transform it by the moves (M1) and (M2) into a graph where we can apply a reduction and it has no leaves (except boundary lollipops). □

Example 19.4. In Figure 73 there are examples of reduced and not reduced graphs. For the latter we show reductions to reduced graphs.

□

Theorem 19.5. *If G without weights is reduced then it is perfectly orientable and the map* $\widetilde{M}_G : \mathbb{R}_{>0}^{F(G)-1} \to$ *cell in* $\mathbf{Gr}_{\geq 0}(k,n)$ *is a bijection. In particular, the dimension of a cell is* $F(G)-1$*, where* $F(G)$ *is the number of faces of* G*.*

Theorem 19.6. *For two reduced graphs,* $G_1 \cong G_2$ *if and only if* G_2 *can be obtained from* G_1 *by moves (M1) and (M2).*

A priori we know that $G_1 \cong G_2$ if G_2 can be obtained by a sequence of moves and reductions. But this result says that we can just go from one to the other at the level of reduced graphs without using reductions.

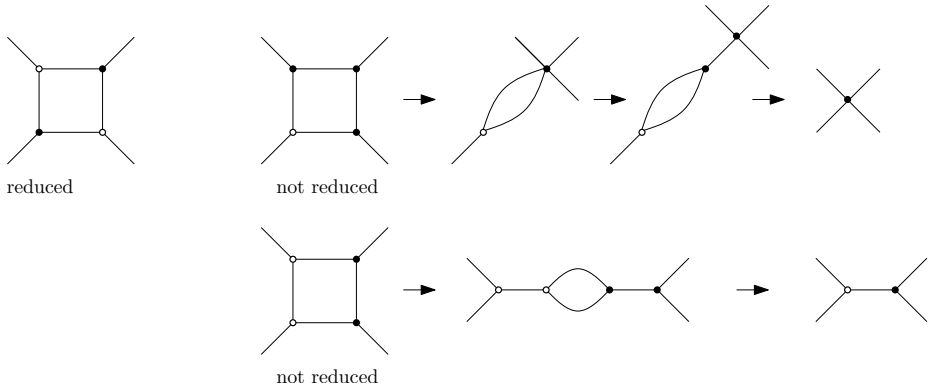

Figure 73: Example of reduced graph and two non reduced graphs and the corresponding reductions to obtain reduced graphs.

Remark 19.7. Such results are parallel to a classical results about reduced decompositions of the symmetric group: if $\mathfrak{S}_n$ is the symmetric group and $s_i = (i, i+1)$ and we have two decompositions of $w = s_{i_1} \cdots s_{i_\ell} = s_{j_1} \cdots s_{j_m}$, we can obtain one from the other by doing Coxeter moves:

$$\begin{cases} s_i s_{i+1} s_i = s_{i+1} s_i s_{i+1} & \\ s_i s_j = s_j s_i & \text{if } |i-j| \geq 2 \\ s_i s_i = id. & \end{cases}$$

But there is a stronger result about reduced decompositions where we do not need to use the relation $s_i s_i = id$. □

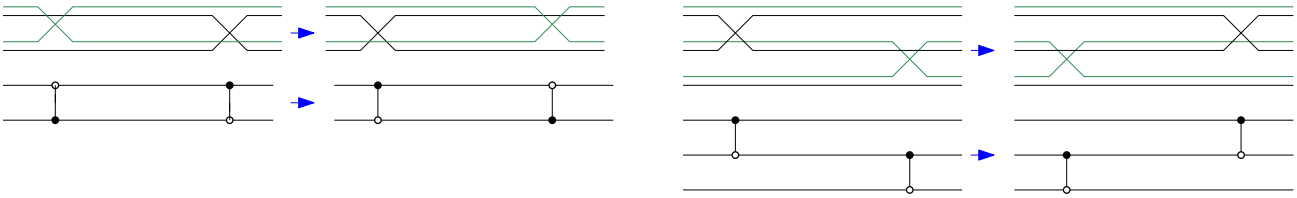

Figure 74: double wiring diagrams.

Question 19.8. *Is there an algorithm to tell whether two graphs are equivalent?*

If you see a black vertex you turn right, if you see a white vertex you turn left.

Example 19.9. For the graph in Figure 75 we obtain the permutation $\pi = \begin{pmatrix} 1 & 2 & 3 & 4 & 5 & 6 \\ 4 & 5 & 1 & 3 & 6 & 2 \end{pmatrix}$. □

Theorem 19.10. *Two reduced graphs without lollipops are equivalent if and only if they have the same permutation π as described above.*

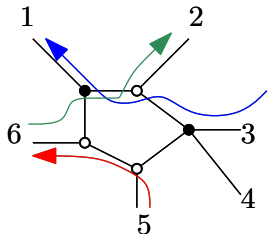

Figure 75: Permutation π associated to graph G. $\pi(3) = 1$, $\pi(5) = 6$.

20 Lecture 20, 4/25/2012

[⋆⋆⋆ missing pictures and revision ⋆⋆⋆]

Notion of **trips** in G. These are the walks that follow the following rules: 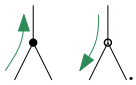 . We obtain a permutation π_G where $\pi_G(i) = j$ if the trip that starts at the ith boundary vertex ends at jth boundary vertex.

Lemma 20.1. *If G' is obtained from G by moves (M1) and (M2) then $\pi_G = \pi_{G'}$.*

Proof. Show permutation does not change with the moves (M1) and (M2). □

Remark 20.2. The reduction moves can change π_G. □

Theorem 20.3. *If G is a plabic graph without vertices of degree 1 and 2 (except boundary lollipops) then G is reduced if and only if*

1. *G has no closed trips,*
2. *G has no trips with a self-intersection except lollipops,*
3. *G has no pair of trips with a* **bad double crossing**.

where a **bad double crossing** *is a pair of trips such that there exist a pair of edges (with vertices of different colors) e_1 and e_2 such that both trips pass through e_1 and then trough e_2 (see Figure 76).*

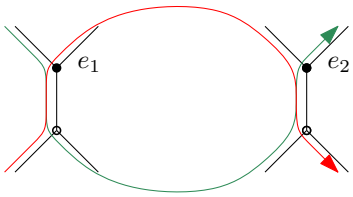

Figure 76: Illustration of a bad double-crossing.

Example 20.4. Figure 77 shows two graphs, one reduced and one that is not reduced. □

Definition 20.5. A **decorated trip permutation** of G is π_G with fixed points $\pi_G(i) = i$, then ith boundary edge is a lollipop. We color a fixed point by its lollipop. □

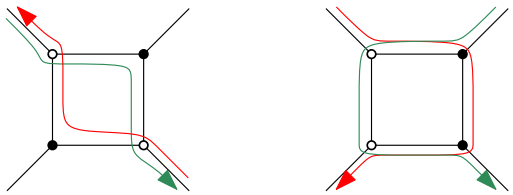

Figure 77: Illustration of a graph without a bad double crossing and one with one.

Example 20.6. The graph G in Figure 78 gives the decorated trip permutation

$$\pi^*_G = \begin{pmatrix} 1 & 2 & 3 & 4 & 5 & 6 & 7 \\ 5 & 7 & 2 & 4 & 1 & 6 & 3 \end{pmatrix}.$$

□

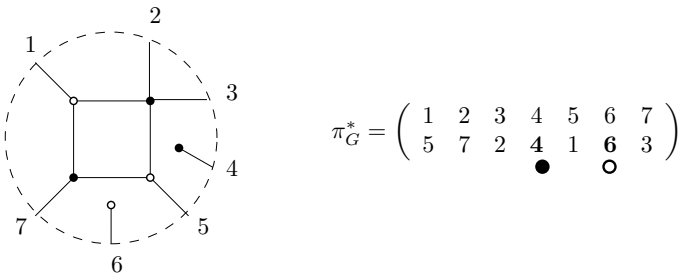

Figure 78: Decorated permutation π^*_G from a graph G. The fixed points are either black or white depending on whether they correspond to black or white lollipops.

The main result of this section is the following.

Theorem 20.7. *2-reduced graphs G_1 and G_2 are move equivalent if and only if $\pi^*_{G_1} = \pi^*_{G_2}$.*

Remark 20.8. The hard direction of this result is to show that if $\pi^*_{G_1} = \pi^*_{G_2}$ then the graphs G_1 and G_2 are move equivalent. □

20.1 Alternating strand diagram

Definition 20.9. A disk with $2n$ marked points on the boundary labelled $1, 1', 2, 2', \ldots, n, n'$ (clockwise) and n directed strands connecting i with j'.

1. Then for any boundary vertex i there is exactly one strand that starts at i, For any boundary vertex j' there is exactly one strand that ends at j'.
2. There are finitely many intersections of the strands.
3. No triple intersections (only exception is a loop 

).
4. No self intersections.
5. Alternating condition (has to start left to right, then right to left, etc) 

6. two strands cannot have two intersections points u and v like the following 

□

We go from a reduced plabic graph to an alternating strand diagram. The first step is to contract all unicolored edges to obtain a bipartite graph. The second step is to make all boundary vertices connected to black vertices. See Figure 79.

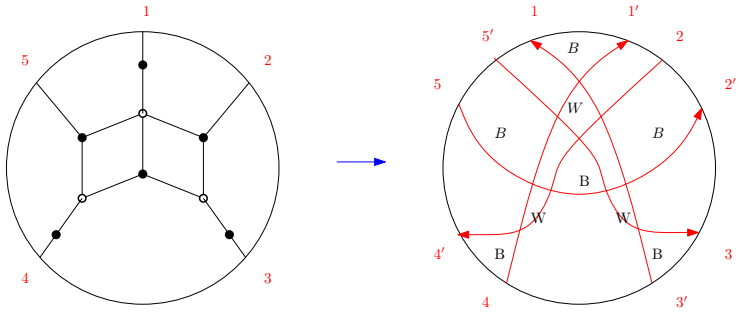

Figure 79: Obtaining an alternating strand diagram from a reduced plabic graph.

Moves of alternating strand diagrams:

M1'

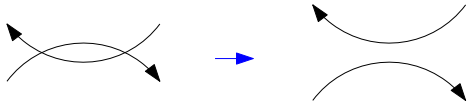

M2'

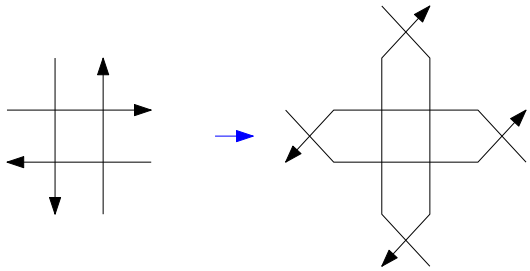

20.2 Triple crossing strand diagrams

These strand diagrams were studied by Dylan Thurston. Same setup as before ($2n$ boundary vertices connected by n directed strands). We allow only triple intersections  .

Example 20.10. Domino tilings can be transformed to triple crossing diagrams (the converse is not true).

□

We can perform flips on domino tilings which correspond to moves on triple crossing diagrams (see Figure 81).

From a reduced plabic graph we can obtain a triple crossing diagrams. First we make all white vertices 3-valent. Second we make the graph bipartite and impose that all boundary edges are connected to black vertices. See Figure 82.

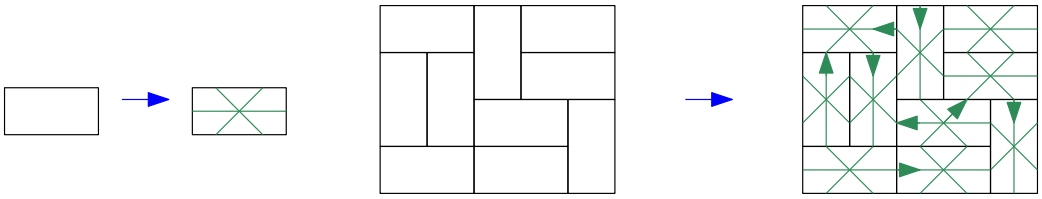

Figure 80: From domino tilings to triple crossing diagrams.

Figure 81: Flips in domino tiling and corresponding move on triple crossing diagrams.

21 Lecture 21, 4/27/2012

21.1 Triple crossing diagrams

These consists of

- n directed strands in a disk
- all intersections have form 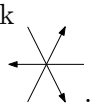 .
- no self intersections
- no bad double crossings

Exercise 21.1. *You can orient direct strands in the triple crossing diagram obtained from a domino tiling.*

Exercise 21.2. *Show that any two domino tilings of the same region are connected by tiling flips.*

21.2 How to go from plabic graphs to triple crossing diagrams

Example 21.3. In Figure 82, a triple crossing diagram is obtained from a plabic graph representing a top cell in $\mathbf{Gr}_{\geq 0}(2,5)$.

□

There is a map between triple crossing diagrams D and plabic graphs G where the vertices of D becomes white vertices of G, counter-clockwise regions of D become black vertices of G, and clockwise regions of D correspond to regions of G. See Figure 83.

Given a permutation π without fixed points construct a triple crossing diagram with this permutation.

Example 21.4. The permutation $\pi_G = \begin{pmatrix} 1 & 2 & 3 & 4 & 5 \\ 2 & 4 & 5 & 1 & 3 \end{pmatrix}$ comes from the plabic graph G in Figure 84. From this graph we construct a triple crossing diagram.

□

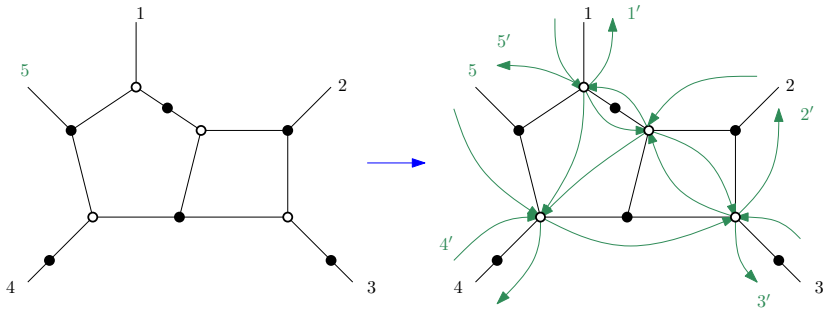

Figure 82: Illustration of how to go from a plabic graph to a triple-crossing diagram.

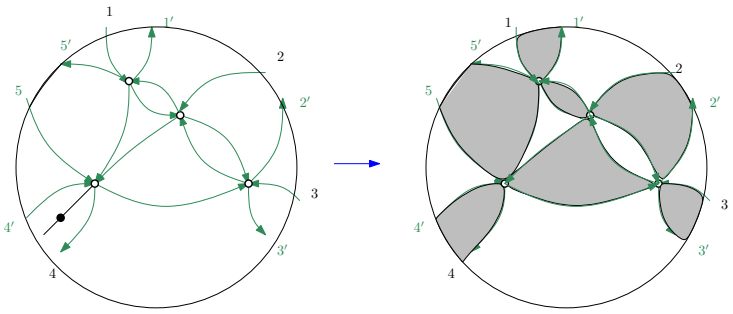

Figure 83: Illustration of map from a triple crossing diagram to a plabic graph.

If you have an even number of strands on top and do crossings.

Summary: The following are in bijection with each other

1. cells in $\mathbf{Gr}_{\geq 0}(k,n)$,
2. hook diagrams contained in $k \times (n-k)$,
3. decorated permutations of type (n,k),
4. move-equivalent classes of perfectly orientable plabic graphs of type (n,k),
5. move-equivalent classes of reduced plabic graphs of type (n,k),
6. move-equivalent classes of alternating strand diagrams of type (n,k),
7. move-equivalent classes of triple crossing diagrams of type (n,k).

There will be three move objects (7)-(10).

The **type** of a plabic graph G is (n,k) where n is the number of boundary vertices and $k-(n-k) = \sum_{u \text{ black vertex}}(\deg(u)-2) - \sum_{v \text{ white vertex}}(\deg(v)-2)$.

Example 21.5. $n=5$ and $k-(n-k) = 3-4$ so $k=2$. This is a top cell in $\mathbf{Gr}(2,5)$. □

The **type** of a decorated permutation π is (n,k) where n is the size of π and

$$\begin{aligned} k &= \#\{i \mid \pi^{-1}(i) > i\} + \#\{\text{white fixed points in } \pi\} \\ &= \#\{i \mid \pi(j) < j\} + \#\{\text{white fixed points in } \pi\} \end{aligned}$$

Example 21.6. For $\pi = \begin{pmatrix} 1 & 2 & 3 & 4 & 5 \\ 2 & 4 & 5 & \underline{1} & \underline{3} \end{pmatrix}$ $\pi(4) < 4$ and $\pi(5) < 5$ so $k=2$. If we compute k through the associated plabic graph G we also obtain the same number. □

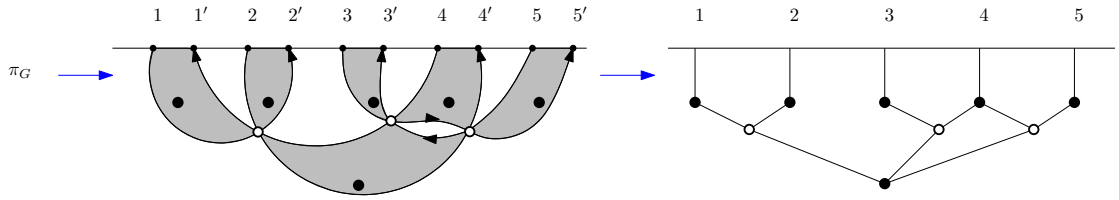

Figure 84: Illustrating how to construct a triple crossing diagram from a permutation $\pi_G = 2\,4\,5\,1\,3$, and then constructing a plabic graph from such a triple crossing diagram.

Theorem 21.7. *Criterion for reduced plabic graphs (no closed trips, no self-intersections, no bad double-crossings:* 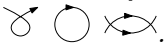 *.*

Theorem 21.8. *For any two reduced graphs G and G' with $\pi^*_G = \pi^*_{G'}$ can be obtained from each other by moves (M1) and (M2).*

Lemma 21.9. *Every connected reduced plabic graph G such that $\pi_G(i) = j$ can be transformed by moves (M1) and (M2) into a graph where this trip goes along the boundary.*

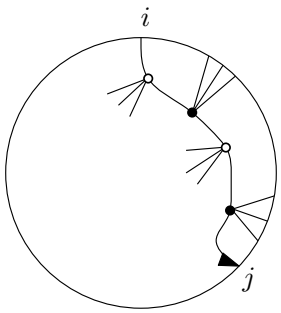

Figure 85: If $\pi_G(i) = j$, Lemma 21.9 states that using moves (M1) and (M2) we can transform the graph into a graph where this trip goes along the boundary.

The situation of the Lemma is illustrated in Figure 85. We will prove all claims together by induction on the number of faces in G.

Proof of Theorem 21.7. If G is not reduced then it has a forbidden segment. Suppose that G is reduced. And assume that G has a forbidden segment. Then

1. There is one face inside this segment. In all cases we can do a reduction. Thus G is not reduced. See Figure 86.

2. There are two or more faces inside the forbidden segment. Let $\widetilde{G}$ be the plabic graph inside this segment. Assume that $\widetilde{G}$ has as few faces as possible in the move equivalence class of G. $\widetilde{G}$ has at least one trip. By Lemma 21.9, we can make it go along the boundary. Take the first face in the *boundary strip*. See Figure 87. In all cases, doing a square move one can decrease the number of faces inside the forbidden segment.

□

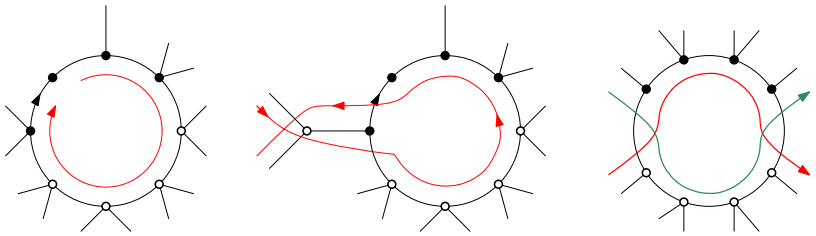

Figure 86: Step 1 of the proof of Theorem 21.7. There is a face with an instance of a closed trip, a self intersection or a double crossing.

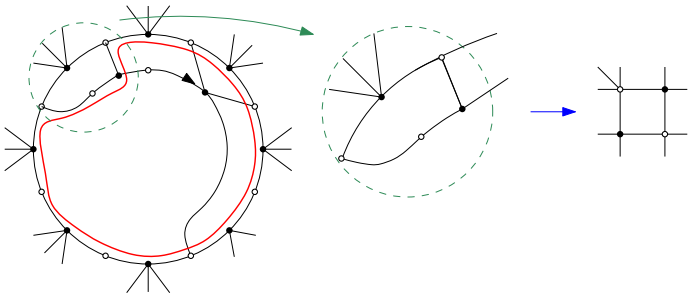

Figure 87: Step 2 of the proof of Theorem 21.7.

Proof of Theorem 21.8. Let G and G' be the graphs with $\pi_G = \pi_{G'}$. Make on trip go along the boundary. The boundary strip should be the exactly the same. For the graphs $\widetilde{G}$ and $\widetilde{G'}$, $\pi_{\widetilde{G}} = \pi_{\widetilde{G'}}$. By induction $\widetilde{G}$ and $\widetilde{G'}$ are related by moves M1 and M2. Thus G and G' are related by moves M1 and M2. □

Proof of Lemma 21.9. Make the number of faces in region A in Figure 88 (a) as small as possible in the move equivalence class of G. If all the faces in A are boundary fatces then the trip goes along the boundary. Make the trip in $\widetilde{G}$ that starts at D go along the boundary (see Figure 88 (b)).

Apply a square move (see Figure 88 (c)). We can always decrease the number of faces to the right of the trip.

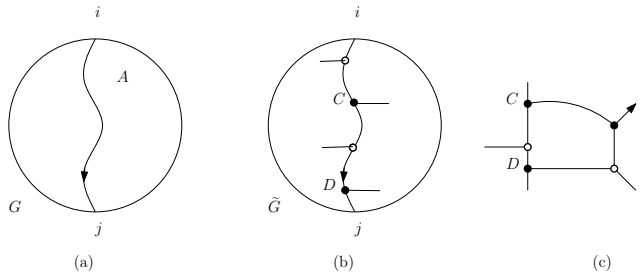

Figure 88: Diagrams for the proof of Lemma 21.9.

□

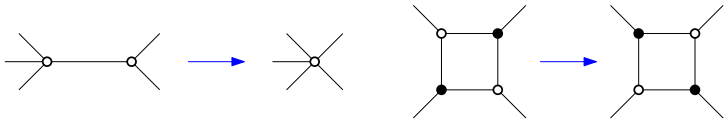

Figure 89: Moves relating reduced graphs in Theorem 21.8.

22 Lecture 22, 5/02/2012

We have proved Theorem 21.7 and Theorem 21.8. In order to prove these results used Lemma 21.9. Next we talk about another object that is in bijection with cells in $\mathbf{Gr}_{\geq 0}(k,n)$.

22.1 Grassmann necklaces

Let $I_1, \ldots, I_n \in \binom{[n]}{k}$ and for all i $I_{i+1} = (I_i \backslash \{i\}) \cup \{j\}$ or $I_{i+1} = I_i$. The indices are taken modulo n.

Example 22.1. $n = 6$ and $k = 3$ let
$$\begin{array}{rcccc} I_1 & = & 1 & 2 & 6 \\ I_2 & = & 2 & 3 & 6 \\ I_3 & = & 3 & 6 & 1 \\ I_4 & = & 5 & 6 & 1 \\ I_5 & = & 5 & 6 & 1 \\ I_6 & = & 6 & 1 & 2. \end{array}$$
□

These objects are in bijection with all the objects we had from before. We show a bijection between Grassmann necklaces and decorated permutations.
From necklaces to decorated permutations: We define π in the following way If $I_{i+1} = (I_i \backslash \{i\}) \cup \{j\}$ then $\pi(i) = j$. There are two kinds of fixed points: a white fixed point if $i \in I_i$, and black fixed point if $i \notin I_i$.

$I_i = \{i \mid \pi^{-1}(i) < i \text{ or } i \text{ is white fixed point}\}$.

I_i is the same procedure with respect to the shifted ordering $i < i+1 < \ldots < n < 1 < \ldots < i-1$.

To obtain the necklace from π, we find I_i by cutting the permutation between i and $i+1$. We look at the chords that go to the left. Their endpoints are the elements of I_i. See Figure 90 for an example.

Example 22.2. For $I_1 = \{1,2,6\} = \{1 \mid \pi^{-1}(i) < i \text{ or } i \text{ is white fixed point}\}$. In general I_i is the same thing as I_1 with the ordering shifted $i < i+1 < \cdots < n < 1 < \cdots < i-1$. See Figure 90 for the decorated permutations obtained from I_1 and I_2.

□

Recall that we had a bijection between the cells in $\mathbf{Gr}_{\geq 0}(k,n)$ and hook diagrams. I_1 corresponds the the shape λ of the hook diagram.

Example 22.3. $n = 6, k = 3$, $I_1 = \{1,2,6\}$ and $\lambda^{(1)} = 3\,3$. The hook diagram is 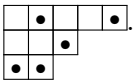 . □

The next goal is the partial order of the cells.

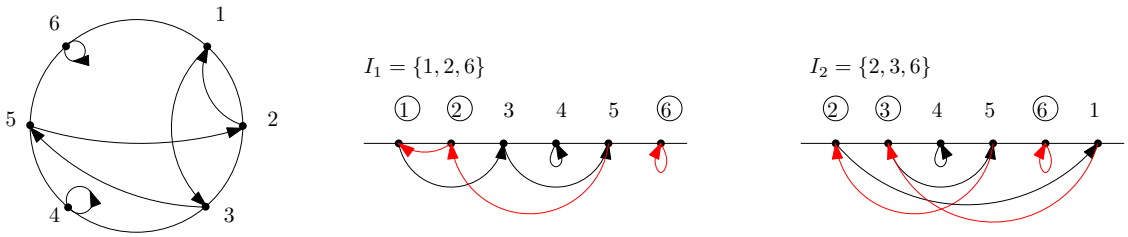

Figure 90: Example of bijection between Grassmann necklaces and decorated permutations.

23 Lecture 23, 05/04/2012

[⋆⋆⋆ missing pictures and revision ⋆⋆⋆]

Last time we discussed a bijection between decorated permutations π and Grassmann necklaces $(I_1, \ldots, I_n)$. The condition on these necklaces was that $I_{i+1} = (I_i \backslash \{i\}) \cup \{j\}$ or $I_{i+1} = I_i$. In this case $\pi(i) = j$.

Given a k element subset I_i we get a Young diagram in $k \times (n-k)$ (we go down for each element in the set and start labeling with i).

Example 23.1. $n = 6$ and $k = 3$ let

$I_1 = 1\ 2\ 6$ $\lambda^{(1)} =$ 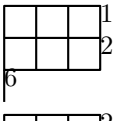

$I_2 = 2\ 3\ 6$ $\lambda^{(2)} =$ 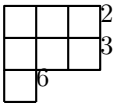

$I_3 = 3\ 6\ 1$ $\lambda^{(3)} =$ 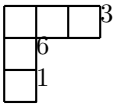

$I_4 = 5\ 6\ 1$ $\lambda^{(4)} =$ 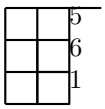

$I_5 = 5\ 6\ 1$ $\lambda^{(5)} =$ 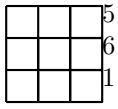

$I_6 = 6\ 1\ 2$ $\lambda^{(6)} =$ 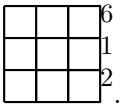 .

□

Theorem 23.2. *The decomposition of* $\mathbf{Gr}_{\geq 0}(k, n)$ *into cells is the common refinement of* n *Schubert decompositions for cyclic shifts. And every cell* C *is the positive part of*

$$\Omega_{\lambda^{(1)}} \cap c\left(\Omega_{\lambda^{(2)}}\right) \cap c^2\left(\Omega_{\lambda^{(3)}}\right) \cap \cdots \cap c^{n-1}\left(\Omega_{\lambda^{(n)}}\right),$$

where $c = (1, 2, \ldots, n)$.

Claim 23.3. *The map* $\pi \leftrightarrow C \leftrightarrow (\lambda^{(1)}, \ldots, \lambda^{(k)})$. *This is the same map as the correspondence between necklaces and* n *Young diagrams.*

Claim 23.4. *If $C \subset \Omega_\lambda$ and via the map above the cell corresponds to a decorated permutation π and this permutation corresponds to $(\lambda^{(1)}, \ldots, \lambda^{(n)})$ then $\lambda = \lambda^{(1)}$.*

Recall that by construction λ is the shape of the corresponding hook diagram.

Example 23.5. $n = 9$, $k = 4$ and $I = \{1, 3, 6, 9\} \in \binom{[9]}{4}$.
$I_1 = \{1, 3, 6, 9\} = I$. □

We can also go directly from the hook diagram to the decorated permutation. We follow the **rules of the road**.

Example 23.6. $\pi(3) = 7$ and $\pi(7) = 8$. □

23.1 Partial order on cells in $\mathbf{Gr}_{\geq 0}(k, n)$

Define the partial order in the following way: $C_1 \leq C_2$ if and only if $C_1 \subseteq \overline{C_2}$.

Recall the partial order on the Schubert cells $\Omega_\lambda \subseteq \overline{\Omega_\mu}$ if and only if $\lambda \subseteq \mu$ if and only if $I \geq J$ in the Gale order where $I = I(\lambda)$ and $J = J(\mu)$.

Theorem 23.7. *For two cells in $\mathbf{Gr}_{\geq 0}(k, n)$ then $C_1 \leftrightarrow (I_1, \ldots, I_n) \leftrightarrow (\lambda^{(1)}, \ldots, \lambda^{(n)})$ and $C_2 \leftrightarrow (J_1, \ldots, J_n) \leftrightarrow (\mu^{(1)}, \ldots, \mu^{(n)})$ then $C_1 \leq C_2$ if and only if $\lambda^{(i)} \subseteq \mu^{(i)}$ for all i if and only if $I_i \geq_i J_i$ for all $i = 1, \ldots n$. Where $\geq_i$ is the Gale order on $\binom{[n]}{k}$ with respect to the* shifted *ordering of numbers $i < i+1 < \ldots < n < 1 < \ldots < i-1$.*

Recall the notion of the strong Bruhat order in $\mathfrak{S}_n$.
such that there is no chord from A to B.

Definition 23.8 (circular Bruhat order on decorated permutations π)**.** $\pi > \widetilde{\pi}$ (covering relation), a simple crossing is there is no chord from A to B and $\widetilde{\pi}(r) = \pi(r)$ for all $r \neq i, j$. There are special cases since we allow $i = \pi(j)$ or $j = \pi(i)$ or both.

□

Exercise 23.9. *Show that the circular Bruhat order is equivalent to the shifted Gale order in Theorem 23.7*

Example 23.10. □

24 Lecture 24, 5/09/2012

24.1 Circular Bruhat order

Last time we defined the circular Bruhat order. What is the rank function in this circular Bruhat order? The chords can be arranged in three ways: crossing, alignment and misalignment (see Figure 91)

Definition 24.1. Let $A(\pi)$ be the number of alignments in π, and $k_i(\pi)$ is the cut π between $i-1$ and i and counts the number of chords going to the left. □

Example 24.2. Let π be the permutation in Figure 92. The alignments are $23, 24, 34, 36, 46, 16$, the crossings are $15, 12, 13, 25, 35$ and the misalignments are $26, 56, 54, 14$. Thus $A(\pi) = 6$. Also $k_3(\pi) = 3$.

□

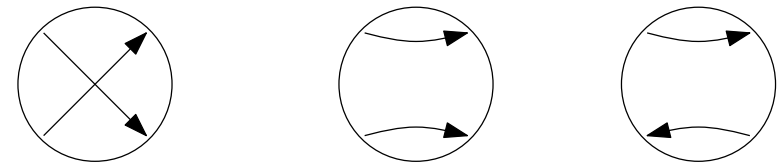

Figure 91: Possible crossings

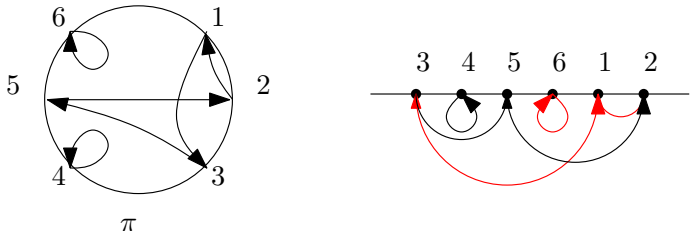

Figure 92: Example of decorated permutation.

Lemma 24.3. *(1)* $k_i(\pi) = k_j(\pi)$ *for all* i, j,
(2) If $\pi > \widetilde{\pi}$ *then* $k_i(\pi) = k_i(\widetilde{\pi})$,
(3) If $\pi > \widetilde{\pi}$ *then* $A(\pi) + 1 = A(\widetilde{\pi})$.

Definition 24.4. Let CB_{K_n} be the partial order on decorated permutations of size n with $k_i(\pi) = k$. The maximum element in CB_{K_n} is the permutation $\pi : i \mapsto i + k \pmod n$. □

Corollary 24.5. *The rank function on* CB_{K_n} *is* $\operatorname{rank}(\pi) = k(n-k) - A(\pi)$.

Let $A_{n,k}$ be the number of permutations $w \in \mathfrak{S}_n$ with k descents (indices i such that $w_i > w_{i+1}$). This is the Eulerian number.

Exercise 24.6. *Show that*

$$\#CB_{K_n} = \sum_{n' \le n} \binom{n}{n'} A_{n',k}.$$

We want to study $\sum_{\pi \in CB_{K_n}} q^{rank(\pi)}$. An explicit expression was proved by Lauren Williams [9].

Theorem 24.7 ([9])**.**

$$\sum_{\pi \in CB_{K_n}} q^{rank(\pi)} = \sum_{i=1}^{k-1} \binom{n}{i} q^{-(k-i)^2} \left([i-k]_q^i [k-i+1]_q^{n-i} - [i-k+1]_q^i [k-i]_q^{n-i} \right), \tag{24.8}$$

where $[a]_q = \frac{1-q^a}{1-q}$.

The formula was proved working with hook diagrams and looking at $F_{n,k}(q) := \sum_{D \subset k \times (n-k)} q^{\#\text{dots}(D)}$ where the sum is over hook diagrams D. If we fix a shape $\lambda \subseteq k \times (n-k)$, let $F_\lambda(q) = \sum_{D \text{ shape } \lambda} q^{\#\text{dots}(D)}$.

Example 24.9. If $\lambda = 22$ then $F_{\square\square\\\square\square}(q) = (1+q)^4 - q^2 - q^3 = 1 + 4q + 5q^2 + 3q^3 + q^4$, since $\begin{array}{|c|c|}\hline \ & \bullet \\ \hline \bullet & \ \\ \hline \end{array}$ and $\begin{array}{|c|c|}\hline \bullet & \bullet \\ \hline \bullet & \ \\ \hline \end{array}$ are not valid. □

24.2 Recurrence relation for $F_\lambda(q)$

Let x be a corner removed. Let $\lambda^{(1)}$ be the shape λ with box x removed, $\lambda^{(2)}$ is the shape λ with ith row removed, $\lambda^{(3)}$ is λ with jth column removed, $\lambda^{(4)}$ is λ with ith row and jth column removed (see Figure 93).

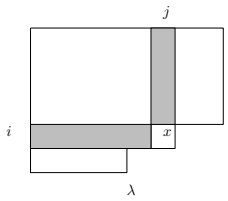

Figure 93:

Lemma 24.10. $F_\lambda(q) = qF_{\lambda^{(1)}} + F_{\lambda^{(2)}} + F_{\lambda^{(3)}} - F_{\lambda^{(4)}}$.

Example 24.11. For $\lambda = 22$ as in the previous example,

$$F_{\square\square\\\square\square} = qF_{\square\square\\\square} + F_{\square\square} + F_{\begin{array}{|c|}\hline \ \\ \hline \ \\ \hline \end{array}} - F_{\square}.$$
$$= q(1+q)^3 + (1+q)^2 + (1+q)^2 - (1+q).$$

□

Next we prove the Lemma.

Proof. The first part $qF_{\lambda^{(1)}}$ corresponds to hook diagrams of shape λ containing dot in x. The rest, $F_{\square\square} + F_{\begin{array}{|c|}\hline \ \\ \hline \ \\ \hline \end{array}} - F_{\square}$, counts hook diagrams where x is empty, then the whole ith row or the whole jth column is empty by the hook diagram condition. □

Exercise 24.12. *Prove formula for $F_{n,k}(q) = \sum_{\lambda \subseteq k\times(n-k)} F_\lambda(q)$ from the recurrence in Lemma 24.10.*

Definition 24.13. $\lambda \subseteq k \times (n-k)$, define a graph $G_\lambda \subset K_{k,n-k}$ such that (i, j') is an edge in G_λ if and only if (i, j) is a box in λ. □

Example 24.14. For $\lambda = 421 \subset 3 \times (7-3)$ we find G_λ in Figure 94.

□

Lemma 24.15. *If $\chi_\lambda(t)$ be the chromatic polynomial of G_λ, then*

$$\chi_\lambda = \chi_{\lambda^{(1)}} - t^{-1}\left(\chi_{\lambda^{(2)}} + \chi_{\lambda^{(3)}} - \chi_{\lambda^{(4)}}\right),$$

where $\lambda^{(1)}, \ldots, \lambda^{(4)}$ is defined as before.

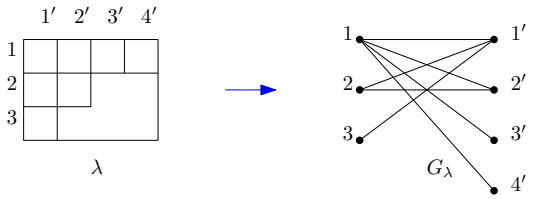

Figure 94: Graph G_λ associated to $\lambda \subset k \times (n-k)$.

Proof. Let e be the edge form vertex A to B. Let $G_{\lambda^{(1)}}$ be the graph G_λ with edge e removed. Let $G_{\lambda^{(2)}}$ be the graph G_λ with all edges from A removed. Let $G_{\lambda^{(3)}}$ be the graph G_λ with all edges from B removed. And let $G_{\lambda^{(4)}}$ be the graph G_λ with all edges from A and B removed.

Pick any proper t-coloring of $G_\lambda \backslash \{A, B\}$.

$t(\chi_{\lambda^{(1)}} - \chi_\lambda) = \chi_{\lambda^{(2)}} + \chi_{\lambda^{(3)}} - \chi_{\lambda^{(4)}}$.

If we have a corner $x = (a, b)$ then G_λ contains a copy of $K_{a,b}$ including edge e. □

Corollary 24.16. *$F_\lambda(1) = (-1)^n \chi_\lambda(-1)$. The LHS counts number of hook diagrams f shape λ (also the number of positive cells in Ω_λ). The RHS counts the number of acyclic orientations of G_λ.*

Exercise 24.17. *Find a bijection between the hook diagrams of shape λ and the acyclic orientation of G_λ. Finding a nice simple bijection is an interesting open question.*

Let $\lambda = k \times (n-k)$ so that we are looking at acyclic orientations of $K_{k,n-k}$. There is a nice way to draw such orientations by drawing a $k \times (n-k)$ grid. Each point corresponds to an edge of $K_{k,n-k}$ and we have to decide the orientation and represent it by doing a crossing or undercrossing. We call these **weak weaving patterns**.

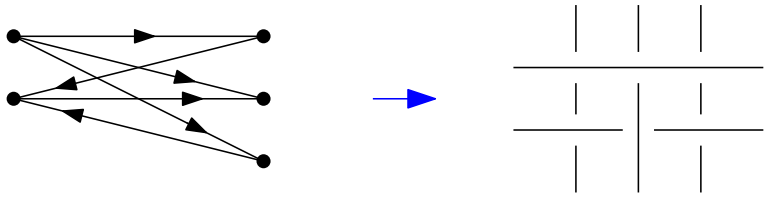

Figure 95: Example of representation of acyclic orientation of $K_{k\times(n-k)}$ and a weak weaving pattern.

24.3 Bijection between hook diagrams and Grassmannian permutations

$\lambda \subseteq k \times (n-k) \Leftrightarrow$ Grassmannian permutations$w_\lambda = w_1 \cdots w_n$ where $w_1 < w_2 < \cdots < w_k, w_{k+1} < \cdots < w_n$.

If in addition we have a hook-diagram on $\lambda \subseteq k \times (n-k)$ we tile the cells of the hook diagram in the following way: if a cell is empty we tile it  , if it has a dot we tile it  . The resulting tiled diagram is called a **pipe dream**. From it we obtain a permutation u in $\mathfrak{S}_n$ (see Figure 96 for an example).

Thus from a hook diagram D we obtain a pair (w_λ, u).

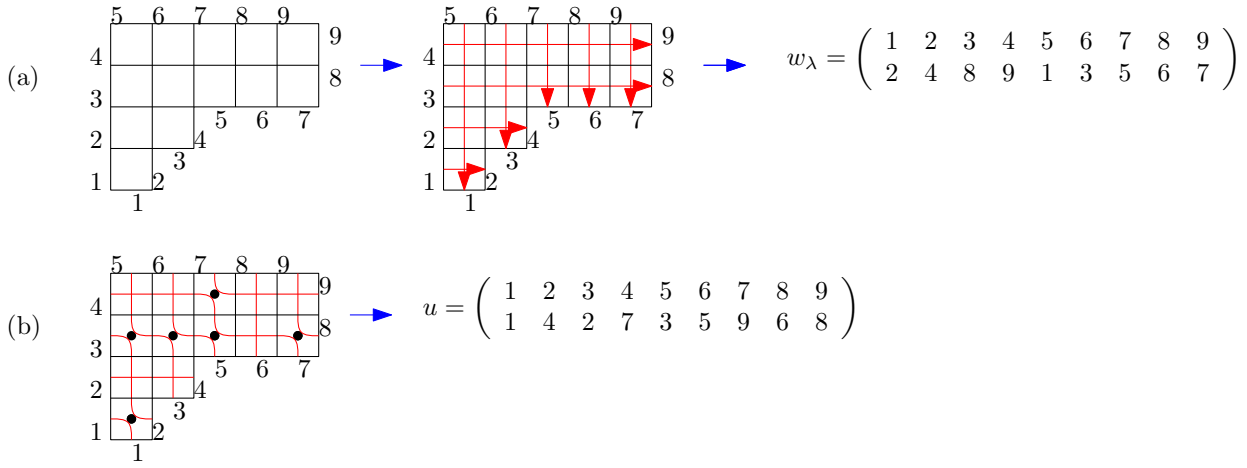

Figure 96: (a) Example of bijection between $\lambda \subset k \times (n-k)$ and Grassmannian permutations w_λ for $k = 4$ and $n = 9$. (b) Example of bijection between hook-diagram and pipe dream given by the permutation u. $u \leq w_\lambda$ in the strong Bruhat order.

25 Lecture 25, 5/11/2012

Last time we saw that from a hook diagram we obtain a pair of permutations (w_λ, u) where w_λ.

Theorem 25.1. *This is a bijection between hook diagram $D \subseteq k \times (n-k)$ and pairs (w, u) where w is Grassmannian and $u \leq w$ in the strong Bruhat order on $\mathfrak{S}_n$.*

From (w, u) we obtain the decorated permutation π where $\pi = w_0 w u^{-1} w_0$ for $w_0 = \begin{pmatrix} 1 & 2 & \dots & n \\ n & n-1 & \dots & 1 \end{pmatrix}$.

Example 25.2. From the previous example $w_\lambda = 248913567$ and $u = 142735968$. Then $\pi = 531476928$. Note that π has two fixed points 4 and 9. We can view π as coming from mirrors (see Figure 97).

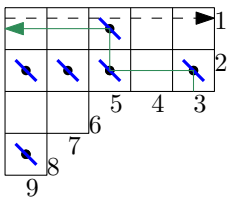

Figure 97: Building the decorated permutation π by placing mirrors on the hook diagram and following the rules of the road. For example $\pi(3) = 1$.

□

25.1 Lex maximal subwords

Claim 25.3. *$w = s_{i_1} \cdots s_{i_\ell}$ is any reduced decomposition. All permutations u such that $u \leq w$ (in the strong Bruhat order) are obtained by taking subwords of $s_{i_1} \cdots s_{i_\ell}$.*

But among these 2^ℓ possible subwords there might be repetitions. We want a way of obtaining all such permutations u in a better way without repetitions. We will use wiring diagrams.

Example 25.4. $w = s_2s_3s_1s_2s_1$ and $u = s_2\hat{s_3}s_1\hat{s_2}\hat{s_1} = \hat{s_2}\hat{s_3}\hat{s_1}s_2s_1 = s_2s_1$ (see Figure 98).

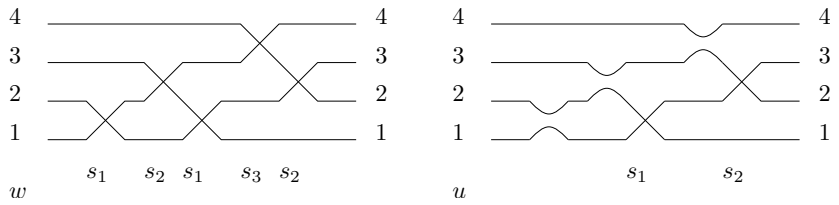

Figure 98: The wiring diagram of $w = s_2s_3s_1s_2s_1$ and of one of its subwords $u = s_1s_2$.

□

Among the subwords we want to find the **lexicographically maximal** subwords (to the left in the wiring diagrams). In the wiring diagram of w replace some crossings by "uncrossings" such that if two strands cross at some point x, they can never cross or touch at a point to the left of x (see Figure 99).

Figure 99: Forbidden moves on wiring diagrams of lex maximal subwords.

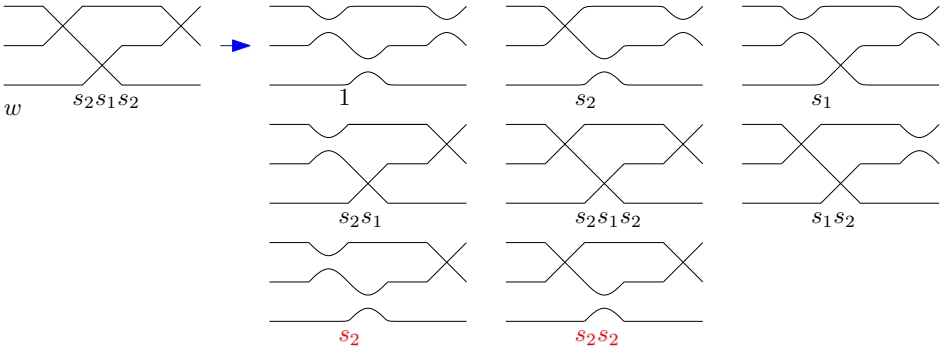

Figure 100: Example of subwords of $w = s_2s_1s_2$. Among the eight subwords (with repetitions) $\hat{s_2}\hat{s_1}s_2$ and $s_2\hat{s_1}s_2$ (in red) contain the forbidden pattern.

Example 25.5. For $w = s_2s_1s_2$, we consider the eight subwords by removing reflections. Among them $\hat{s_2}\hat{s_1}s_2$ and $s_2\hat{s_1}s_2$ contain the forbidden pattern. See Figure 100. □

Theorem 25.6. *The lex maximal subwords give all $u \leq w$ without repetitions.*

Proof. If we have a forbidden pattern then either subword is not reduced or it is not lex maximal located in $w = s_{i_1} \cdots s_{i_\ell}$. The opposite direction is left as an exercise. □

If we have no dot in a cell this corresponds to a crossing. a dot in a cell corresponds to an uncrossing. Each dot in a hook-diagram corresponds to eliminating a reflection from the reduced decomposition.

Example 25.7. We apply the above construction to w_λ for $\lambda = 5521$ (see Figure 96). $w_\lambda = s_7s_6s_8s_1s_3s_5s_7s_2s_4s_6s_3s_5s_4$ and $u = \hat{s_7}s_6s_8\hat{s_1}s_3s_5s_7s_2\hat{s_4}\hat{s_6}\hat{s_3}s_5s_4$. See Figure 101.

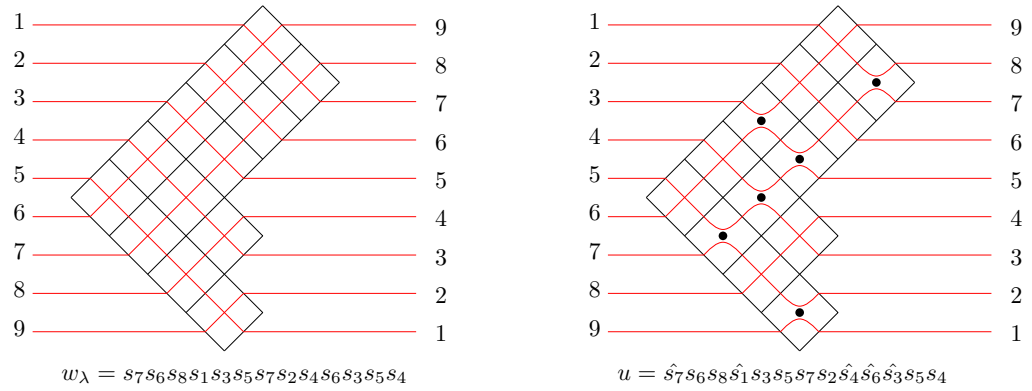

Figure 101: Example of how to get w_λ from a tiling of λ, and obtaining u as a lex maximal subword from a dot diagram in λ.

□

Theorem 25.8. *Under this correspondence the hook condition is equivalent to the lex maximal condition.*

Proof. ($\Leftarrow$)

If the wiring diagram has one of the two forbidden patterns (see Figure 99) they correspond to a hook condition in the diagram (see Figure 102 (a)).

($\Rightarrow$) pick a minimal hook condition pattern (with $a + \ell$ minimal). By the choice of a and ℓ there are no dots in the rectangle defined by this pattern (except for the NW corner of the rectangle). If we draw red wires we see we have one of the two forbidden patterns (see Figure 102 (b)).

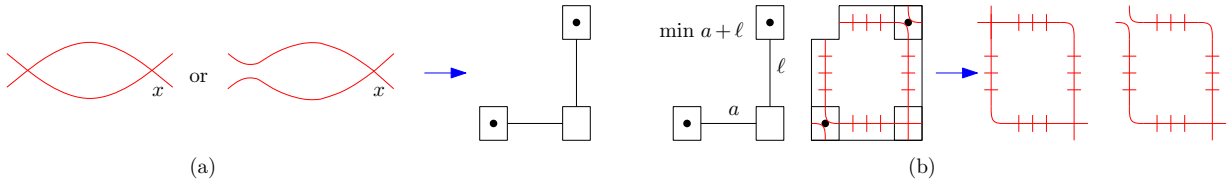

Figure 102: Diagrams for the proof of Theorem 25.8.

□

25.2 General diagrams

A **dot diagram** is a placement of dots in λ. We have some moves:

Exercise 25.9. *Each move-equivalence class of dot diagrams has a unique valid hook diagram.*

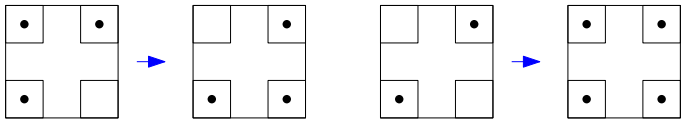

Figure 103: Moves of dot diagrams, the inner squares are empty.

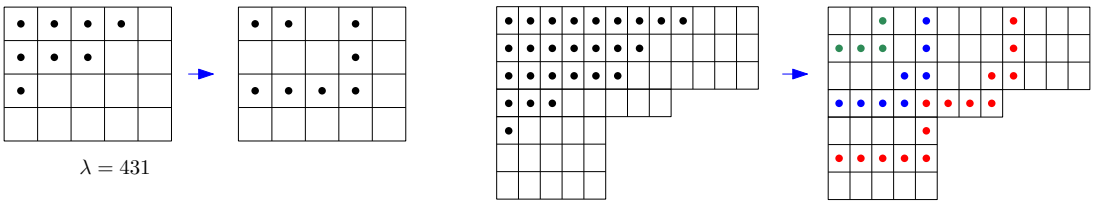

Figure 104: Examples of moving dots to obtain a hook diagram.

26 Lecture 26, 5/16/2012

26.1 Grassmannian formula for scattering amplitudes in $N = 4$ Super Yang-Mills theory

This is based on the work of Nima Arkhani-Hamed, Freddy Cachazo, et.al.

This is an alternative to doing computations with Feynman diagrams.

$$\int_{\text{some contour in } \mathbf{Gr}(k,n,\mathbb{C})} \frac{\prod dc_{ij}}{< 12\cdots k >< 23\cdots k+1 > \cdots < n1\ldots k-1 >} \delta^{4/4}(C \cdot Z), \qquad (26.1)$$

where $< i_1, \ldots, i_K >$ is a maximal $k \times k$ minors C is a $k \times n$ matrix whose entries are c_{ij}. The integrand is invariant under $\mathbf{GL}_k$ so we get a form in $\mathbf{Gr}(k, n, \mathbb{C})$.

To calculate such integrals one would look at a contour and we would obtain a sum of residues.

Claim 26.2. *The singularities of this form on* $\mathbf{Gr}(k, n, \mathbb{C})$ *live exactly in* **positroid varieties** *where such varieties are defined to be the Zariski closure of the positive cells of* $\mathbf{Gr}_{\geq 0}(k, n, \mathbb{R})$.

Example 26.3. In the function $\frac{1}{x(x+yz)}$ there are more than two possibilities for the poles. For instance if $x \to 0$ then $x + yz \to yz$ thus there are two more cases $y \to 0$ and $z \to 0$. Thus, as we set the simple minors in (26.1) to zero we get some complicated branching. □

Question 26.4. *See in a direct combinatorial way that all the possibilities of setting minors to zero (this branching procedure) correspond to the objects described in this class to be in bijection with positroid cells in* $\mathbf{Gr}_{\geq 0}(k, n, \mathbb{R})$.

The physical data is $\lambda, \widetilde{\lambda}$ which are 2-dimensional planes in $\mathbb{C}^n$,

$$\lambda = \begin{array}{c} n \\ \square \\ 2 \end{array}, \quad \widetilde{\lambda} = \begin{array}{c} n \\ \square \\ 2 \end{array}$$

(encodes momenta). If V is a k-dimensional subspace in $\mathbb{C}^n$ then $\lambda \subset V$ and $V \perp \widetilde{\lambda}$. This corresponds to a subvariety of codimension $2n-4$ in $\mathbf{Gr}(k, n)$ which is a Schubert variety $\widetilde{\Omega}_{(k-2)\times(n-k-2)}$ (not in the standard basis but an arbitrary basis).

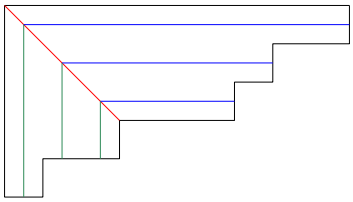

Figure 105: Example of Fröbenius notation of Young diagrams.

Then (26.1) becomes a sum over positive cells Π_D of dimension $2n-4$. You have to find the intersection points $\Pi_D \cap \widetilde{\Omega}_{(k-2)\times(n-k-2)}$ (both find the number of points and a description of the points). There is a nice paper of Knutson-Lam-Speyer [4] that looks at $\#(\Pi_D \cap \widetilde{\Omega}_\lambda)$ (this is related to *juggling patterns* and *affine Stanley symmetric functions*).

26.2 Non-planar plabic graphs

A white trivalent vertex corresponds to $\mathbf{Gr}(1,3) = \mathbb{P}^2$ and a black trivalent vertex corresponds to $\mathbf{Gr}(2,3)$ (see Figure 106(a-b)). We have looked at graphs embedded in disks. Can we generalize this to graphs that are not planar. We eliminate variables for internal edges.

Example 26.5. For the graph G in Figure 106(c) we get the equations $\frac{w_1}{a} = \frac{w_2}{b} = \frac{w_5}{c}, ew_3 + fw_4 + dw_5 = 0$, we eliminate w_is corresponding to internal edges. $w_5 = -\frac{ew_3+fw_4}{d}$, $\frac{w_1}{a} = \frac{w_2}{b}, \frac{w_1}{a} = -\frac{ew_3+fw_4}{cd}$ this corresponds to a plane in $\mathbb{C}^4$, i.e., a point in $\mathbf{Gr}(2,4)$. □

Example 26.6. For the graph in Figure 106(d) there is no perfect orientation and we cannot do such an elimination. □

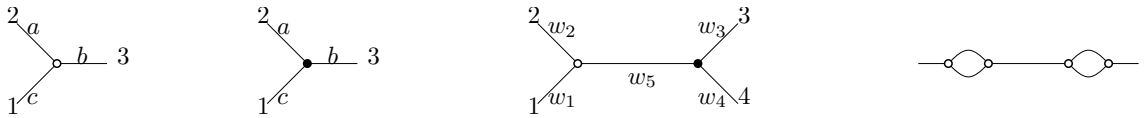

Figure 106: (a) White trivalent vertex corresponds to $\mathbf{Gr}(1,3) = \mathbb{P}^2$ $(a:b:c)$ $\frac{w_1}{a} = \frac{w_2}{b} = \frac{w_3}{c}$. (b) Black trivalent vertex corresponds to the plane given by $aw_1 + bw_2 + cw_3 = 0$. (c) Planar graph that corresponds to the equations $\frac{w_1}{a} = \frac{w_2}{b} = \frac{w_5}{c}$ and $ew_3 + fw_4 + dw_5 = 0$, if we eliminate the weight w_5 corresponding to the internal edge we obtain a plane in $\mathbb{C}^4$ which is a point in $\mathbf{Gr}(2,4)$. (d) Planar graph that corresponds to four linear equations.

Conjecture 26.7. *The elimination procedure described above works if and only if G has a perfect orientation.*

In the planar case if we start from a graph and do square moves repeatedly and get back to the original graph. Each square move changes the parameters but at the end when we return to the same graph the final transformation of parameters is the identity i.e., the monodromy is trivial. This is no longer the case in the nonplanar case. For instance if the graph has one hole. Lam and Pylyavskyy showed that in the case of one hole the monodromy is the symmetric group.

Question 26.8. *Describe the monodromy group in the non-planar case. What is it for two holes?*

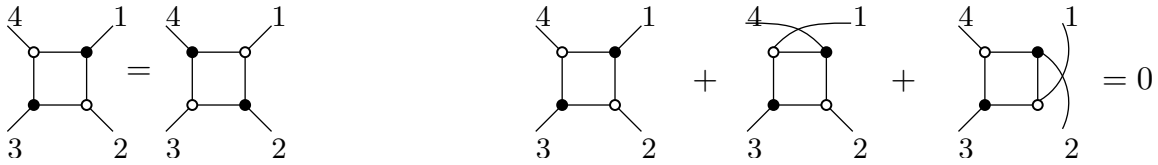

Figure 107: Square move and Jacobi-type identity of graphs.

Question 26.9. *Understand this set of graphs under the Jacobi type identity (see right of Figure 107).*

26.3 BCFW recurrence for tree-level amplitudes

This was first defined in terms of Feynman diagrams. Let $M_{k,n}$ be a certain linear combination of plabic graphs for $\mathbf{Gr}(k,n)$ (see Figure 108).

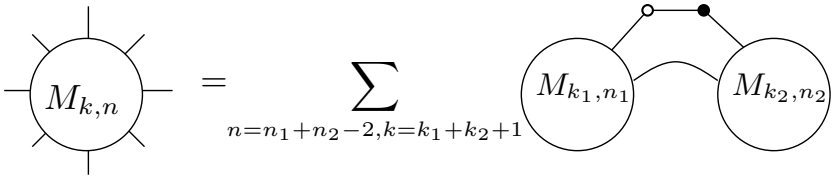

Figure 108: BCFW recurrence for tree-level amplitudes in terms of plabic graphs.

Claim 26.10. *$M_{k,n}$ involves Narayana number of graphs.*

Figure 109: $M_{k,n}$ involves Narayana number of graphs.

$M_{k,n}$ is a sum of plabic graphs corresponding to binary trees with $k-2$ right edges and $n-k-2$ left edges (see Figure 110(a) for rules).

Example 26.11. The plabic graph in Figure 110(b) with $n = 12$ external edges and $k = 7$ external edges incident to black vertices. This graph corresponds to a cell of dimension $2n-4$ and it is associated to a binary tree with $k-2 = 5$ right edges and $n-k-2 = 3$ left edges. The intersection $\Pi_D \cap \widetilde{\Omega}_{(k-2)\times(n-k-2)}$ has exactly one point. □

See Figure 111 for the six-term identity of $M_{3,6}$.

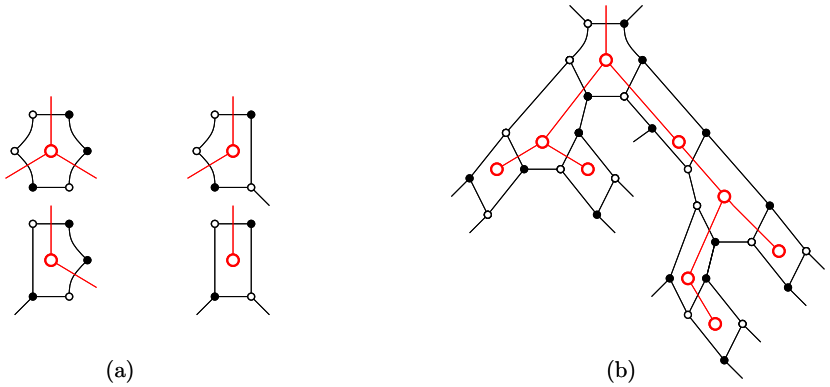

Figure 110: (a) Rules for correspondence between plabic graph and binary tree (in red). (b) Example of plabic graph and its associated binary tree (in red).

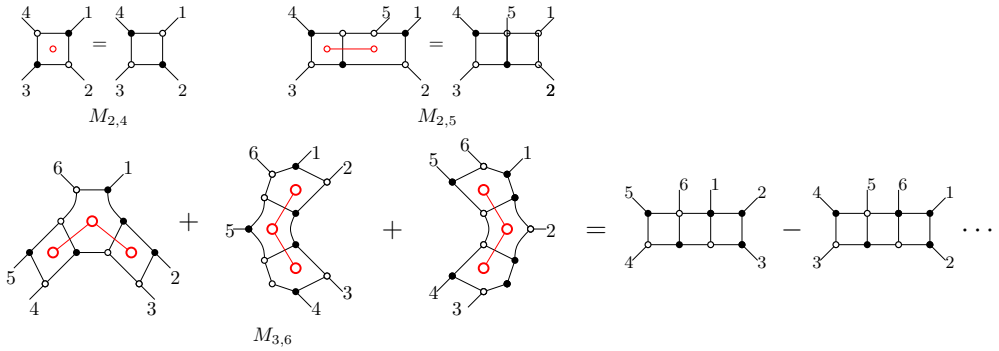

Figure 111: Identities for $M_{2,4}, M_{2,5}$ and $M_{3,6}$. The RHS of the latter involves six graphs.

Conjecture 26.12. *The six-term identity implies cyclic symmetry of* $M_{k,n}$.

Another way of representing the graphs in $M_{k,n}$ is as two trees in the disk. We add extra vertices such that every region is a quadrilateral (see Figure 112).

Thanks: to Darij Grinberg, Nan Li, Taedong Yun, Yufei Zhao and Tom Roby for comments, proofreading and board photos!

References

[1] Emeric Deutsch and Bruce E Sagan. Congruences for catalan and motzkin numbers and related sequences. *J. Number Theory*, 117(1):191–215, 2006.

[2] I. M Gelfand, R. M Goresky, R. D MacPherson, and V. V Serganova. Combinatorial geometries, convex polyhedra, and schubert cells. *Adv. in Math.*, 63(3):301–316, 1987.

[3] Oleg Gleizer and Alexander Postnikov. Littlewood-richardson coefficients via yang-baxter equation. *Internat. Math. Res. Notices*, (14):741–774, 2000.

[4] Allen Knutson, Thomas Lam, and David Speyer. Positroid varieties: Juggling and geometry. *arXiv*, math.AG, Nov 2011.

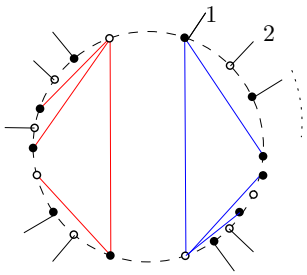

Figure 112: Example of alternative way of representing $M_{k,n}$ as two trees (one in red and the other in blue) in the disk such that every region is a quadrilateral.

[5] Allen Knutson and Terence Tao. Puzzles and (equivariant) cohomology of grassmannians. *Duke Math. J.*, 119(2):221–260, 2003.

[6] Ricky Ini Liu. Matching polytopes and specht modules. *Trans. Amer. Math. Soc.*, 364(2):1089–1107, 2012.

[7] Alexander Postnikov. Total positivity, grassmannians, and networks. *arXiv*, math.CO, Sep 2006. 79 pages.

[8] Kelli Talaska. Combinatorial formulas for $gamma$-coordinates in a totally nonnegative grassmannian. *J. Combin. Theory Ser. A*, 118(1):58–66, 2011.

[9] Lauren K Williams. Enumeration of totally positive grassmann cells. *Adv. Math.*, 190(2):319–342, 2005.